THE UNIVERSITY OF CHICAGO

OPTOGENETIC ANALYSIS OF RHO FAMILY GTPASES DURING MORPHOGENESIS AND POLARIZATION

A DISSERTATION SUBMITTED TO
THE FACULTY OF THE DIVISION OF THE BIOLOGICAL SCIENCES
AND THE PRITZKER SCHOOL OF MEDICINE
IN CANDIDACY FOR THE DEGREE OF
DOCTOR OF PHILOSOPHY

GRADUATE PROGRAM IN CELL AND MOLECULAR BIOLOGY

BY
ASHLEY RICH

CHICAGO, ILLINOIS
JUNE 2020

Table of Contents

LIST OF FIGURES vi

LIST OF TABLES viii

ACKNOWLEDGMENTS ix

ABSTRACT xii

1 INTRODUCTION 1
- 1.1 Actomyosin-mediated tissue internalization during development 3
  - 1.1.1 Rho1 drives invagination of the *Drosophila* ventral furrow 5
  - 1.1.2 Cdc42 drives endoderm invagination in the *C. elegans* embryo 12
  - 1.1.3 Actomyosin-mediated neural tube closure in *Xenopus* 13
  - 1.1.4 Open questions 14
- 1.2 PAR proteins promote cortical polarity and asymmetric cell division 17
  - 1.2.1 PAR protein polarization in the *C. elegans* zygote 21
    - 1.2.1.1 Rho family GTPases and cortical flows play a critical role in the polarization of *C. elegans* zygotes 22
    - 1.2.1.2 Mutually antagonistic PAR domains maintain polarity in the *C. elegans* zygote 23
    - 1.2.1.3 Multiple, dynamic PAR complexes exist during polarization 23
  - 1.2.2 PAR polarity underlies asymmetric cell division in *Drosophila* neuroblasts 24
    - 1.2.2.1 Neuroblast polarity cues 25
    - 1.2.2.2 aPKC is a key player in neuroblast polarization 26
    - 1.2.2.3 The role of Rho family GTPases during neuroblast polarization is unclear 27
    - 1.2.2.4 Linking cortical polarity to the mitotic spindle 27
  - 1.2.3 Open Questions 28
- 1.3 Optogenetics: A method for subcellular control of protein activity 30
  - 1.3.1 Light sensitive channels revolutionized neuroscience 31
  - 1.3.2 Optogenetic approaches adapted for cell biology 32
  - 1.3.3 Application of optogenetic tools to developmental cell biology 36
    - 1.3.3.1 Optogenetic dissection of cell fate specification 36
    - 1.3.3.2 Optogenetic control of Rho family GTPases during development 37
    - 1.3.3.3 Optogenetic probes provide definitive proof for longstanding models in developmental biology 39
    - 1.3.3.4 Optogenetic manipulation of polarity within tissues 40
    - 1.3.3.5 Generating force via optogenetics 41
- 1.4 Summary 41

2 RHO1 ACTIVATION RECAPITULATES EARLY GASTRULATION EVENTS IN THE VENTRAL, BUT NOT DORSAL, EPITHELIUM OF *DROSOPHILA* EMBRYOS . . . 43
2.1 Abstract . . . 43
2.2 Introduction . . . 43
2.3 Results . . . 46
2.3.1 A LOV domain-based optogenetic system controls Rho1 activity in *Drosophila* . . . 46
2.3.2 Rho1 activation is sufficient to induce reversible invaginations in the *Drosophila* embryonic epithelium . . . 51
2.3.3 Rho1 activation induces distinct apical constriction in the dorsal and ventral epithelium . . . 53
2.3.4 Genetic requirements for ventral-specific responses . . . 57
2.3.5 Spreading of deformations within the endogenous ventral furrow region 66
2.3.6 Differential responses of cells flanking the Rho1 activation zone in the dorsal and ventral epithelium . . . 66
2.4 Discussion . . . 68
2.4.1 A robust, ubiquitously expressed optogenetic system for use in *Drosophila* 70
2.4.2 Optogenetically-induced invaginations are reversible . . . 70
2.4.3 PR-GEF and RhoGEF2-CRY2 induce distinct cellular responses . . . 71
2.4.4 Requirements for ventral-specific responses to Rho1 activation . . . 72
2.4.5 Ventral and dorsal epithelia exhibit different material properties . . . 73
2.4.6 Conclusion . . . 75
2.5 Methods and Materials . . . 75
2.5.1 Plasmids . . . 75
2.5.2 Fly stocks . . . 75
2.5.3 S2 cells . . . 76
2.5.4 Preparation of *Drosophila* tissues for live imaging . . . 76
2.5.5 Live imaging and optogenetic experiments . . . 77
2.5.6 Image processing and cell shape analysis . . . 78
2.5.7 Statistics . . . 79
2.6 Acknowledgements . . . 79

3 OPTOGENETIC DISSECTION OF *DROSOPHILA* NEUROBLAST POLARIZATION . . . 86
3.1 Abstract . . . 86
3.2 Introduction . . . 87
3.3 Results . . . 89
3.3.1 Detecting endogenous Cdc42 activity . . . 89
3.3.2 Optogenetic manipulation of Cdc42 activity . . . 91
3.3.3 Optogenetic control of Bazooka . . . 95
3.3.4 Optogenetic control of aPKC . . . 96
3.4 Discussion . . . 98

3.5 Methods and Materials . . . 106
3.5.1 Plasmids . . . 106
3.5.2 Fly stocks . . . 107
3.5.3 S2 cells . . . 107
3.5.4 Preparation of *Drosophila* tissues for live imaging . . . 107
3.5.5 Live imaging and optogenetic experiments . . . 108
3.5.6 Image processing . . . 109
3.6 Acknowledgements . . . 109

4 DISCUSSION AND FUTURE DIRECTIONS . . . 115
4.1 Summary . . . 115
4.2 Rho1 and morphogenesis in *Drosophila* . . . 116
4.2.1 What protein activity enables ventral-specific responses to Rho1 activation? . . . 116
4.2.2 How are tissue level shape changes **sustained** *in vivo*? . . . 118
4.2.3 Is Rho1 activity sufficient to induce junctional rearrangements in Drosophila? . . . 120
4.2.4 What is the biological significance of pulsed contractility? . . . 122
4.2.5 Using optogenetic activation of Rho1 to delineate the contributions of distinct pools of actomyosin . . . 123
4.3 What is the role of Cdc42 in neuroblast polarity? . . . 124
4.4 Technological hurdles limiting optogenetic control of Rho family GTPases . . . 129
4.5 Moving beyond optogenetic control of Rho1 and Cdc42 in *Drosophila* . . . 131
4.6 Conclusion . . . 135

REFERENCES . . . 137

List of Figures

1.1 Schematic of GTPase signaling. 2
1.2 Rho family GTPase signaling in the context of morphogenesis and polarization. 3
1.3 Actomyosin contractility can drive apical constriction. 4
1.4 Adherens junctions connect cells within a tissue. 5
1.5 Apical constriction drives tissue level shape changes in diverse morphogenetic events. 6
1.6 Ventral furrow formation in the *Drosophila* embryo 8
1.7 Cortical polarity enables asymmetric cell division in the *Drosophila* neuroblast and *C. elegans* zygote. 18
1.8 Known PAR protein interactions 20
1.9 Inscuteable and Pins link apical cortical polarity with the spindle in *Drosophila* neuroblasts. 28
1.10 General approaches to optogenetic control of protein activity. 32

2.1 Optogenetic control of Rho1 in *Drosophila*. 48
2.2 Recruitment of PR-GEF activates Rho1 in all tissues tested. 50
2.3 Ectopic Rho1 activation is sensitive to light dose. 51
2.4 Inactivation kinetics of the LOV domain dictate the off rate of optogenetic-induced Rho1 activity. 52
2.5 Local Rho1 activation is sufficient to induce ectopic invaginations in the embryonic epithelium. 54
2.6 Optogenetic-induced invaginations revert following cessation of Rho1 activation. 55
2.7 Rho1 activation induces distinct apical constriction in dorsal and ventral epithelial cells. 56
2.8 Quantification of endogenous ventral furrow formation. 58
2.9 WT ventral, but not dorsal, cells exhibit large changes in the magnitude and alignment of anisotropy in response to Rho1 activation. 59
2.10 Comparisons of angle and magnitude of anisotropy before and after optogenetic Rho1 activation. 61
2.11 Optogenetic activation of Rho1 induces precocious cell shape changes in the ventral epithelium. 62
2.12 Dorsal is required for and Twist promotes aligned, anisotropic apical constriction in response to ectopic Rho1 activation. 63
2.13 Optogenetic Rho1 activation specifically induces cell non-autonomous responses in the ventral epithelium. 67
2.14 Non-activated cells bend towards ectopic invaginations specifically in the ventral epithelium. 69
2.15 Schematic of data collection and analysis for local activation experiments. 79

3.1 Putative Cdc42 biosensors respond to Cdc42 overexpression in S2 cells. 90
3.2 tagRFP-Par6$^{CRIB-PDZ}$ responds to Cdc42 activity *in vivo*. 92
3.3 Optogenetic control of Cdc42 in *Drosophila*. 94

3.4 PR-Baz is photosensitive and nucleates a complex with aPKC and Par6. 97
3.5 PR-aPKC co-recruits Par6 and displaces Numb. 99
3.6 PR-aPKC co-recruits a fragment of Par6. 101

4.1 Junctional proteins reorganize during ventral furrow formation. 122
4.2 Distinct pools of actomyosin exist during cell and tissue shape changes. 124
4.3 Proposed model for Baz(PAR-3) and Cdc42 during polarization of the *Drosophila* neuroblast and *C. elegans* zygote. 128
4.4 Hypothesis for optogenetic induction of pulsatile Rho1 activity with CRY2 - RhoGEF2(DHPH). 134

List of Tables

1.1 PAR proteins 19

2.1 Chapter 2 Plasmids Used 80
2.2 Chapter 2 Plasmids Used (Cont.) 81
2.3 Chapter 2 Genotypes and Reproducibility 82
2.4 Chapter 2 Genotypes and Reproducibility (Cont.) 83
2.5 Chapter 2 Activation Protocols 84
2.6 Recruitable GEF Viability Tests 85

3.1 Chapter 3 Plasmids Generated 111
3.2 Chapter 3 Plasmids Generated (Cont.) 112
3.3 Chapter 3 Plasmids Generated (Cont.) 113
3.4 Chapter 3 Genotypes 114

ACKNOWLEDGMENTS

This thesis would not have been possible without the support of many inspiring mentors, exemplary colleagues, encouraging friends, and supportive family members. First and foremost, I thank Michael Glotzer. He took a chance when he hosted me in his lab as an unexperienced REU student. In so doing, he opened the door to what has been an incredible intellectual experience. Michael's creativity and enthusiasm are infectious, and they have deeply impacted me as a scientist and a person. I am grateful for his unwavering support and encouragement throughout graduate school, and I will always appreciate the high standards he holds for his science and his trainees. May my future work reflect the rigorous training he has provided.

I am also deeply grateful to Rick Fehon, who has generously accepted me as an honorary member of his lab over the last seven years. Bringing *Drosophila* into the Glotzer lab would not have been possible without Rick's sharing of knowledge, time, reagents, and incubator space. My thesis work and my development as a scientist have both benefited from thoughtful discussions with Rick and his research group.

I further thank my thesis committee, Rick Fehon, Ed Munro, and Sally Horne-Badovinac, for their interest in my research, their technical and conceptual suggestions, and their continued encouragement. My committee gave me immense space to pursue a high risk project, and they maintained faith in my competence, even when I did not. I am grateful for their confidence in me as well their investment in my development as a scientist. I am also incredibly thankful to Ed Munro for helping me rediscover the joy of science on many occasions.

I am honored to have been a part of the hardworking and driven Glotzer lab. Katrina Longhini-Aldis keeps the Glotzer lab running smoothly and knows where just about every reagent we own is stored. I have benefited greatly from her technical assistance throughout my time at UChicago. Moreover, Katrina has been a constant source of encouragement and friendship during my time in the Glotzer lab. Amruta Nayak's excitement about fruit fly

morphogenesis is inspiring, and I wish her the best as she begins her own graduate school journey. Alana Koscove has brought much enthusiasm to the Glotzer lab, and I am grateful for her input on my project. I am also grateful to many former members of the Glotzer lab who helped shape my graduate school experience. Angika Basant continues to inspire me as a scientist and a person. Her graduate career set a standard to which I aspired, and I continue to be inspired and encouraged by her work. I am also deeply grateful for our continued friendship. I also appreciate the many discussions, scientific and otherwise, that I had with Kristen Witte. My science continues to be impacted by Kristen's thoughtful questioning.

My graduate school experience has been enriched by many colleagues outside of the lab. I thank Katie Homa for setting an incredible example of top notch science as well as for her unwavering friendship from Cell Bio I to the present day. Alyssa Harker generously and patiently helped me get my footing in SQL and R, and I continue to value her selfless friendship. Ana Beiriger has been a source of constant encouragement, and it has been a pleasure to write and defend our theses alongside each other. I thank current and past members of the Fehon lab for welcoming me into their discussions and generously sharing their technical expertise, including Jiajie Xu and Will Yee. I also thank Audrey Williams, Allison Zajac, and Sherzod Tokamov for keeping me abreast of fascinating new research and always being willing to speculate wildly about new results in the 9th floor fly room.

I give warm thanks to Aaron Turkewitz. I believe his continued support of the MGCB REU program played a large role in me being accepted into UChicago's CMB graduate program. Moreover, I appreciate his continued advocacy for graduate students. Working with Aaron to develop the MGCB Journal Club was a highlight of my graduate studies.

Behind the scenes, the hard work of many administrators allowed me to keep my focus on my science. I appreciate their efforts and their speedy responses to my never-ending questions. In particular, I thank Kristine Gaston, Catherine Will, Sue Levison, and Mary-

Ann Johnson.

Beyond UChicago, I benefited from an incredible support system. My parents, Randy and Andrea Rich, were a constant source of encouragement. Their work ethic and drive to succeed continue to inspire me, and I thank them for believing in me always. I thank my sister, Aireca Smith, for her continued support and for always picking up the phone when I needed to vent. Last, but definitely not least, I thank Andrew Baker. He has ridden every high and every low of graduate school with me. This work and this degree would not have been possible without his support, patience, and encouragement.

ABSTRACT

Organismal development is a complex process that involves cell growth and proliferation, specification of cell fates, and reorganization of tissues relative to one another. The generation of subcellular asymmetries is fundamental to many of these developmental events. For example, the building and contracting of actomyosin networks at precise positions within cells effects cell shape changes. Coupling these cell shape changes across a tissue drives tissue morphogenesis and reorganization of germ layers. Additionally, the polarization of cellular contents prior to cell division results in an asymmetric cell division that generates two daughter cells of distinct fates. Rho family GTPases, including Rho1/RhoA and Cdc42, play key roles in the formation of subcellular asymmetries. For example, Rho1 drives the formation of actomyosin structures that induce apical constriction and tissue invagination during ventral furrow formation in the *Drosophila* embryo, and Cdc42 promotes cortical polarity in *Drosophila* neuroblasts. However, the formation of these subcellular asymmetries is dynamic, and many questions about their formation and function remain. What protein activity is sufficient to initiate the formation of a subcellular structure? Does cell cycle progression regulate this inducer's activity? Once subcellular domains form, are they self-sustaining? Addressing these and related questions necessitates experimental approaches that afford acute control over protein activity in space and time. Toward this end, this thesis documents the development of optogenetic probes that acutely activate two Rho family GTPases, Rho1 and Cdc42, in *Drosophila*. I first describe the application of the Rho1 optogenetic probe to morphogenesis during *Drosophila* gastrulation. Using this tool, we discovered that Rho1 activity is sufficient to induce ectopic morphogenesis throughout the *Drosophila* embryo. However, the cell shape changes that underlie these ectopic morphogenetic events differ between cells in the dorsal and ventral epithelium. The response of ventral, but not dorsal, cells recapitulates cellular behaviors normally observed during ventral furrow formation, the first step in *Drosophila* gastrulation. Our work indicates that a Rho1-independent,

ventral-specific activity exists and cooperates with Rho1 during ventral furrow formation. This challenges the common Rho1-centric view of this morphogenetic event. Additionally, I describe the development of a Cdc42 biosensor and a Cdc42 optogenetic probe for use in monitoring and effecting Cdc42 activity during *Drosophila* neuroblast polarization. The optogenetic tools developed here promise to be widely useful for furthering our understanding of the roles of Rho1 and Cdc42 in generating subcellular asymmetries during *Drosophila* development.

CHAPTER 1

INTRODUCTION

The development of an organism from a single cell into a multilayered, adult form is a complex process. During this time, cells grow and proliferate, and cell types are specified, giving rise to distinct germ layers and tissue types. Morphogenetic movements rearrange these cell types relative to one another, ultimately generating complex body plans. Critical to many of these developmental events is the construction of subcellular domains and structures that enable asymmetric allocation of cellular factors. How such subcellular asymmetries are built with sufficient spatial and temporal precision during organismal development is a central focus of developmental cell biology.

One example of a subcellular asymmetry is the building of contractile structures at specific places within cells that are subsequently used to effect cell shape changes. Coupling several of these contractile structures and cell shape changes across cells within a tissue can generate a tissue level shape change. Another example of subcellular asymmetry during development is that of asymmetric cell division. During this process, cells segregate their contents unequally among daughters, generating two differently fated cells. Before cellular cargo can be asymmetrically segregated, cortical and/or cytoplasmic domains must be generated in the mother cell to polarize its contents.

The specific molecules that generate subcellular asymmetries in diverse organisms and cell types can vary, but a general cast of molecular players underlies these events. For example, small GTPases, which function as small molecular switches, often regulate the formation of subcellular asymmetries. GTPases cycle between active, GTP-bound, and inactive, GDP-bound, states (Figure 1.1). Guanine nucleotide exchange factors (GEFs) and GTPase activating proteins (GAPs) promote the activation and inactivation of GTPases, respectively [Reiner and Lundquist, 2018]. Examples of GTPases include Ras, Rap1, and the Rho family GTPases, RhoA/Rho1, Cdc42, and Rac1.

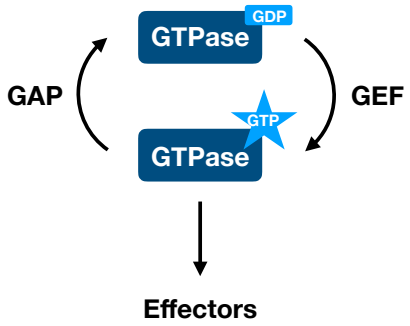

Figure 1.1: **Schematic of GTPase signaling.** GTPases are active when bound to GTP and inactive when bound to GDP. In their active state, GTPases can promote the activity of downstream effectors. Guanine nucleotide exchange factors (GEFs) activate GTPases by promoting the exchange of GDP for GTP. GTPase activating proteins (GAP) inactivate GTPases by promoting their hydrolysis of GTP.

My thesis work focused on two Rho family GTPases, RhoA/Rho1 and Cdc42, as they are conserved regulators of subcellular asymmetries that effect tissue level shape changes and asymmetric cell divisions [Jaffe and Hall, 2005]. In their active state, Rho family GTPases activate downstream effectors, including formins, which drive the assembly of filamentous actin, as well as Rho kinase (Rok) and MRCK-1, which activate myosin (Figure 1.2) [Kumfer et al., 2010, Jaffe and Hall, 2005]. Once assembled, these actin and myosin structures work together to alter cell shape and segregate cellular contents. Chapter 2 of this thesis focuses on the role of Rho1 in morphogenesis. Specifically, I ask how does Rho1 activity promote the formation and contraction of actomyosin networks in the context of mesoderm internalization in the *Drosophila* embryo. Chapter 3 investigates the role of Cdc42 in cell polarization. Specifically, I interrogate how Cdc42 promotes the building and maintaining of cortical asymmetries during asymmetric cell division in *Drosophila* neuroblasts.

The following sections of this introductory chapter introduce these two developmental processes and summarize the mechanistic understanding of how they occur. I compare both mesoderm internalization and neuroblast polarization to similar developmental events in other organisms to emphasize their conservation as well as to highlight outstanding open questions. These summaries of *Drosophila* mesoderm internalization and neuroblast po-

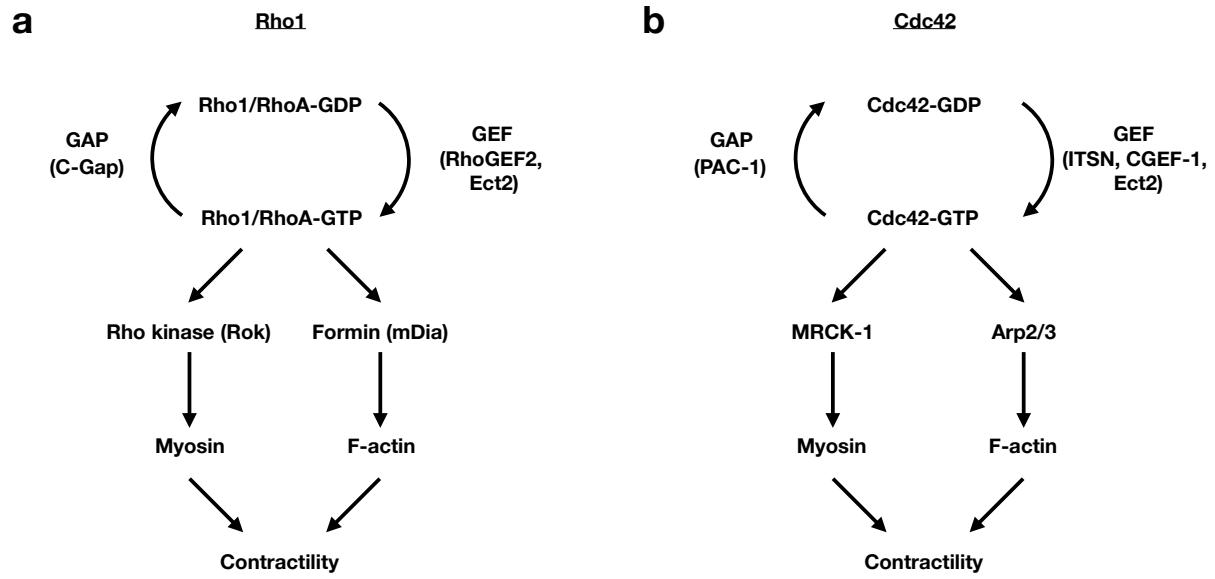

Figure 1.2: **Rho family GTPase signaling in the context of morphogenesis and polarization.** Once activated by their respective GEFs, Rho1 (a) and Cdc42 (b) activate downstream effectors that ultimately drive actomyosin-mediated contractility. The GEFs, GAPs, and effectors diagrammed correspond to the proteins discussed in this thesis.

larization will underscore the dynamic nature of both tissue internalization and cortical polarization, emphasizing that a complete understanding of these processes will require approaches that allow dynamic measurements and perturbations of protein activity. Toward this end, the final section of this introduction will discuss the application of optogenetic approaches to questions in cell and developmental biology and argue that optogenetic manipulation of Rho family GTPase activity can advance our understanding of both tissue morphogenesis and cell polarity.

1.1 Actomyosin-mediated tissue internalization during development

Tissue level shape changes convert simple embryonic body plans into multilayered adult organisms. Diverse morphogenetic movements can achieve this end, including involution, epiboly, and invagination [Solnica-Krezel, 2005, Warga and Kimmel, 1990, Campos-Ortega

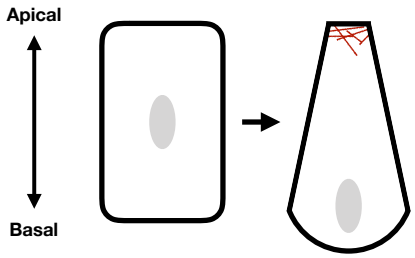

Figure 1.3: **Actomyosin contractility can drive apical constriction.** Schematic of a single columnar cell undergoing apical constriction. Apical constriction involves the shrinking of the apical cell surface. Conservation of volume leads to expansion of the basal cell surface.

and Hartenstein, 1985]. Tissue level shape changes are brought about by individual cell shape changes. One of the best studied cell shape changes is apical constriction, where the apical domain of a cell shrinks, or constricts, converting a formerly columnar cell into a wedge-shaped cell (Figure 1.3) [Martin and Goldstein, 2014]. The transient assembly and contraction of actomyosin networks is a common driving force for this cell shape change [Martin and Goldstein, 2014]. In cases where cell volume is conserved, apical constriction results in cell lengthening along the apicobasal axis as well as expansion of the basal cell surface [Gelbart et al., 2012]. However, apical constrictions that occur alongside reductions in cell volume can also occur [Saias et al., 2015].

Cells within epithelial tissues are coupled to one another through junctional complexes, including tight junctions and adherens junctions. Tight junctions (septate junctions in flies) perform the barrier function of epithelial cells by preventing leakage of fluids between epithelial cells [Miyoshi and Takai, 2005]. Adherens junctions, which are composed in part of E-cadherin, β-catenin, and α-catenin, link cells within an epithelium to one another [Harris, 2012, Harris and Tepass, 2010]. The cytoplasmic faces of adherens junctions connect to the actin cytoskeleton, coupling the cytoskeletons of individual epithelial cells across the tissue (Figure 1.4). Thus, through adherens junctions, autonomous apical constrictions, which alter the apices of individual cells, are coupled throughout an epithelial sheet and drive tissue bending.

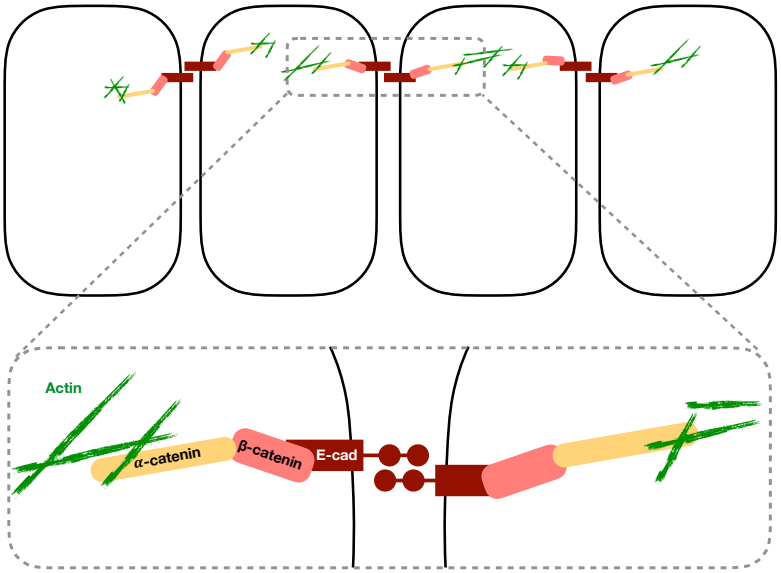

Figure 1.4: **Adherens junctions connect cells within a tissue.** Schematic of a simplified adherens junction. The extracellular cadherin repeats of E-cadherin homodimerize in trans to adhere neighboring cells together within tissues. The intracellular, cytoplasmic face of E-cadherin connects to the actin cytoskeleton through α- and β-catenin.

The following sections will discuss how Rho family GTPases drive the formation of actomyosin structures and promote tissue internalization in well-studied models of embryonic development, with the goal of highlighting and emphasizing similarities among the systems as well as open questions.

1.1.1 Rho1 drives invagination of the Drosophila ventral furrow

Ventral furrow formation is the first step in *Drosophila* gastrulation. It begins shortly after the completion of cellularization and proceeds rapidly, completing in about 15 minutes [Sweeton et al., 1991, Turner and Mahowald, 1977]. Proper execution of ventral furrow formation is critical, as it internalizes the cells of the embryonic mesoderm. Once internalized by the ventral furrow, the mesodermal precursors undergo an epithelial to mesenchymal transition (EMT), losing their cell-cell adhesions and eventually migrating dorsally [Leptin, 1999].

During ventral furrow formation, approximately 1000 ventrally located epithelial cells

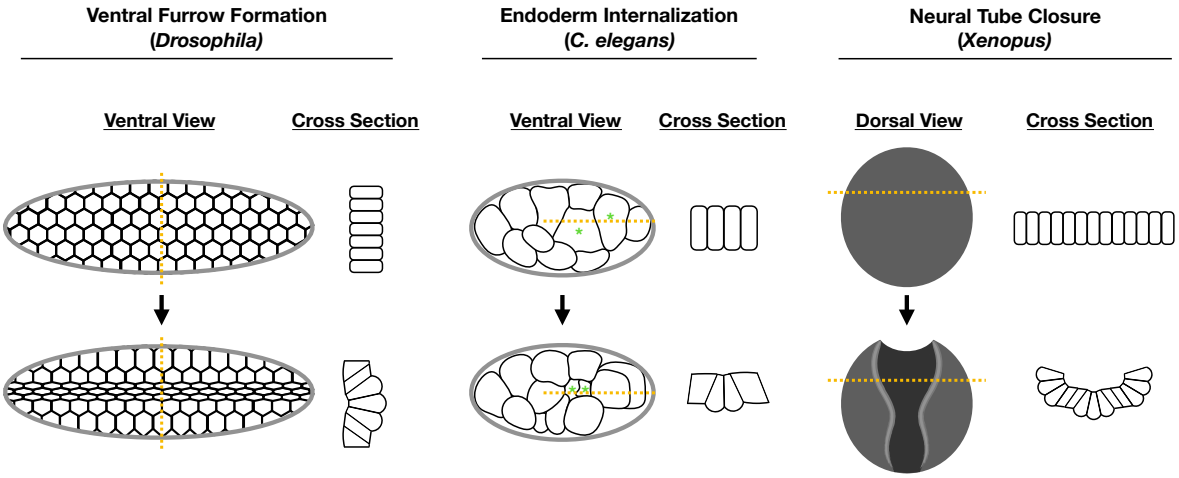

Figure 1.5: **Apical constriction drives tissue level shape changes in diverse morphogenetic events.** During ventral furrow formation in the *Drosophila* embryo (left), approximately 1000 ventral cells apically constrict and drive mesoderm invagination. (Anterior is to the left.) During endoderm internalization in the *C. elegans* zygote (middle), two endodermal precursors apically constrict before moving into the embryo. (Anterior is to the left. Adapted from [Goldstein and Nance, 2020, Nance et al., 2005].) During neurulation in *Xenopus* (right), subsets of neural plate cells apically constrict to promote neural tube closure. (Anterior is to the top. Adapted from [Suzuki et al., 2012].) Yellow dashed lines correspond to cross sections shown to the right of ventral and dorsal views.

constrict, or shrink, their apical surfaces and invaginate (Figure 1.5) [Sweeton et al., 1991, Leptin and Grunewald, 1990, Turner and Mahowald, 1977]. Rho1 activity drives the formation of apical, contractile actomyosin networks in individual ventral cells to promote their constriction and invagination [Martin et al., 2009, Fox and Peifer, 2007]. The coupling of these cell shape changes, via adherens junctions, across the ventral epithelium generates an invagination [Martin et al., 2010]. Thus, *Drosophila* ventral furrow formation provides an excellent example of how contractile structures, built with subcellular precision, drive cell shape changes and, ultimately, tissue morphogenesis.

The cellular events upstream of Rho1 activation during ventral furrow formation are well understood. A series of classic transplantation experiments identified a polarizing activity in perivitelline fluid that specifies ventral cell fate when injected into mutant embryos that would otherwise develop as completely dorsalized embryos [Stein and Nusslein-Volhard, 1992,

Stein et al., 1991]. This polarizing activity includes a maternally contributed, extracellular protease cascade that activates the ligand Spatzle [Schneider et al., 1994]. Once activated, Spatzle binds Toll, a transmembrane receptor, and signaling downstream of activated Toll allows Dorsal, a transcription factor, to enter the nucleus [Lewis et al., 2013, Weber et al., 2007]. This results in a gradient of active, nuclear Dorsal along the dorsal-ventral axis, with the ventral-most cells containing the highest amounts of Dorsal in their nuclei [Morisato and Anderson, 1995]. In the presumptive mesoderm, where its activity is greatest, Dorsal drives the expression of two additional transcription factors, Snail and Twist [Ip et al., 1992, Jiang et al., 1991]. Twist, in turn, promotes the expression of T48, a transmembrane protein, and Fog, a secreted ligand [Kölsch et al., 2007, Costa et al., 1994]. Snail indirectly promotes the expression of a G protein coupled receptor (GPCR), Mist [Manning et al., 2013]. The ligand Fog binds Mist and activates Concertina, a maternally contributed Gα protein [Manning et al., 2013, Dawes-Hoang et al., 2005, Parks and Wieschaus, 1991]. Activated Concertina, T48, and an additional, maternally contributed GPCR, Smog, all cooperate to apically localize and activate RhoGEF2, a guanine nucleotide exchange factor that promotes Rho1 activity and actomyosin accumulation [Kerridge et al., 2016, Manning et al., 2013, Nikolaidou and Barrett, 2004, Kölsch et al., 2007, Barrett et al., 1997, Häcker and Perrimon, 1998]. These intracellular actomyosin networks within cells are coupled via adherens junctions to ultimately generate a supracellular actomyosin network that promotes apical constriction and robust ventral furrow formation (Figure 1.6) [Yevick et al., 2019, Martin et al., 2010].

Rho1 activity and myosin accumulate in a pulsatile manner at the apical surface of each cell during ventral furrowing, and these pulses of Rho1 and myosin translate into pulsed apical constrictions [Martin et al., 2009, Mason et al., 2016]. Pulsatile protein activity can be generated by local, positive feedback coupled to global and/or delayed negative feedback [Michaux et al., 2018, Bement et al., 2015, Kumar et al., 2014, Allard and Mogilner, 2013]. In the case of ventral furrow formation, the positive signal comes from a Rho1 GEF, RhoGEF2,

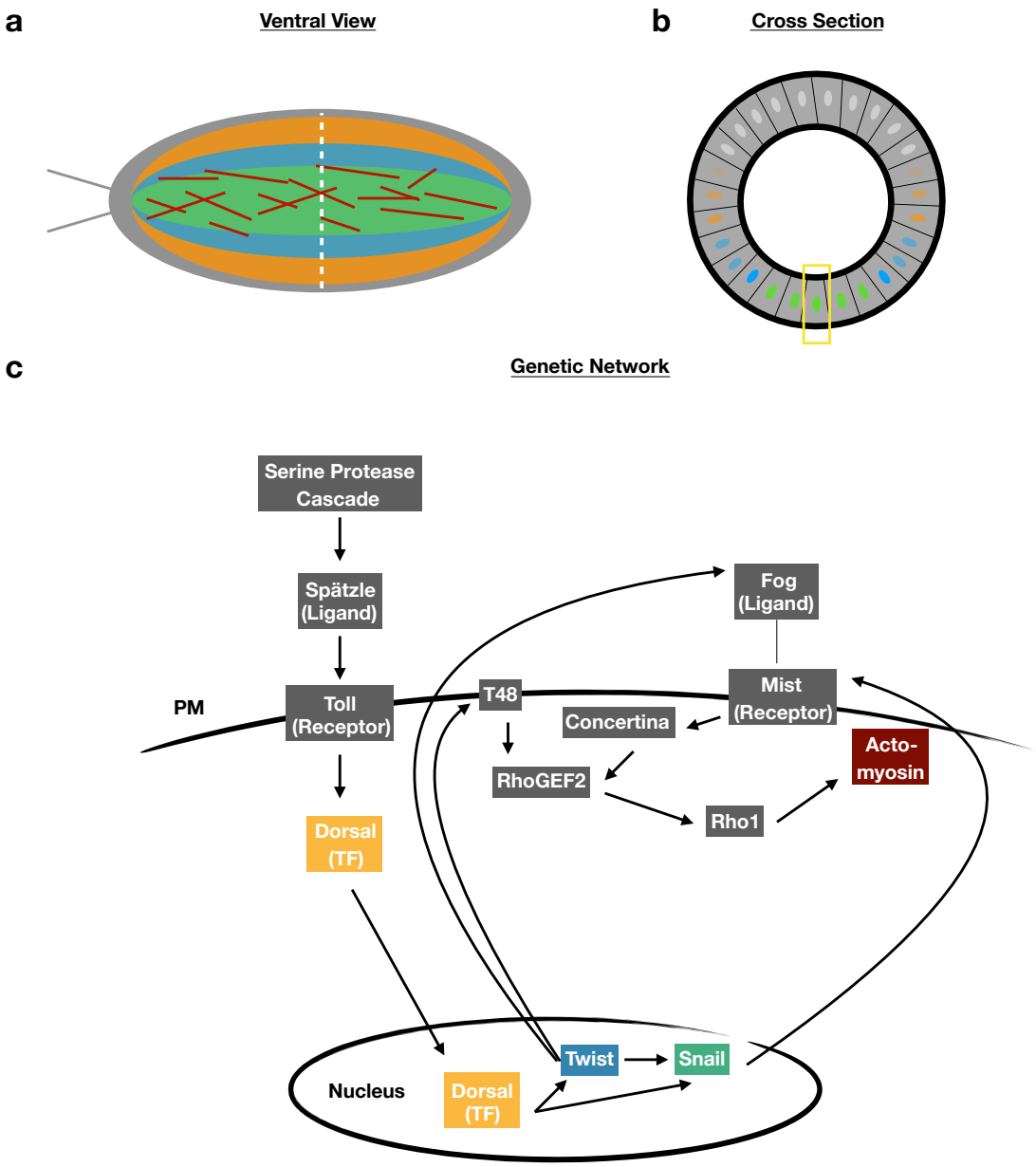

Figure 1.6: **Ventral furrow formation in the *Drosophila* embryo.** a) Schematic ventral view of *Drosophila* embryo exhibiting domains of Dorsal (orange), Twist (blue), and Snail (green) expression. One known downstream output of these transcription factors is the formation of a supracellular actomyosin network (red) in the ventral mesoderm. (Anterior is to the right.) b) Schematic of a cross-sectional view of a *Drosophila* embryo (dashed white line in (a)). Nuclei exhibit a single color for simplicity. Green nuclei express Snail, Twist, and Dorsal. Blue nuclei express Twist and Snail. Orange nuclei express only Dorsal. (Dorsal is to the top.) c) Gene expression profile of a ventral cell (yellow box in (b)).

which accumulates in pulses that precede myosin pulse accumulation [Mason et al., 2016, Häcker and Perrimon, 1998, Barrett et al., 1997]. The negative regulator in this system is C-Gap, a Rho1 GAP that inhibits Rho1 activity [Mason et al., 2016]. C-Gap is required for Rho1 and myosin pulses during ventral furrow formation [Mason et al., 2016]. The initial pulses of apical constriction are not ratcheted and relax to their pre-constriction state following dissolution of actomyosin punctae. Ventral cells eventually transition to a phase of ratcheted constriction, where actomyosin-driven cell shape changes are stabilized [Xie and Martin, 2015, Martin et al., 2009]. The molecular nature of the ratchet that maintains the apically constricted state of ventral cells is not known, but it requires the transcription factor Twist [Martin et al., 2009]. Despite extensive characterization of the biochemical and cellular pulses during ventral furrow formation and the insights into the molecules underlying these pulses, their biological importance is unproven. Testing whether pulsatile Rho1 activity is necessary to drive this tissue-level shape change will necessitate acute, persistent Rho1 activation in the absence of the endogenous activator of ventral cell contractility.

Much focus has been placed on the role of apical-medial actomyosin during ventral furrow formation. However, a recent study raises the possibility that actomyosin cables running along the apico-basal axis might also contribute to ventral furrow invagination [Gracia et al., 2019]. Specifically, the authors demonstrate that apico-basal cables of myosin in the presumptive mesoderm exist and are under tension. Laser cutting experiments that disrupted the apico-basal myosin cables did not impair ventral furrowing. In contrast, combining laser ablation of the apico-basal cables with laser cuts at the anterior and posterior most regions of the ventral furrow, which isolate the contractile domain from the ends of the embryo, severely disrupted ventral furrow formation. Thus, while these apico-basal cables are not essential, they may contribute to the robustness of ventral furrow formation and/or act as a redundant mechanism for internalizing mesoderm. Notably, this work relied exclusively upon laser ablation of apico-basal cables. It is possible that the laser cuts that disrupted the

apico-basal cables or the apical actomyosin network also damaged other cellular structures. More targeted disruption or activation of these structures would provide a clearer understanding of their contribution to ventral furrow formation. Outside of *Drosophila*, there is precedent for the involvement of apico-basal structures during tissue internalization. Endoderm invagination in ascidians involves both myosin-mediated apical constriction as well as myosin-mediated apical-basal shortening [Sherrard et al., 2010]. The existence of similar apico-basal actomyosin structures in the *Drosophila* mesoderm suggests that actomyosin structures other than those found in the well-studied apical-medial punctae may contribute to the invagination of the ventral furrow.

The intracellular signaling cascade described above explains how individual cells within the ventral epithelium effect the constriction of their apical surfaces. In addition to these cell autonomous actions, several aspects of ventral furrow formation suggest that individual cellular behaviors may be coordinated among cells of the ventral furrow. For example, ventral cells constrict anisotropically during this morphogenetic movement, decreasing their width along the dorsal-ventral axis much more than along the anterior-posterior axis [Sweeton et al., 1991, Martin et al., 2009]. If individual apical constrictions did not influence the behavior of neighboring cells, one would predict uniform, or isotropic, apical constriction. Furthermore, cells adjacent to constricting cells appear more likely to constrict than cells more distant to constricting cells [Gao et al., 2016, Sweeton et al., 1991]. Finally, several rows of cells neighboring the ventral furrow bend toward it as it invaginates; this behavior is indicative of efficient transmission of forces over long distances in the ventral epithelium [Rauzi et al., 2015, Costa et al., 1994, Leptin et al., 1992]. Thus, intercellular transmission of forces likely plays a role in the cell- and tissue-level behaviors that occur during ventral furrow formation.

The model of ventral furrow formation discussed above centers on Rho1-mediated actomyosin contractility. However, accumulating evidence suggests that Rho1-mediated contrac-

tility alone may not explain this morphogenetic event. For example, adherens junctions may play a role in ventral furrowing. Junctional proteins, including E-cadherin and β-catenin (Armadillo), move from a sub-apical position prior to ventral furrow formation to an apical position and become more densely packed during ventral furrow formation [Weng and Wieschaus, 2016, Mathew et al., 2011, Kölsch et al., 2007]. The molecular mechanism driving this junctional rearrangement is unclear, but myosin activity is required [Weng and Wieschaus, 2016, Kölsch et al., 2007]. Furthermore, Fog or T48 overexpression is sufficient to induce ectopic apical accumulation of E-cadherin or β-catenin, respectively [Weng and Wieschaus, 2016, Kölsch et al., 2007]. Though its function is unclear, TNF-receptor-associated factor 4 (Traf4) is also required for the apical concentration of β-catenin. Embryos lacking maternal and zygotic Traf4 exhibit compromised apical constriction and delayed ventral furrowing [Mathew et al., 2011], demonstrating that these junctional rearrangements contribute to the robustness of this morphogeneitc movement.

Consistent with the importance of junctional proteins during ventral furrowing, embryos expressing a version of E-cadherin lacking the proximal half of its extracellular domain fail to form a ventral furrow [Haruta et al., 2010]. These ventral cells still apically constrict, but ventral cell shape changes are no longer coordinated across the ventral epithelium, and furrows often regress after they form. Similarly, embryos lacking Rap1 GTPase, which fail to form an apical adherens junction belt of E-cadherin, exhibit uncoordinated apical constriction and delayed ventral furrowing [Spahn et al., 2012]. Taking these data together, it is intriguing to speculate that E-cadherin molecules may interact in trans to coordinate the cell shape changes that occur during ventral furrow formation and to stabilize this tissue-level shape change.

Besides junctional proteins, endocytosis may be another Rho1-independent mediator of ventral furrowing. Depletion of Rab35, a small GTPase involved in endocytic trafficking, or its GEF, Sbf (SET domain binding factor), impairs apical constriction and ventral furrowing

[Miao et al., 2019]. Endocytosis may contribute to apical constriction by remodeling apical cell membranes following actomyosin-mediated constriction. However, it is unlikely that membrane remodeling alone would stabilize apical constrictions, as membrane is quite fluid. Taken together, these works emphasize that an actomyosin-centric view of ventral furrow formation and invagination is incomplete; additional mechanisms contribute to remodeling the apical surfaces of ventral cells and internalizing the presumptive mesoderm.

1.1.2 Cdc42 drives endoderm invagination in the C. elegans embryo

Another well studied model of actomyosin-mediated tissue morphogenesis is endoderm internalization in the *C. elegans* zygote. This first gastrulation event in the embryo occurs at the 26-28 cell stage (Reviewed in Goldstein and Nance [2020]). During endoderm internalization, two endodermal precursors on the ventral surface of the embryo constrict their apical surfaces and move into the interior of the embryo over a period of 15-20 minutes (Figure 1.5) [Goldstein and Nance, 2020, Lee and Goldstein, 2003, Nance and Priess, 2002]. As in *Drosophila* mesoderm internalization, actomyosin accumulation at the apical, or outside, surface of these cells underlies their constriction [Nance and Priess, 2002, Lee and Goldstein, 2003].

Similar to *Drosophila* ventral furrow formation, the molecular events upstream of actomyosin contractility in the *C. elegans* endodermal precursors are well understood, and they center around Rho family GTPase activity. However, in the *C. elegans* endoderm CDC-42, rather than RHO-1, activates actomyosin. Two GEFs, CGEF-1 and ECT-2, function in parallel to activate CDC-42 at the endodermal precursor cortex [Chan and Nance, 2013]. CDC-42 activity is restricted to the apical cortex by PAC-1, a CDC-42 GAP, which is recruited to cell-cell contacts and inhibits CDC-42 activity at basolateral membranes [Anderson et al., 2008]. Apically active CDC-42 recruits MRCK-1, which activates myosin and drives apical constriction in these cells [Marston et al., 2016, Anderson et al., 2008]. Myosin

activity is pulsatile during endoderm invagination [Roh-Johnson et al., 2012]. However, as in the *Drosophila* ventral furrrow, the biological importance of this pulsatile myosin, versus continuous myosin activity, is unclear. Notably, the first pulses of actomyosin observed in endodermal cells do not deform the apical membrane. As this morphogenetic event progresses, a molecular clutch appears to engage in these cells, coupling actomyosin pulses to membrane deformation [Roh-Johnson et al., 2012]. The molecule underlying this clutch has not been identified, but it is possible that the same molecule that underlies this clutch also underlies the ratcheting of pulsed apical constriction in the *Drosophila* ventral furrow formation.

In addition to apical cell surface shrinkage, cadherin complexes reorganize during endodermal precursor internalization. Specifically, in the *C. elegans* endodermal precursors, E-cadherin, α-catenin, and β-cataenin concentrate at the apical-most contacts between the invaginating endodermal cells [Marston et al., 2016]. This cadherin relocalization requires myosin [Marston et al., 2016]. Thus, in both flies and worms, apical surface shape changes occur alongside junctional rearrangements. However, in both systems, the importance of this junctional reorganization needs to be investigated: Is it required for proper internalization? Is myosin activity sufficient to drive this junctional rearrangement?

1.1.3 Actomyosin-mediated neural tube closure in Xenopus

Actomyosin-mediated apical constriction and tissue internalization is also important during vertebrate morphogenesis. For example, apical constriction promotes tissue invagination during *Xenopus* neural tube closure (Figure 1.5) [Itoh et al., 2014, Lee et al., 2007, Haigo et al., 2003]. Apical junctions parallel to the mediolateral axis of the neural plate also shrink and contribute to the reduction in apical surface area of *Xenopus* neuroepithelial cells [Christodoulou and Skourides, 2015]. As in the two invertebrate systems already discussed, actomyosin contractility is associated with these apical cell surface shape changes during *Xenopus* neurulation [Itoh et al., 2014, Haigo et al., 2003], indicating conservation of, at

least the downstream, effectors of apical constriction and tissue bending during vertebrate development.

The molecular mechanisms underpinning apical constriction and tissue invagination during *Xenopus* neural tube closure are not as well studied as the invertebrate systems discussed above. Shroom, an actin binding protein that activates Rho kinase (Rok), and GEF-H1, a RhoA specific GEF, are required for the apical constriction observed during neural tube closure [Itoh et al., 2014, Lee et al., 2007, Haigo et al., 2003]. However, the mechanisms by which GEF-H1 or Shroom is localized or activated at the correct subcellular location during neural tube closure remain to be determined.

Recently, live imaging experiments showed that apical pulses of actin precede the apical constrictions observed during *Xenopus* neurulation [Christodoulou and Skourides, 2015]. Thus, pulsatile actomyosin activity during apical constriction appears to be conserved from invertebrates to vertebrates.

1.1.4 Open questions

Taking the morphogenetic events described above together, a general theme emerges: Transient assembly and contraction of actomyosin structures at the apical surface of cells drives apical constriction and promotes morphogenesis during development in diverse organisms. Despite our ever-improving molecular knowledge of the morphogenetic events described above, several questions remain.

Is actomyosin contractility sufficient to drive these, and other, morphogenetic movements?

Contraction of actomyosin networks occurs concomitant with each of the morphogenetic events discussed above. However, is actomyosin contractility alone sufficient to drive these tissue-level shape changes? Altering the gene expression program of *C. elegans* germline cells such that they acquire endodermal fate results in their ectopic apical constriction and inter-

nalization, reminiscent of normal endodermal cells [Marston et al., 2016]. This ectopic internalization is preceded by MRCK-1 accumulation at the apical surface of the cells converted to endodermal fate. This raises the possibility that CDC-42 activity and subsequent actomyosin contractility may be sufficient to drive endodermal invagination. However, it is also possible that Wnt signaling, which is involved in specifying endodermal cell fate [Lee et al., 2006d, Herman and Wu, 2004], drives the expression of additional factors that cooperate with CDC-42 activity and/or actomyosin contractility to recapitulate endoderm internalization. Experimental approaches that acutely activate CDC-42 or actomyosin contractility and assess whether endodermal precursor invagination was recapitulated will distinguish between these possibilities.

Similarly, the current model of ventral furrow formation suggests that this morphogenetic event arises from spatiotemporally defined Rho1 activity in the *Drosophila* ventral epithelium [Gilmour et al., 2017, Ko and Martin, 2020]. In the simplest iteration of this model, an asymmetric zone of Rho1 should recapitulate the cell- and tissue-level behaviors observed during endogenous ventral furrow formation [Doubrovinski et al., 2018]. Consistent with this model, ectopic expression of signaling components upstream of Rho1, such as Fog, throughout the embryonic epithelium is sufficient to globally induce cell shape changes that are normally restricted to the ventral furrow, namely apical cell surface flattening [Morize et al., 1998, Costa et al., 1994]. Moreover, optogenetic experiments that locally activated Rho1, via recruitable RhoGEF2, demonstrated that Rho1 activity is sufficient to induce an ectopic invagination in the dorsal *Drosophila* embryonic epithelium [Izquierdo et al., 2018]. Despite proving the sufficiency of Rho1 to intiate morphogenesis, this study did not assess whether Rho1 activity is sufficient to recapitulate all aspects of ventral furrow formation, including sustained tissue-level shape changes and coordinated cellular behaviors. Furthermore, this study did not investigate whether distinct regions of the embryonic epithelium, such as the dorsal and ventral surfaces, respond similarly to ectopic Rho1 activation.

What is the role of pulsatile actomyosin in morphogenesis?

Pulsatile actomyosin accompanies all three of the morphogenetic movements discussed above. However, is this pulsing necessary for these morphogenetic movements? The pulses of myosin observed in the *C. elegans* embryo, before the molecular clutch engages, are not sufficient to deform the cellular membranes [Roh-Johnson et al., 2012], and the *C. elegans* zygote polarizes its cortex in the absence of myosin pulses [Motegi et al., 2011, Zonies et al., 2010]. Thus, pulsed myosin activity may be dispensable in these systems. In contrast, ablation of medial myosin pulses during *Drosophila* germband extension relaxes junctional shrinkage, suggesting that the medial pulses in this system actively drive cell shape changes [Rauzi et al., 2010]. However, this experiment does not determine whether a pulse of myosin activity is needed or whether sustained medial myosin activity might drive the same cell shape change. Determining whether pulsatile Rho1 and/or actomyosin activity is required for morphogenetic movement or whether pulses are a consequence of the underlying biochemistry will require determining whether these morphogenetic events can be reproduced with sustained rather than pulsed Rho1 activation.

What is the role of junctional rearrangements in apical constriction and tissue internalization?

Junctional rearrangements accompany the internalization of both the *Drosophila* mesoderm and the *C. elegans* endoderm. In both systems, cadherin complexes concentrate at the apical most part of the lateral cell membranes at the onset of morphogenesis. What drives these rearrangements? In both systems, myosin activity is required for the apical concentration of cadherin complexes [Weng and Wieschaus, 2016, Marston et al., 2016, Kölsch et al., 2007]. However, it is unclear whether myosin-dependent contractility is sufficient to drive these junctional rearrangements. Fog or T48 overexpression throughout the *Drosophila* embryo is sufficient to drive junctional protein rearrangement [Weng and Wieschaus, 2016, Kölsch et al., 2007], but both of these proteins could activate factors in addition to myosin.

Moreover, the biological importance of these junctional rearrangements has not been elucidated. An approach that permits the direct activation of myosin-mediated contractility in combination with live imaging of E-cadherin dynamics is needed to determine whether myosin activity alone is sufficient to induce junctional rearrangement. Although the biological significance of junctional rearrangements remains unclear, it is intriguing to speculate that this junctional reorganization may contribute to stabilizing apical constriction and tissue-level shape changes and/or coordinating cell shape changes across tissues.

1.2 PAR proteins promote cortical polarity and asymmetric cell division

Asymmetric cell division segregates cellular contents unequally among daughter cells such that they become physically and/or molecularly distinct from one another. In the *C. elegans* zygote, asymmetric cell division generates an anterior AB and a posterior P1 cell, which give rise to distinct embryonic tissues (Figure 1.7a) [Gönczy and Rose, 2005]. In the *Drosophila* neuroblast, asymmetric cell division generates a self-renewing neuroblast and a differentiating daughter cell that gives rise to neurons and glial cells (Figure 1.7b) [Hartenstein and Wodarz, 2013].

Cell polarization is a critical upstream step in asymmetric cell division that involves the generation and maintenance of distinct subcellular domains. One of the best studied examples of cell polarization occurs in *S. cerevisae* when this single-celled organism breaks symmetry at its cortex and forms a single daughter bud (Reviewed in [Chiou et al., 2017, Bi and Park, 2012, Park and Bi, 2007]). This polarization event occurs at a specific point in the cell cycle and ensures proper segregation of genetic material between mother and daughter cells during this asymmetric cell division. Though the molecular details differ, cell polarization also underlies the asymmetric cell division of *C. elegans* zygotes and *Drosophila* neuroblasts. In both cases, domains of distinct molecular content form on the cell cortex

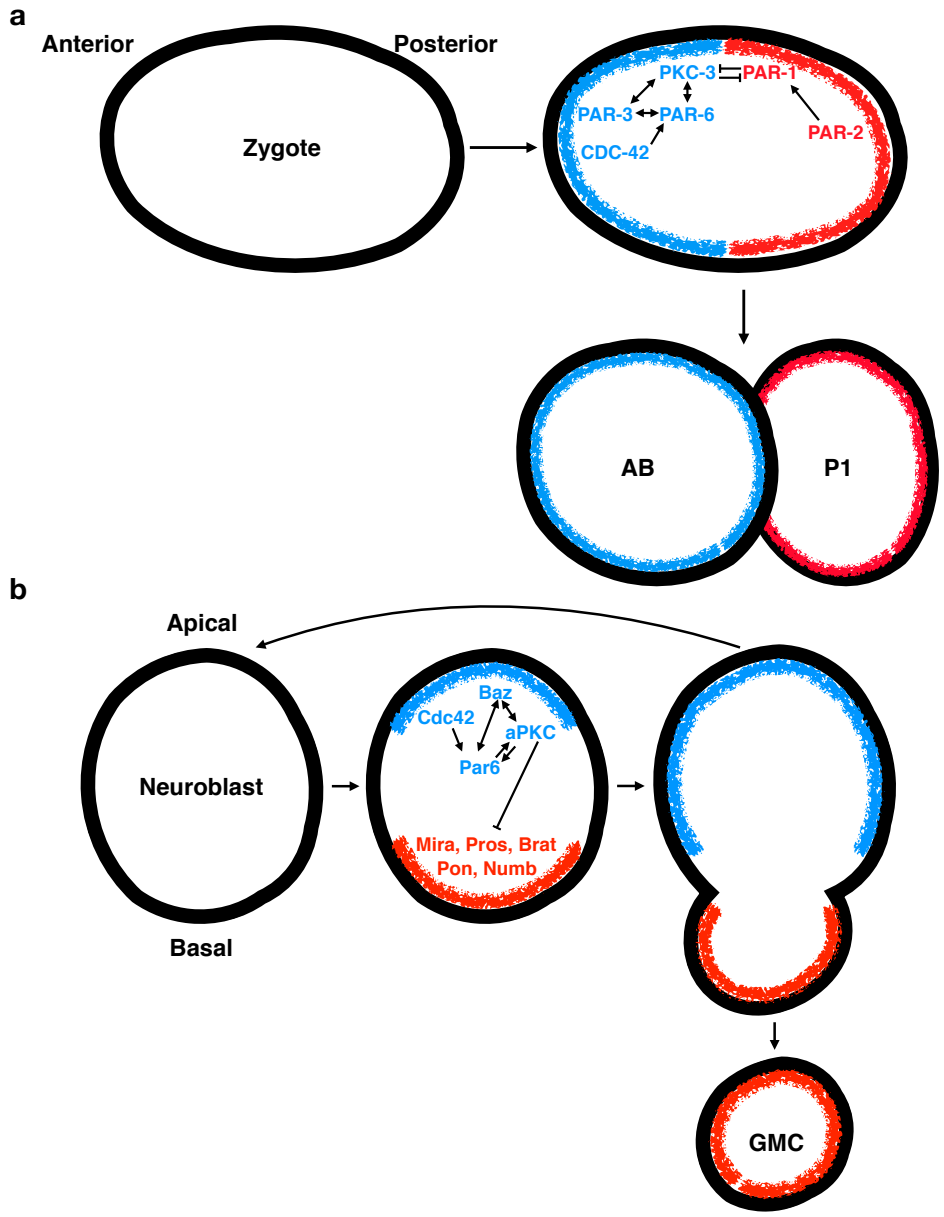

Figure 1.7: **Cortical polarity enables asymmetric cell division in the *Drosophila* neuroblast and *C. elegans* zygote.** a) *C. elegans* zygotes undergo an asymmetric cell division to generate an anterior AB cell and a posterior P1 cell. Two complementary PAR domains form in C. elegans: anterior PARs (blue) and posterior PARs (red).
b) *Drosophila* neuroblasts undergo an asymmetric cell division that generates a self-renewing neuroblast and a differentiating ganglion mother cell. PAR proteins form an apical crescent (blue), excluding cell fate determinants and their adaptor proteins (red) from the apical cortex and relegating them to the basal cortex.

prior to division, and this cortical polarization ensures the asymmetric segregation of cell fate determinants between daughter cells.

A core set of proteins, the PAR proteins, underlies asymmetric cell division by mediating cell polarization in diverse organisms and cell types. This group of proteins includes Bazooka (Baz)/PAR-3, aPKC/PKC-3, Par6, Cdc42, Par1, Par2, and Lgl (Table 1.1). PARs were initially discovered in *C. elegans* as proteins required for asymmetric cell division and were later shown to be conserved throughout metazoa, where they mediate cell polarity and are implicated in tumor formation [Gotta et al., 2001, Jantsch-Plunger et al., 2000, Tabuse et al., 1998, Watts et al., 1996, Guo and Kemphues, 1995, Etemad-Moghadam et al., 1995, Kemphues et al., 1988, Gateff, 1978]

Apical/Anterior	**Basal/Posterior**
Drosophila/*C. elegans*/Mammals	*Drosophila*/*C. elegans*/Mammals
Bazooka(Baz)/PAR-3/Par3	Par1/PAR-1/Par1
Par6/PAR-6/Par6	/PAR-2/
aPKC/PKC-3/aPKC	Lgl/LGL-1/Lgl
Cdc42/CDC-42/Cdc42	

Table 1.1: **PAR proteins**

The interactions among PAR proteins have been extensively studied in a variety of model organisms, cell types, and in vitro assays (Figure 1.8). Par3/Baz is a large, multi-domain protein that exhibits a variety of interactions with other PAR proteins. Par3/Baz has three PDZ domains. PDZ1 of Par3/Baz interacts with Par6's PDZ domain in mammalian tissue culture, *Drosophila* embryos, and *C. elegans* zygotes [Renschler et al., 2018, Morais-de Sa et al., 2010, Li et al., 2010b, Lin et al., 2000, Joberty et al., 2000]. However, disrupting this PDZ-PDZ interaction does not compromise the polarization of PAR-6 in the *C. elegans* zygote, suggesting that this interaction is either not important for PAR protein polarization *in vivo* or that it acts redundantly with other PAR protein interactions [Li et al., 2010b].

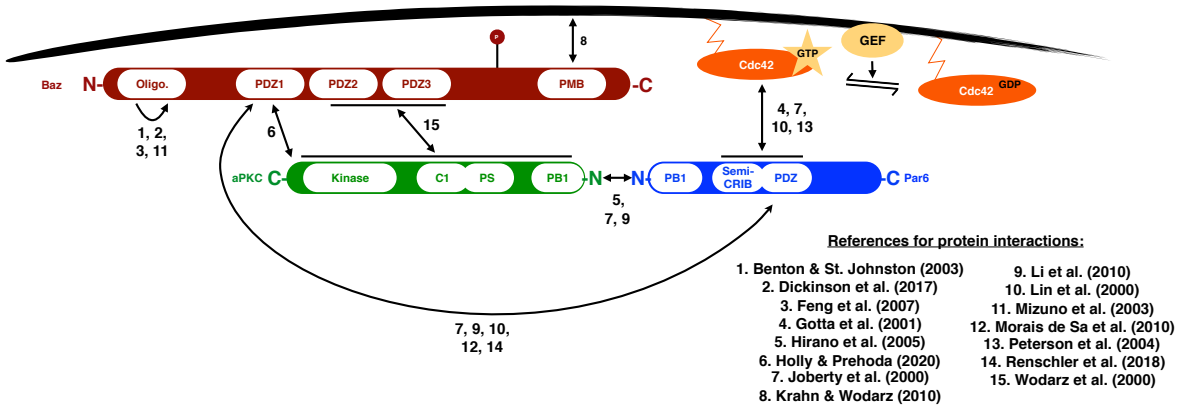

Figure 1.8: **Known PAR protein interactions.** Schematic of anterior/apical PAR proteins. Identified protein-protein interactions are indicated. Numbers indicate references that identified the interaction.

PDZ2 and PDZ3 of Par3/Baz interact with aPKC in *Drosophila* tissue culture [Wodarz et al., 2000], and recent work demonstrated that PDZ2 of Baz interacts with a C-terminal PDZ binding motif in aPKC [Holly et al., 2020].

In addition to interacting with other PAR proteins, Baz self-oligomerizes through an N-terminal domain [Dickinson et al., 2017, Li et al., 2010a, Feng et al., 2007, Mizuno et al., 2003, Benton and St Johnston, 2003a] and binds PIP3 [PtdIns(3,4,5)P3] through a C-terminal stretch of 20 amino acids [Krahn et al., 2010]. This ability to cluster at the plasma membrane is consistent with this multi-domain, multi-interaction protein forming a signaling hub at the plasma membrane during cell polarization in a variety of systems.

PAR proteins can interact with one another independent of Par3/Baz. For example, Par6 binds aPKC in vitro, and this interaction is thought to occur primarily through the N-terminal PB1 domains in each protein [Li et al., 2010b, Hirano et al., 2005, Joberty et al., 2000]. The binding of Par6 to aPKC relieves autoinhibition of aPKC [Graybill et al., 2012]. Furthermore, PAR-1 and PAR-2 directly interact, and this interaction promotes the recruitment of PAR-1 to the posterior cortex of the *C. elegans* zygote [Motegi et al., 2011, Boyd et al., 1996].

Unlike the PAR proteins discussed thus far, Cdc42 is conserved in *S. cereivisae* and *S.*

pombe, where it is a critical regulator of cell polarity (Reviewed in [Chiou et al., 2017]). Thus, Cdc42 is likely to play an important role in cell polarization across species. In the context of PAR polarity, Cdc42 binds the semiCRIB-PDZ region of Par6 [Joberty et al., 2000, Lin et al., 2000, Gotta et al., 2001]; this binding event activates the PDZ domain of *Drosophila* Par6 [Peterson et al., 2004].

My thesis work focuses on cell polarity in the context of asymmetric cell division in *Drosophila* neuroblasts. However, work in the *C. elegans* zygote pioneered our understanding of PAR protein polarization and asymmetric cell division. Thus, below I begin with a brief summary of how the above-described PAR proteins polarize in the *C. elegans* zygote, focusing on insights from this model system that inform cell polarization in the *Drosophila* neuroblast. I then review the current model for PAR protein polarization in *Drosophila* neuroblasts. Finally, I articulate areas open for investigation.

1.2.1 PAR protein polarization in the C. elegans zygote

Cell polarization in the *C. elegans* zygote occurs in two phases: Establishment and Maintenance. This polarization event results in two distinct domains of PAR proteins (Figure 1.7a). At the anterior cortex, a PAR domain that includes PKC-3(aPKC), PAR-3(Baz), PAR-6, and CDC-42 forms. At the posterior cortex, a second PAR domain that includes PAR-1 and PAR-2 forms (Reviewed in [Lang and Munro, 2017]). These cortical domains ultimately ensure an asymmetric cell division that segregates the germ plasm, including P-granules, into a posterior P1 cell (Figure 1.7a). The anterior AB cell retains factors that promote the specification of somatic tissue (Reviewed in [Griffin, 2015]).

1.2.1.1 Rho family GTPases and cortical flows play a critical role in the polarization of *C. elegans* zygotes

Just after fertilization, anterior PAR proteins, including PAR-3, PAR-6, and PKC-3, localize uniformly to the plasma membrane of the *C. elegans* zygote [Cowan and Hyman, 2007, Hung and Kemphues, 1999]. Myosin is also uniformly cortical [Munro et al., 2004]. Approximately 30 minutes after fertilization, cortical actomyosin contractility is locally inhibited around the site of sperm entry [Munro et al., 2004]. This leads to RHO-1- and myosin-dependent cortical flows towards the anterior that remove anterior PAR proteins from the posterior cortex and establish polarity in the zygote [Motegi and Sugimoto, 2006, Munro et al., 2004]. The local inhibition of contractility occurs through Aurora A, which is localized at the sperm-derived centrosome and displaces Ect-2, an activator of RHO-1, from the posterior cortex [Kapoor and Kotak, 2019, Klinkert et al., 2019, Zhao et al., 2019, Motegi and Sugimoto, 2006, Cowan and Hyman, 2004].

During the maintenance phase of zygote polarization, CDC-42 acts through MRCK-1 to drive cortical flows and is required to maintain PAR polarization [Sailer et al., 2015, Kumfer et al., 2010, Motegi and Sugimoto, 2006, Aceto et al., 2006, Kay and Hunter, 2001, Jantsch-Plunger et al., 2000]. Strong depletion of CDC-42 disrupts polarity establishment [Schonegg and Hyman, 2006], suggesting CDC-42 may also be required in the establishment phase. Taken together, these data demonstrate that active cortical flows downstream of Rho family GTPases promote the polarization of the *C. elegans* zygote. In addition to driving cortical flows, CDC-42 also promotes the association of PKC-3/Par6 complexes with the cortex [Sailer et al., 2015, Aceto et al., 2006, Gotta et al., 2001].

Notably, PAR proteins still polarize in the absence of cortical flows. The sperm-derived centrosome promotes the cortical association of PAR-2 and PAR-1 with the posterior cortex, independent of its role in generating cortical flows [Motegi et al., 2011, Zonies et al., 2010].

Thus, redundant sperm-derived cues can generate anterior and posterior PAR domains in the *C. elegans* zygote [Tse et al., 2012, Motegi et al., 2011, Zonies et al., 2010].

1.2.1.2 Mutually antagonistic PAR domains maintain polarity in the *C. elegans* zygote

Once polarity is established, inhibitory interactions between anterior and posterior complexes contribute to maintaining this polarity. For example, PKC-3 phosphorylates PAR-1, PAR-2, and LGL-1, preventing them from associating with the anterior cortex [Motegi et al., 2011, Hoege et al., 2010]. Conversely, PAR-1 phosphorylates PAR-3 [Motegi et al., 2011], presumably inhibiting it from self-oligomerizing and associating with the membrane [Sailer et al., 2015, Benton and St Johnston, 2003b]. CHIN-1, a CDC-42 GAP, prevents CDC-42 activity on the posterior zygote cortex during polarity maintenance [Kumfer et al., 2010], and LGL-1 opposes PKC-3 localization at the posterior cortex [Hoege et al., 2010, Beatty et al., 2010]. Collectively, these antagonistic relationships yield multiple polarity circuits that contribute to the robustness of *C. elegans* zygote polarization [Sailer et al., 2015, Beatty et al., 2013].

1.2.1.3 Multiple, dynamic PAR complexes exist during polarization

The cell biology experiments that initially characterized protein localization in wildtype *C. elegans* zygotes reported overlapping signals for PAR-3, PKC-3, PAR-6, and CDC-42 [Hung and Kemphues, 1999, Tabuse et al., 1998, Watts et al., 1996]. These observations were consistent with a model in which anterior PAR proteins exist and act in a single constitutive complex. However, a subsequent study demonstrated that PAR-6/PKC-3 complexes localize to the *C. elegans* zygote cortex independent of PAR-3 when CDC-37, a Hsp90 co-chaperone, is co-depleted [Beers and Kemphues, 2006]. This finding challenges the model that anterior proteins form a single, constitutive complex and suggests that PKC-3/PAR-6 complexes can

associate with the cortex in two distinct manners: via interaction with PAR-3 or with CDC-42. Consistent with this finding, CDC-42 depletion increases PAR-6 clustering in the zygote, while PAR-3 depletion decreases PAR-6 clustering [Rodriguez et al., 2017], confirming that CDC-42 and PAR-3 differentially affect PKC-3/PAR-6 complexes. Furthermore, Rodriguez et al. [2017] developed a version of PKC-3 that is fused to a C1B domain and can be directly recruited to the plasma membrane upon the addition of PMA, even in the absence of PAR-3. Experiments using this C1B-PKC3 fusion demonstrated that PKC-3 is active as a kinase in the absence of PAR-3 but not in the absence of PAR-6 or CDC-42. Taken together, all of these findings strongly support the hypothesis that PKC-3 and PAR-6 form distinct complexes with PAR-3 versus CDC-42, each having differential diffusivities and activities.

1.2.2 PAR polarity underlies asymmetric cell division in Drosophila neuroblasts

Another well-studied example of PAR protein polarization is the *Drosophila* neuroblast. Neuroblasts are the precursors to the embryonic and larval central nervous system. They delaminate from the embryonic ventral neuroectoderm and undergo repeated rounds of asymmetric division along the apicobasal axis to produce a larger, apical, self-renewing neuroblast and a smaller, basal, ganglion mother cell that subsequently differentiates into neurons and glia (Figure 1.7b) [Hartenstein and Wodarz, 2013]. At the end of embryonic neurogenesis, neuroblasts either undergo apoptosis or become quiescent. Quiescent neuroblasts re-enter the cell cycle during early larval development and undergo their characteristic asymmetric divisions to generate the adult nervous system [Hartenstein and Wodarz, 2013].

Polarization of PAR proteins in neuroblasts begins at the onset of mitosis [Wodarz et al., 2000, Schober et al., 1999, Wodarz et al., 1999]. Similar to the anterior PAR proteins in the *C. elegans* embryo, Bazooka(PAR-3), Par6, and aPKC form an apical crescent in the neuroblast. These apically localized polarity proteins exclude cell fate determinants, such

as Numb, Prospero (Pros), and Brain Tumor (Brat), from the apical neuroblast membrane, relegating them into a basal crescent (Figure 1.7b). The adaptor proteins Partner of Numb (Pon) and Miranda (Mira) promote the localization of these cell fate determinants at the plasma membrane. This cortical polarity ensures that, following cytokinesis, an apical, self-renewing neuroblast, and a basal, differentiating ganglion mother cell are generated (Reviewed in [Prehoda, 2009]).

As in the *C. elegans* zygote, antagonistic interactions between PAR proteins do occur in *Drosophila* neuroblasts. For example, in the absence of Lgl, aPKC spreads into the basal domain of the neuroblast cortex and displaces basal Mira from the cortex. However, this phenotype is not completely penetrant [Lee et al., 2006b]. Moreover, PAR-1-mediated phosphorylation of Baz(PAR-3) is not necessary for neuroblast polarization. Par1 does, however, seem to play a role in maintaining the axis of neuroblast polarity [Krahn et al., 2009]. Thus, while antagonistic PAR protein interactions do occur in *Drosophila* neuroblasts, they may not be essential for this polarization process.

1.2.2.1 Neuroblast polarity cues

The point of sperm entry specifies axis of *C. elegans* zygote polarity. In *Drosophila* neuroblasts, the specifier of the polarity axis varies depending on whether the neuroblast exists in the *Drosophila* embryo or larva. In embryonic neuroblasts, the overlying ectoderm is a critical regulator of the polarity axis. Cultured neuroblasts that remain in contact with the overlying epithelium polarize with normal kinetics and exhibit a consistent axis of polarity across many cell divisions [Siegrist and Doe, 2006]. In contrast, cultured neuroblasts that are isolated from all epithelial cells exhibit delayed polarization and a random axis of polarity over repeated mitoses. The inducing signal from the overlying ectoderm requires expression of the G protein coupled receptor (Tre1) in the neuroblast [Yoshiura et al., 2012]. Tre1 acts through the G protein Goα, which recruits Pins, a protein known to interact with the mitotic

spindle (see below for Pins) [Yoshiura et al., 2012].

In larval neuroblasts, centrioles play a major role in specifiying the axis of polarity. Unlike embryonic neuroblasts, not all larval neuroblasts remain in contact with an overlying epithelium [Egger et al., 2008]. However, larval neuroblasts still maintain their axis of polarity through subsequent divisions via a mechanism that requires centrioles [Januschke and Gonzalez, 2010]. Thus, in both the *C. elegans* zygote and larval *Drosophila* neuroblasts, centrioles/centrosomes are key regulators of symmetry breaking. However, centrioles likely act through distinct PAR proteins in the *C. elegans* zygote and the *Drosophila* neuroblast, as Par1 is not required for proper neuroblast polarization [Krahn et al., 2009]. Work in the *Drosophila* embryonic epithelium has identified a positive feedback mechanism between Baz and centrioles [Jiang et al., 2015], and it is intriguing to speculate that centrioles play a similar role in promoting Baz accumulation in neuroblasts. More recent work has also shown that the ganglion mother cell (GMC) from the previous neuroblast division also plays a role in specifying the axis of neuroblast polarity in larval neuroblasts: Ablation of the most recently born GMC increases the randomness of the division axis [Loyer and Januschke, 2018].

1.2.2.2 aPKC is a key player in neuroblast polarization

Downstream of initiation, aPKC is the linchpin in current models of neuroblast polarization. It localizes to the apical cortex downstream of Baz and phosphorylates basal factors, such as Mira and Numb, antagonizing their association with the apical cortex [Atwood and Prehoda, 2009, Smith et al., 2007, Rolls et al., 2003]. Despite the central role of aPKC in neuroblast polarization, it is still unclear whether aPKC kinase activity itself can instruct polarization in this cell type. Furthermore, the possibility that aPKC activity is controlled by the cell cycle has not been fully explored. Work in *Drosophila* neuroblasts and sensory organ precursors found that Aurora A phosphorylation of Par6 activates the aPKC/Par6 complex such that

it can phosphorylate and release Lgl. In turn, this activated aPKC/Par6 complex can form a new complex with Baz [Wirtz-Peitz et al., 2008]. Aurora A kinase is activated at the onset of mitosis [Crane et al., 2004, Bischoff et al., 1998, Glover et al., 1995], so these data raise the possibility that aPKC's kinase activity may be tied to the neuroblast cell cycle. Experiments that directly assess the ability of aPKC to manipulate basal factor localization in intact neuroblasts will be needed to directly test this hypothesis.

1.2.2.3 The role of Rho family GTPases during neuroblast polarization is unclear

Unlike in the *C. elegans* zygote, the role of Rho family GTPases during neuroblast polarization is not well understood. Neuroblasts lacking Cdc42 fail to polarize aPKC or Par6 and exhibit uniformly cortical Mira. Thus, Cdc42 contributes to aPKC activity. This function of Cdc42 is likely indirect through Par6, as Cdc42 binding directly affects the structure of Par6's semiCRIB domain [Peterson et al., 2004], and disrupting Par6's ability to bind Cdc42 precludes Par6 from associating with the cortex. However, modulating aPKC's kinase activity may not be the only role of Cdc42 during neuroblast polarization. When and where Cdc42 is active during neuroblast polarization has not been determined. Furthermore, the possibility that Cdc42 plays an instructive role in neuroblast polarity crescent formation has not been tested.

1.2.2.4 Linking cortical polarity to the mitotic spindle

Downstream of PAR protein polarization, the mitotic spindle must be oriented with cortical polarity to ensure proper positioning of the cleavage furrow and segregation of cell fate determinants. In neuroblasts, the linking of apical polarity and spindle position occurs through Inscuetable (Insc). Insc forms an apical crescent in mitotic neuroblasts, coincident with the Baz/aPKC/Par6 crescent. Loss of Insc leads to randomization of the mitotic

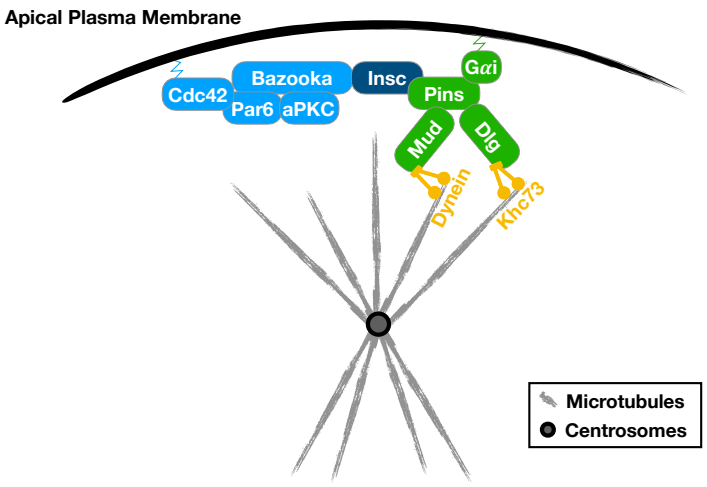

Figure 1.9: **Inscuteable and Pins links apical cortical polarity with the spindle in *Drosophila* neuroblasts.** Inscuteable binds both apical polarity proteins (light blue) and Pins (green). Pins interacts with Gαi, Dlg, and Mud. Dlg and Mud, in turn, interact with two microtbule binding motors: Khc73 and Dynein, respectively. These motor proteins exert pulling forces on aster microtubules to orient the spindle with the apical polarity crescent. (Adapted from [Siller and Doe, 2009].)

spindle relative to cortical polarity [Kraut et al., 1996]. Insc localizes downstream of Baz [Wodarz et al., 1999] and binds directly to Pins [Schaefer et al., 2000], a TPR/GoLoco domain containing protein that regulates G-proteins [Yu et al., 2000]. Pins crescents form in the absence of Insc expression, but Insc is required for Pins directed spindle orientation to be coupled to cortical polarity [Siegrist and Doe, 2005]. Once at the cortex, Pins interacts with Gαi, Mud (NuMA), and Dlg to orient the microtubules of the mitotic spindle with the apical polarity crescent (Figure 1.9) [Nipper et al., 2007, Izumi et al., 2006, Siller et al., 2006, Bowman et al., 2006, Siegrist and Doe, 2005].

1.2.3 Open Questions

The two examples presented above demonstrate that PAR protein polarization is a dynamic process. The dynamic nature of this process is best understood in the context of *C. elegans* zygote polarization, due in large part to pioneering live imaging studies and image analysis

[Dickinson et al., 2017, Rodriguez et al., 2017, Robin et al., 2014, Munro et al., 2004]. A complete understanding of cell polarization, especially in the *Drosophila* neuroblast, will require tools that can both assay protein activity and localization in real time as well as modulate protein activity with high spatiotemporal resolution. Specific areas open for further investigation are highlighted below.

Do cortical flows contribute to neuroblast polarization?

Although not strictly essential, RHO-1- and CDC-42-mediated cortical flows contribute to efficient polarization of the *C. elegans* zygote [Motegi et al., 2011, Kumfer et al., 2010, Munro et al., 2004]. To date, cortical flows have not been implicated in *Drosophila* neuroblast polarization. However, recent work offers a dynamic picture of PAR proteins during neuroblast polarization, reminiscent of PAR protein behavior during *C. elegans* zygote polarization. Live imaging of aPKC-GFP shows that aPKC first forms punctae on the apical cortex early in mitosis. These punctae coalesce in an apical cap by metaphase and subsquently flow toward the cleavage furrow later in mitosis [Oon and Prehoda, 2019]. Similar behavior for Baz, aPKC, and Par6 has been observed in *Drosophila* tissue culture [Kono et al., 2019]. Live imaging of Mira-mCherry, expressed at near endogenous levels, revealed that this basal factor also exhibits dynamic localization throughout the neuroblast cell cycle. Specifically, Mira is uniformly cortical during interphase, displaces completely from apical cortex upon mitotic entry, and accumulates in a strong basal crescent after nuclear envelope breakdown [Hannaford et al., 2018]. Actin is required for both the aPKC and Mira dynamics observed in neuroblasts [Oon and Prehoda, 2019, Hannaford et al., 2018]. Thus, cortical flows may play a previously unappreciated role in neuroblast polarization. Consistent with this possibility, myosin flows have been observed in the context of neuroblast cytokinesis, and they contribute to cleavage furrow positioning in the *Drosophila* neuroblast [Roubinet et al., 2017].

What factors are sufficient to instruct neuroblast polarization?

CDC-42 activity plays key roles in the polarization of *S. cerevisiae* and the *C. elegans* zygote, and optogenetic experiments have demonstrated that Cdc42 activity is sufficient to specify bud site selection in *S. cerevisae* [Witte et al., 2017]. Despite the high conservation of Cdc42 from yeast to flies to mammals, the role of Cdc42 in *Drosophila* neuroblast polarization remains unclear. In part, this is due to the lack of an activity sensor for Cdc42 in *Drosophila*. Additionally, approaches that can precisely manipulate Cdc42 in an *in vivo* context would shed light on the ability of Cdc42 to initiate polarization in this system.

Additionally, it remains to be tested whether aPKC is sufficient to polarize a *Drosophila* neuroblast. Overexpression of aPKC-CAAX, which is constitutively on the neuroblast membrane, prevents basal factors from associating with the neuroblast cortex. However, can an acute, subcellular focus of aPKC initiate an "apical" polarity crescent or disrupt an already formed crescent of basal factors?

1.3 Optogenetics: A method for subcellular control of protein activity

Making progress on the open questions discussed above, in both actomyosin-mediated tissue morphogenesis and PAR protein-mediated polarization, will require moving beyond identifying the genetic requirements for these processes and towards determining when and where polarity factors act during these processes. Moreover, answering these open questions will necessitate acutely and specifically manipulating polarity factor activity in space and time.

Toward this end, chemically-inducible dimers demonstrated the feasibility of controlling protein activity with temporal precision. One iteration of this approach utilized FRB and FKBP, which dimerize in the presence of rapamycin, to recruit constitutively active GTPases, dominant negative GTPases, and GEF domains to the plasma membrane. This afforded acute activation or inhibition of signaling downstream of the recruited GTPases [Inoue et al., 2005]. Despite the temporal precision afforded by chemically inducible dimers,

these systems do not offer spatial precision nor are they reversible. In contrast to a chemical stimulus, which must be delivered to the entire cell, a light stimulus can be delievered with subcellular precision. Furthermore, light stimuli can be removed by simply turning off the light. Thus, optogenetic approaches, which use light to reversibly manipulate protein localization and/or activity with high spatiotemporal precision, are ideally-suited to answering the open questions about morphogenesis and polarization posed above.

1.3.1 Light sensitive channels revolutionized neuroscience

The first generation of optogenetic tools were applied in neuroscience. One early iteration involved ectopically expressing photocaged agonists as well as ligand-gated ion channels that could be stimulated by these agonists in cultured neurons. This enabled temporally precise activation of these neurons [Zemelman et al., 2003]. This approach was subsequently adapted for use in *Drosophila*, where optogenetic stimulation of distinct neurons, via uncaging of the photocaged agonist, elicited a variety of behaviors specific to the neuron type stimulated, including jumping and flying [Lima and Miesenbock, 2005]. These experiments in *Drosophila* required the generation of transgenic flies that express the photocaged agonist-responsive ion channels as well as microinjection of the photocaged agonist into *Drosophila* tissue.

A technically simpler iteration of this approach was made possible by the discovery of Channelrhodopsin2 (ChR2), a cation-selective channel that is directly stimulated by light (Figure 1.10a) [Nagel et al., 2003]. Subsequent work demonstrated excitatory and inhibitory synaptic events could be induced in a light-dependent manner in cultured neurons expressing ChR2 [Boyden et al., 2005]. Importantly, this approach required expression of a single, light-sensitive transgene. Subsequent applications of this optogenetic approach enabled the precise mapping of neuronal circuits in mammalian brains [Zhang et al., 2010, Gradinaru et al., 2009]. As a result of these and many other informative experiments, optogenetic tools are now integral to the neurobiology experimental toolkit. Optogenetics promises to

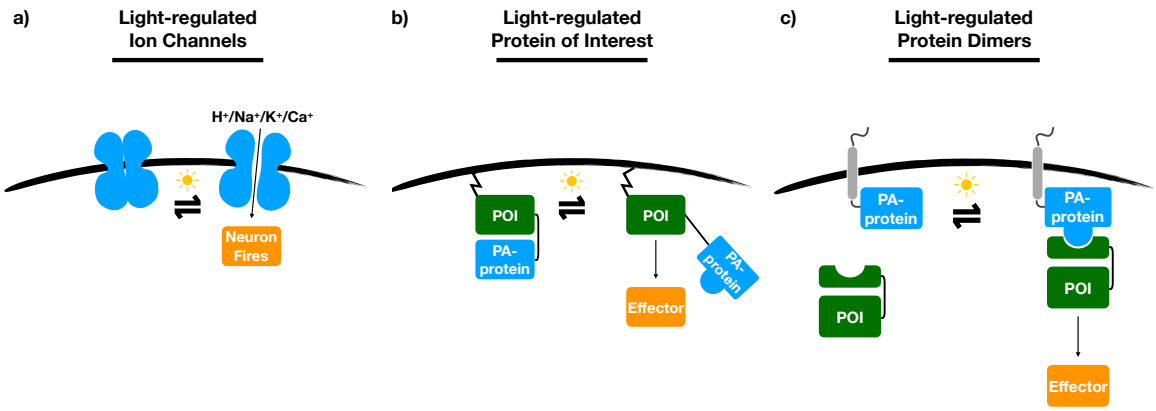

Figure 1.10: **General approaches to optogenetic control of protein activity.** a) Light-regulated ion channels, often used in neurobiology, open in response to light and permit the entry of ions into neurons, ultimately inducing the neurons to fire. b) Light-regulated proteins comprise a protein of interest (POI) fused to a light-sensitive protein or domain (PA-protein). Photoactivation of the fusion protein releases the protein of interest, allowing it to activate or inhibit effectors. c) Light-regulated dimers utilize a naturally occurring or engineered pair of dimers that specifically interact in the presence of light. Fusion of a protein of interest to one of dimers allows the protein of interest to be recruited to a specified location upon photoactivation where it can subsequently activate its effectors.

be similarly transformative for cell and developmental biology.

1.3.2 Optogenetic approaches adapted for cell biology

Outside of neuroscience, few biological processes can be controlled by light-sensitive ion channels. Moreover, like chemically inducible dimers, light-sensitive ion channels fail to provide researchers with subcellular spatial control over perturbations. Thus, realizing the promise of optogenetics in non-neuronal cells necessitated further adaptation of photosensitive proteins such that they could control protein activation with high temporal and spatial precision.

Towards this end, a host of photosensitive proteins and domains have been adapted for optogenetic purposes, including phytochromes, cryptochromes, and LOV domains. Phytochromes and cryptochromes are photoreceptors originally identified for their role in regulating plant growth [Guo et al., 1998, Ahmad and Cashmore, 1993, Quail, 1991]. The light oxygen voltage (LOV2) domain is a photosensitive domain derived from a flavoprotein

photoreceptor that also regulates phototropism in plants [Christie et al., 1998, Liscum and Briggs, 1995].

The photochemistry of these proteins and domains has been extensively studied. Phytochromes covalently associate with tetrapyrrole chromophores, such as phycocyanobilin (PCB) [Quail, 2002]. Once bound to a phytochrome, the chromophore undergoes a conformational change in response to a red light stimulus, allowing the phytochrome to interact with a phytochrome interacting factor [Quail, 2002]. This red light-induced conformational change is stable, but can be reversed by a far-red light stimulus [Ni et al., 1999]. In contrast to phytochromes, cryptochromes and LOV domains undergo conformational changes in response to a blue light stimulus [Liu et al., 2008, Christie et al., 1998]. Upon photoactivation, Cryptochrome2 (CRY2) interacts with its cognate binding partner, Cryptochrome-interacting basic-helix-loop-helix (CIB1) [Liu et al., 2008]. Photoactivation of AsLOV2 induces a conformational change that releases and unfolds its C-terminal Jα helix [Harper et al., 2003].

One successful, early application of optogenetic technology to cell biology was the generation of photoactivatable Rac1 (PA-Rac1) [Wu et al., 2009]. Constitutively active Rac1 was directly fused to the photosensitive LOV domain, such that the LOV domain inhibited Rac1 activity in the dark (Figure 1.10b). Photoactivation of this fusion protein induces a conformational change in LOV, permitting Rac1 activity. PA-Rac1 controlled protrusion formation and directed cell migration. Despite the attractiveness of this single component optogenetic approach, direct fusion of photosensitive proteins to proteins of interest has not been widely successful.

A more generalizable approach to light-regulated protein activity has been light-inducible dimerization (Figure 1.10c). These techniques build on the utility of chemically-inducible dimers, which afford temporal but not spatial control over protein activity. Several groups have adapted naturally occuring light-inducible dimers for use in cell biology. For example,

localizing the photosensitive PhytochromeB (PhyB) to the plasma membrane and fusing PIF, the binding partner of PhyB, to Rac1- or Cdc42-specific GEFs, enabled control of Cdc42 or Rac1 activity with light in NIH3T3 cells. Notably, optogenetic Rac1 or Cdc42 activity induced lamellopodia formation [Levskaya et al., 2009]. The light-sensitive Phy/PIF interaction has been further adapted to control membrane recruitment of SOS, a RasGEF that acts upstream of ERK signaling [Toettcher et al., 2013]. Combining this PIF-SOS system with careful titrations of activating light demonstrated that different thresholds of ERK signaling yield distinct outputs.

In parallel, a second light inducible dimer system, based on the photosensitive LOV domain, was developed [Yazawa et al., 2009]. In this system, FKF1, which contains a LOV domain, was fused to constitutively active Rac1, and its binding partner, GIGANTEA, was fused to the plasma membrane. Blue light activation induced recruitment of constitutively active Rac1 to the membrane and lamellipodia formation in mammalian tissue culture cells [Yazawa et al., 2009]. Notably, this optogenetic system uses a large photosensory protein (1173 amino acids) and exhibits slow photoactivation (several minutes) and recovery (hours) kinetics [Yazawa et al., 2009]. In addition to this LOV-domain based approach, photosensitive CRY2, a cryptochrome, and CIB1, the binding partner of CRY2, were used in tissue culture cells to control transcription in a light-dependent manner [Kennedy et al., 2010].

In contrast to the light-inducible dimers discussed above, which rely on evolutionarily tuned light-dependent interactions, Tunable Light-inducible Dimerization Tags (TULIPs) utilizes an engineered light-dependent dimer [Strickland et al., 2012]. In this system, the Jα helix of the LOV2 domain is fused to an engineered peptide epitope, which docks against the LOV domain in the dark. Upon photoactivation, LOV2 undergoes a conformational change which releases the Jα helix and allows the fused peptide epitope to bind an engineered PDZ domain. This system was first used in budding yeast to demonstrate that recruitment of Ste5, a scaffold, or Ste11, a kinase, could stimulate the MAPK pathway and activate the

budding yeast mating pathway in the absense of α-factor, the ligand that normally activates this pathway. In the same study, TULIPs was also used to show that recruitment of Cdc24, a Cdc42 GEF, to a region on the budding yeast cortex was sufficient to specify the orientation of a mating projection. Importantly, unlike the Phy/PIF system, light-dependent dimerization in TULIPs does not require the addition of an external chromophore, such as phycocyanobilin (PCB). Furthermore, the photosenitive LOV domain is much smaller (approximately 125 amino acids) than the photosensitive protein, FKF1 (>1000 amino acids), used in the previously mentioned LOV-domain based optogenetic system [Strickland et al., 2012, Yazawa et al., 2009]. The LOV2 domain has also been fused to the bacterial SsrA peptide such that it recruits SspB fusion proteins upon photoactivation [Guntas et al., 2015, Levskaya et al., 2009].

More recent optogenetic experiments expanded upon the initial application of TULIPs and demonstrated that the recruitment of both Cdc24, a Cdc42 GEF, as well as Bem1, a scaffolding protein, could induce symmetry breaking and bud site formation in *S. cerevisiae* [Witte et al., 2017]. Unexpectedly, the ability of Bem1, but not Cdc24, to generate active Cdc42 is dependent on Cdk1 activation. Adaptation of TULIPs to control RhoA in mammalian tissue culture revealed that RhoA is sufficient to initiate contractile ring formation independent of spindle positioning and cell cycle cues, suggesting any negative regulation that specifies cleavage furrow positioning in normal cytokinesis acts upstream of RhoA activity [Wagner and Glotzer, 2016]. Thus, the spatiotemporal precision afforded by TULIPs enabled the detection of a new regulatory step in *S. cerevisiae* bud site selection as well as a better understanding of the mechanisms regulating cleavage furrow formation in mammalian cells. The insights gained from the TULIPs and Phy/PIF experiments mentioned above demonstrate that GTPase activity via light-sensitive GEF recruitment is particularly amenable to optogenetic manipulation [Toettcher et al., 2013, Strickland et al., 2012].

In addition to using optogenetics to control protein recruitment to the plasma membrane,

a variety of approaches have exploited the ability of optogenetics to drive light-dependent protein oligomerization. For example, signaling downstream of FGFR, PDGRF, Integrins, and β-catenin have all been optogenetically induced in tissue culture [Dine et al., 2018, Bugaj et al., 2015, Grusch et al., 2014, Kim et al., 2014, Bugaj et al., 2013]. Additionally, a system for light-induced protein sequestration has been developed (LARIAT, [Lee et al., 2014]), and a method to sequester and release proteins of interest in the dark versus light, respectively exists (LOVTRAP, [Wang et al., 2016]) . While these and other specific optogenetic approaches have merit, they are beyond the scope of this discussion.

1.3.3 Application of optogenetic tools to developmental cell biology

1.3.3.1 Optogenetic dissection of cell fate specification

The extensive optogenetic experiments performed to date in cell culture and yeast demonstrate the power of these approaches to probe cell biological processes in space and time. These tools are now being applied to questions in developmental cell biology. One particularly fruitful application has been optogenetically controlling signaling pathways to understand how their activity over time is integrated into cell fate specification. For example, optogenetic control of ERK signaling, via light-mediated recruitment of the GEF SOS, determined the developmental window in which *Drosophila* embryos are sensitive to elevated ERK signaling. Moreover, because the amount of ERK activation could be titrated through light dosage, this approach proved that the cumulative load, rather than the absolute duration, of ERK signaling instructs cell fate decisions in the *Drosophila* embryo [Johnson and Toettcher, 2019, Johnson et al., 2017]. In a separate study, optogenetic inactivation of the transcription factor Bicoid enabled the determination of when Bicoid acts during embryonic patterning in the *Drosophila* embryo [Huang et al., 2017]. The authors found that anterior gap genes require functional Bicoid protein for a longer time than posterior gap genes, indicating that Bicoid's window of action differs depending on the specific gene target.

Optogenetic approaches have also been used to interrogate signaling dynamics in zebrafish, including the development of a light-inducible Nodal receptor [Sako et al., 2016]. Application of this probe revealed that while optogenetic activation of the Nodal receptor for two hours induced high expression of *sox17*, a marker of endodermal fate, longer activation of the Nodal receptor for three hours yields low levels of *sox17* expression. Subsequent experiments showed that these different outcomes arise because optogenetic activation of the Nodal receptor for three hour upregulates *goosecoid*, a repressor of endodermal fate and *sox17* expression. Thus, the temporal precision of optogenetically induced Nodal signaling demonstrated that the duration of Nodal signaling is important to distinguish between cell fate types, such as endoderm and prechordal plate progenitors. The ability to acutely turn these proteins on or off with light, rather than chronic genetic ablation or overexpression, was critical to the biological insights described above.

1.3.3.2 Optogenetic control of Rho family GTPases during development

In addition to probing cell fate decisions, optogenetic control of Rho family GTPase activity has informed our understanding of the role of these small GTPases during organismal development. For example, expression of photoactivatable Rac1 (PA-Rac1 [Wu et al., 2009]) in *Drosophila* border cells, which form the micropylar channel, revealed that Rac1 activation is sufficient to instruct the collective migration direction of border cells in the *Drosophila* ovary [Wang et al., 2010]. Moreover, Rac1 activation in a single border cell increased protrusion formation in the activated cell, while simultaneously suppressing protrusion formation in neighboring border cells. Thus, this optogenetic approach revealed that protrusive behavior is coordinated among border cells during their collective migration [Wang et al., 2010]. Further optogenetic experiments showed that myosin activity is necessary for down regulating protrusive activity outside of the Rac1 activation zone [Mishra et al., 2019] and that this intercellular communication requires E-cadherin [Cai et al., 2014].

Recently, an optogenetic system for controlling Rho1 activity in the early *Drosophila* embryo has been developed. This system comprises a membrane localized CIB domain and a recruitable, photosensitive CRY2 fused to RhoGEF2, a Rho1-specific GEF [Izquierdo et al., 2018]. Use of this system in the newly cellularized *Drosophila* embryo showed that Rho1 activity is sufficient to induce ectopic invaginations in the dorsal *Drosophila* embryonic epithelium. Intriguingly, certain optogenetic activation protocols induced pulsatile Rho1 activity in these embryos, suggesting that this epithelium may exhibit an intrinsic ability to respond to Rho1 activation with sustained, pulsatile Rho1 activity. However, the period of these pulses did not change over a variety of activation protocols, and it was much longer than the periodity seen in endogenous ventral furrow cells [Xie and Martin, 2015]. Furthermore, experiments presented in Chapter 2 of this thesis show that pulsatile Rho1 activity is not always an outcome of Rho1 activation in the embryonic epithelium. Nevertheless, these experiments establish the feasibility of modulating actomyosin contractility in intact tissues [Izquierdo et al., 2018]. Subsequent experiments used this probe to demonstrate that myosin at the basal surface of cells, which plays a role in completing cellularization in the *Drosophila* embryo, must be removed to allow for ventral furrow formation, the next step in development [Krueger et al., 2018].

More recently, this probe that activates Rho1 was used to directly interrogate the actin cytoskeleton during *Drosophila* cellularization [Krueger et al., 2019]. Previous work had shown that during the slow phase of cellularization in the *Drosophila* embryo, actin filaments exist in hexagonal arrays [Schejter and Wieschaus, 1993]. Later in cellularization, these hexaongal structures reorganize into more compact actin rings that eventually contract to complete cellularization [Royou et al., 2004, Thomas and Wieschaus, 2004, Schejter and Wieschaus, 1993]. Interestingly, the hexagonal actin structures observed in the slow phase of cellularization are refractory to optogenetic activation of Rho1, while the contraction of the ring like actin structures is accelerated by optogenetic activation of Rho1 [Krueger et al.,

2019]. Follow up genetic experiments showed that this differential sensitivity to ectopic Rho1 activation likely arises from differential organization of actin at these two time points. Bottleneck and two actin crosslinkers, Fimbrin and Filamin, mediate this actin network organization. This work demonstrates that optogenetic approaches are well suited to probe the underlying mechanical states of actomyosin networks.

1.3.3.3 Optogenetic probes provide definitive proof for longstanding models in developmental biology

Because they can acutely probe signaling pathways and activate proteins with subcellular precision, optogenetic approaches are well-suited to test existing molecular models. One such example is the testing of the molecular model for nuclei dispersion in the syncytial *Drosophila* embryo. For the roughly three hours between fertilization and ventral furrow formation, the *Drosophila* embryo exists as a syncytium, with all nuclei sharing a common cytoplasm. At the earliest nuclear cycles, these nuclei exist in a cluster in the common cytoplasm. During subsequent nuclear cycles, the nuclei spread out and become uniformly localized around the cortex of the syncytium [Foe and Alberts, 1983]. It has long been suggested that cytoplasmic flows driven by rearrangement of the actin and/or myosin cytoskeleton are the driving force for nuclei dispersion [Royou et al., 2002, von Dassow and Schubiger, 1994]. More recent experiments identified that localized PP1 phosphatase activity regulates cortical myosin accumulation during this phase of *Drosophila* embryonic development [Deneke et al., 2019]. Furthermore, this work suggested that contraction of these PP1-mediated myosin gradients induced cytoplasmic flow to disperse nuclei. Deneke et al. [2019] directly tested this model by using the above-discussed CRY2/CIB optogenetic probe to activate Rho1 and myosin in the early syncytial embryo. Uniform optogenetic activation of Rho1 prior to nuclei dispersion disrupted cytoplasmic flows and prevented dispersion of the nuclei. Alternatively, optogenetic activation of myosin contraction in one pole of the embryo induced nuclei to

accumulate in the opposite pole, proving that asymmetric myosin contraction at the cortex drives cytoplasmic flows and nuclei dispersion in the syncytial embryo.

Prior to the formation of the syncytial embryo and nuclei dispersion discussed above, the anterior-posterior axis of the *Drosophila* embryo is specified. Accumulation of oskar mRNA determines the posterior pole of the eventual *Drosophila* embryo during oogenesis (Reviewed in [van Eeden and St Johnston, 1999, Lasko, 1999]). Both kinesin-1, a plus end director motor, and Myosin-V, along with their respective cytoskeletal tracks, microtubules and actin, are required for proper localization of oskar mRNA [Krauss et al., 2009, Cha et al., 2002, Palacios and St Johnston, 2002, Brendza et al., 2000]. One model for oskar mRNA localization is that myosin-V and kinesin-1 compete in a molecular tug of war: Kinesin-1, walking along microtubules, displaces oskar mRNA where microtubule density is high in the anterior and lateral oocyte cortex. In contrast, myosin-V outcompetes kinesin-1 to anchor oskar mRNA in the posterior cortex, where actin exists and microtubule density is much lower [Lu et al., 2020]. Striking support for this model was provided by the generation and use of optogenetically recruitable spastin (Klp10A), which depolymerizes microtubules. Optogenetically-induced microtubule depolymerization led to ectopic accumulation of Staufen, a proxy for oskar mRNA localization, even at the lateral cortex [Lu et al., 2020]. Collectively, these two examples demonstrate the power of precise optogenetic experiments to directly test molecular mechanisms underlying developmental events.

1.3.3.4 Optogenetic manipulation of polarity within tissues

The application of optogenetics to cell polarization within tissues is less extensive than the other processes discussed thus far. However, work in zebrafish demonstrates the plausibility of manipulating cell polarity in the context of tissues [Buckley et al., 2016]. Specifically, a Phy/PIF approach was used to generate a subcellular domain of Pard3 (Par3) in zebrafish neuroepithelial cells. Par6 colocalizes with this optogenetically induced domain of Pard3.

Moreover, performing these experiments in mitotic neuroepithelial cells forced an asymmetric division, where one daughter cell inherited more Pard3 than the other. The functional consequences of this ectopic asymmetric cell division were not investigated.

1.3.3.5 Generating force via optogenetics

A final noteworthy application of optogenetics in development is a technique to modulate spindle positioning in the *C. elegans* zygote. As discussed above, the factors that connect cortical polarity to spindle positioning during asymmetric cell division are known; they include LGN/Pins/GPR1/2, NuMA/Mud/Lin5, and dynein. Optogenetically-induced membrane recruitment of two of these spindle orientation factors, GPR1/2 or Lin5, exerts pulling forces on the mitotic spindle in the *C. elegans* zygote [Fielmich et al., 2018]. Importantly, recruitment of Lin5 exerts pulling forces on the mitotic spindle even in the absence of GPR1/2. Thus, this work shows that factors acting upstream of Lin5 primarily act to localize Lin5 rather than physically modulate the mitotic spindle. Related optogentic experiments in human tissue culture cells also found that optogenetically recruited NuMA can exert pulling forces on the mitotic spindle [Okumura et al., 2018]. Moreover, this work demonstrates that optogenetic probes can be used to apply physical forces in addition to controlling local protein activity.

1.4 Summary

In summary, the works highlighted above demonstrate that optogenetic approaches afford acute spatial and temporal control over protein activity, often with subcellular precision. A pioneering round of experiments demonstrated the promise and practicality of applying optogenetic approaches to outstanding questions in cell and developmental biology. In the following chapters, I describe the adaptation of LOV domain-based optogenetic probes for controlling Rho1 and Cdc42 activity during *Drosophila* development. I also briefly discuss the

optogenetic manipulation of other polarity factors, including aPKC and Baz(Par3). Moreover, I document my progress in applying these probes to the open questions emphasized above.

CHAPTER 2

RHO1 ACTIVATION RECAPITULATES EARLY GASTRULATION EVENTS IN THE VENTRAL, BUT NOT DORSAL, EPITHELIUM OF *DROSOPHILA* EMBRYOS

2.1 Abstract

Ventral furrow formation, the first step in *Drosophila* gastrulation, is a well-studied example of tissue morphogenesis. Rho1 is highly active in a subset of ventral cells and is required for this morphogenetic event. However, it is unclear whether spatially patterned Rho1 activity alone is sufficient to recapitulate all aspects of this morphogenetic event, including anisotropic apical constriction and coordinated cell movements. Here, using an optogenetic probe that rapidly and robustly activates Rho1 in *Drosophila* tissues, we show that Rho1 activity induces ectopic deformations in the dorsal and ventral epithelia of *Drosophila* embryos. These perturbations reveal substantial differences in how ventral and dorsal cells, both within and outside the zone of Rho1 activation, respond to spatially and temporally identical patterns of Rho1 activation. Our results demonstrate that an asymmetric zone of Rho1 activity is not sufficient to recapitulate ventral furrow formation and reveal that additional, ventral-specific factors contribute to the cell- and tissue-level behaviors that emerge during ventral furrow formation.

2.2 Introduction

Tissue morphogenesis underlies the development of multicellular organisms. The molecular and cellular mechanisms that govern tissue morphogenesis remain a central challenge in developmental cell biology. Extensive genetic and biochemical experiments have defined the factors required for many morphogenetic movements. Furthermore, methods for imaging

and quantitatively describing cell shape changes are ever-improving. Despite this progress, questions remain. For example, how pliable are tissues before and while they are deforming? To what degree does the underlying cytoskeleton of cells within a tissue limit their ability to deform, and to what degree and by what mechanism are shape changes of neighboring cells coordinated?

Ventral furrow formation in the *Drosophila* embryo is one of the best studied examples of tissue morphogenesis; it is the first step in *Drosophila* gastrulation. Ventral furrow formation occurs when a rectangular zone of approximately 1000 cells, arranged in 18 rows, on the ventral surface of the embryonic epithelium apically constrict and invaginate into the embryo, ultimately giving rise to the embryonic mesoderm [Leptin and Grunewald, 1990, Sweeton et al., 1991]. Many molecules required for ventral furrow formation have been identified: An extracellular serine protease cascade activates the transcription factor Dorsal which drives the expression of two additional transcription factors, Snail and Twist, in a subset of ventral cells, inducing them to adopt mesodermal fates [Morisato and Anderson, 1995, Ip et al., 1992, Jiang et al., 1991]. Snail and Twist then induce the expression of secreted and cell surface molecules, including the ligand Fog, the G-protein-coupled receptor (GPCR) Mist, and the transmembrane protein T48 [Dawes-Hoang et al., 2005, Costa et al., 1994, Kölsch et al., 2007, Manning et al., 2013]. Together with Concertina, a maternally contributed Gα protein, and Smog, a maternally contributed GPCR, these factors recruit and activate RhoGEF2, a Rho1-specific guanine nucleotide exchange factor, at the apical membrane of ventral cells [Parks and Wieschaus, 1991, Kölsch et al., 2007, Nikolaidou and Barrett, 2004, Kerridge et al., 2016]. RhoGEF2 then activates Rho1 to assemble a contractile actomyosin network [Fox and Peifer, 2007]; these networks within single cells are coupled through adherens junctions between neighboring cells into a supracellular actomyosin network that promotes apical constriction and robust ventral furrow formation [Martin et al., 2010, Yevick et al., 2019]. Notably, both RhoGEF2 accumulation and Rho1 activation are pulsatile [Martin et al., 2010, Mason et al.,

2016].

The intracellular signaling cascade described above activates Rho1 within individual presumptive mesoderm cells. This could, in principle, account for ventral furrow formation [Gilmour et al., 2017, Ko and Martin, 2020]. However, several features of the ventral furrow suggest that ventral cells exhibit a high degree of intercellular coupling, which may influence the outcome of the genetically encoded contractility. For example, ventral cell apical constriction is anisotropic, occurring more along the dorsal-ventral than the anterior-posterior axis of the embryo [Sweeton et al., 1991, Martin et al., 2010]. If individual ventral cells constrict and invaginate without being influenced by their neighbors, one would predict isotropic apical constriction. Additionally, the apical constriction of individual cells appears coordinated, with cells adjacent to constricting cells more likely to constrict than their more distant counterparts [Sweeton et al., 1991, Gao et al., 2016]. Furthermore, multiple rows of cells lateral to the furrow bend towards it, indicating that forces are transmitted over long distances in the ventral epithelium [Rauzi et al., 2015, Costa et al., 1994, Leptin et al., 1992].

Taken together, this wealth of previous results suggests that ventral furrow formation results from a combination of intracellular Rho1-mediated contractility and intercellular coupling of those contractile forces. In the simplest iteration of this model, an asymmetric zone of Rho1 activation is sufficient to recapitulate both the intra- and intercellular aspects of ventral furrow formation [Doubrovinski et al., 2018]. Indeed, it was recently shown that an asymmetric zone of local Rho1 activation is sufficient to induce an ectopic invagination in the dorsal *Drosophila* epithelium [Izquierdo et al., 2018]. However, it remains unclear whether local Rho1 activation alone is sufficient to induce sustained tissue morphogenesis and recapitulate all aspects of ventral furrow formation. Alternatively, ventral-specific gene expression may endow ventral cells with factors that collaborate with active Rho1 to generate the observed cell shape changes. If this is the case, an asymmetric zone of Rho1 activity would yield distinct cell shape changes in the dorsal versus the ventral embryonic epithelium.

Addressing these and related questions necessitates the ability to activate Rho1 with high spatial and temporal precision without otherwise perturbing the embryo. Optogenetic techniques utilize photosensitive proteins to control protein localization and/or activity with light; these techniques are, therefore, well-suited to interrogate the basis for the anisotropic and coordinated nature of apical constriction during ventral furrow formation. Importantly, the ideal optogenetic approach will activate Rho1 in response to light alone.

Here, we use a LOV-domain based optogenetic probe to acutely activate Rho1 in *Drosophila*. We demonstrate that this system expresses ubiquitously throughout *Drosophila* development and is well tolerated. Optogenetic activation of Rho1 induces ectopic deformations in both the dorsal and ventral embryonic epithelium at the onset of gastrulation. We find that ventral cells specifically respond to ectopic Rho1 activation with aligned, anisotropic apical constriction. This ventral-specific response requires Dorsal and Twist expression. Furthermore, we provide evidence that the transmission of contractile forces over long distances is specific to the ventral epithelium.

2.3 Results

2.3.1 A LOV domain-based optogenetic system controls Rho1 activity in Drosophila

To study the cellular consequences of acute Rho1 activation and probe the impact of Rho1 activation on cells neighboring the activation region, we adapted an optogenetic system for use in *Drosophila*. This two-component system consists of a membrane tethered LOV domain fused to the SsrA peptide and a cytoplasmic SspB protein fused to a protein of interest (Figure 2.1a) [Guntas et al., 2015, Strickland et al., 2012]. Blue light exposure induces a conformational change in the LOV domain, exposing the SsrA peptide and recruiting the SspB fusion protein to the plasma membrane (Figure 2.1a). As a proof of concept, we

first expressed the membrane localized LOV domain and an SspB-mScarlet fusion from the ubiquitin promoter. Local activation of a region of the dorsal embryonic epithelium with blue light induces rapid recruitment of SspB-mScarlet to the plasma membrane (Figure 2.1b). SspB-mScarlet remains associated with the plasma membrane as long as blue light activation is sustained but rapidly (∼1 min) returns to its dark state, cytoplasmic localization, upon cessation of photoactivation (Figure 2.1b).

To control Rho1 activation, we replaced mScarlet with the catalytic Dbl homology (DH) domain of LARG to generate photorecruitable SspB-GFP-LARG(DH) (hereafter called PR-GEF) (Figure 2.1c). LARG is a human RhoA-specific GEF; the DH domain of LARG has previously been used in a related optogenetic system to control RhoA activity in mammalian tissue culture cells [Wagner and Glotzer, 2016]. We used the DH domain of LARG alone to ensure that the recruitable GEF's function is divorced from all endogenous regulation and only sensitive to optogenetic activation. Homozygous flies expressing the membrane localized LOVSsrA and PR-GEF from the ubiquitin promoter are viable and fertile, indicating that these transgenes are well tolerated. Global activation of the dorsal embryonic epithelium with blue light induces strong recruitment of PR-GEF to the plasma membrane within seconds, and this global PR-GEF recruitment induces cortical myosin accumulation within 1 minute (Figure 2.1d). Myosin accumulates both medially and junctionally (Figure 2.1d). Optogenetically-induced cortical myosin completely disappears within 3 minutes of cessation of photoactivation (Figure 2.1d). Thus, using conventional instruments, this optogenetic system rapidly, robustly, and reversibly activates Rho1 in the embryonic epithelium. This system also activates Rho1 in all *Drosophila* tissues tested, including the pupal notum, follicular epithelium, larval wing imaginal disc, and larval central nervous system (Figure 2.2). In the larval wing peripodial epithelium, optogenetic activation of Rho1 can induce myosin accumulation with subcellular precision (Figure 2.2c). Optogenetic activation of Rho1 is sensitive to light dosage; attenuating the activating light induced less myosin-

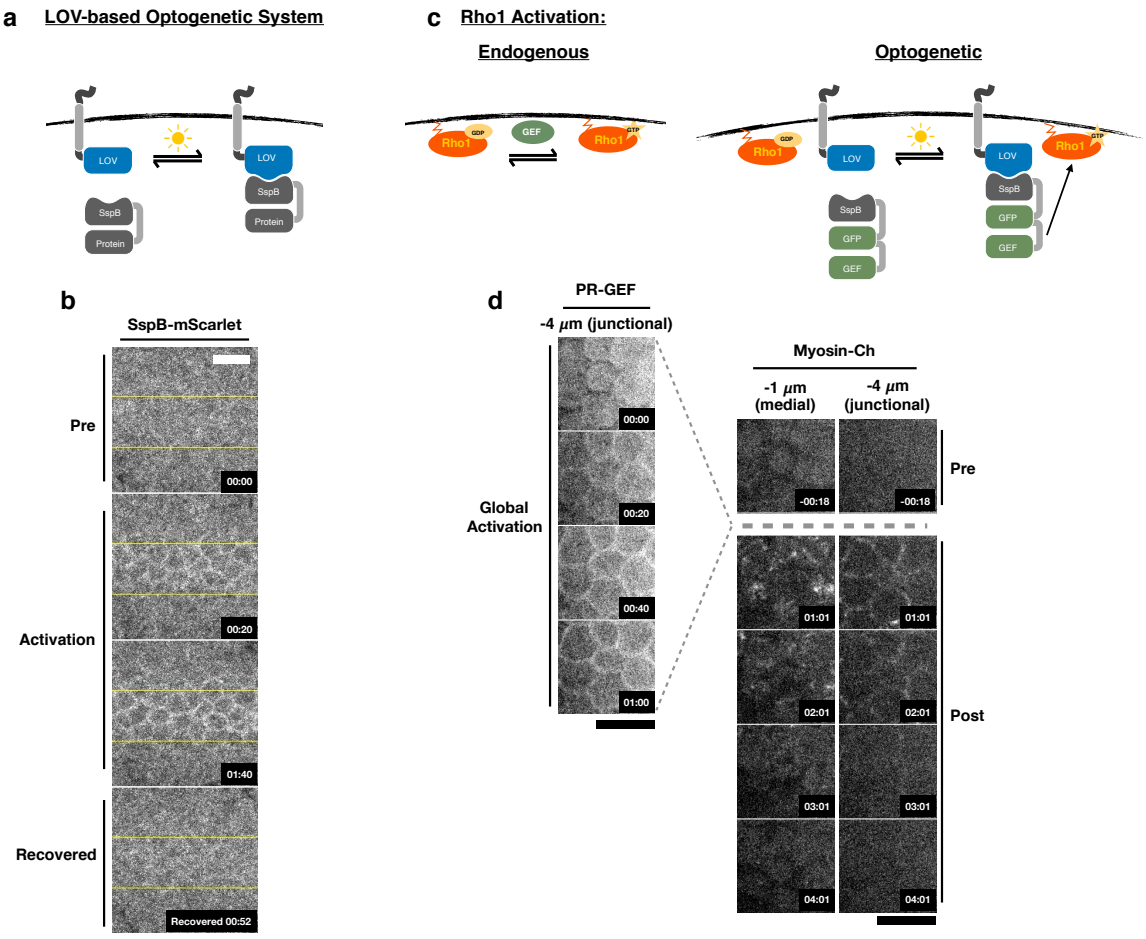

Figure 2.1: **Optogenetic control of Rho1 in *Drosophila*.**
a) Generic LOV domain-based optogenetic system consisting of a membrane localized LOVSsrA protein and a recruitable SspB protein. SspB can be fused to any protein of interest. Blue light induces a conformational change in the LOV domain, allowing it to recruit SspB fusion proteins to the membrane. b) Dorsal epithelium of an embryo expressing the membrane-localized LOVSsrA and SspB-mScarlet at the onset of gastrulation before, during, and after photo-activation in the indicated region (yellow box). Data representative of 4/4 embryos. c) Optogenetic system for activating Rho1: SspB is fused to GFP and the Dbl homology (DH) domain of LARG (PR-GEF). Photoactivation induces recruitment of the PR-GEF to the membrane and Rho1 activation. d) Dorsal epithelium of an embryo expressing a membrane-localized LOVSsrA and PR-GEF at the onset of gastrulation. The distribution of PR-GEF and myosin are shown before, during, and at the indicated times after global photoactivation. Data representative of 5/5 embryos. Time zero indicates the beginning of photoactivation. Scale bars are 10 µm.

Ch accumulation, indicating lower levels of Rho1 activation (Figure 2.3). Above a certain threshold of activating light, Rho1 becomes globally activated, despite precisely defined activation regions (Figure 2.3). Thus, this LOV domain-based optogenetic probe is capable of controlling Rho1 activation with high spatial and temporal resolution. Furthermore, the level of Rho1 activation can be tuned by modulating light dosage.

While this LOV domain-based optogenetic probe recovers to its dark state activity level within minutes (Figure 2.1), some biological phenomena may require faster recovery kinetics. To increase the inactivation rate of our optogenetic probe, we introduced a previously identified point mutation, I427V, into the LOV domain, which increases the rate at which the LOV domain returns to the dark state [Christie et al., 2007]. I427V increases the inactivation rate of the optogenetic system in *Drosophila* S2 cells expressing a membrane localized LOV domain containing this mutation and a cytoplasmic, recruitable tagRFP-SspB (Figure 2.4a,b). Increasing the recovery rate of the LOV domain also decreases the maximum recruitment of tagRFP-SspB (Figure 2.4a,b), demonstrating the trade off between rapid inactivation and total recruitment. Global activation of the rapid cycling LOV domain in *Drosophila* larval brains induced robust Rho1 activation, as scored by accumulation of a Rho1 biosensor (Figure 2.4c); this Rho1 activity dissipated within a minute of cessation of global optogenetic activation. In contrast, Rho1 remained active a minute after global activation of the wild type LOV domain (Figure 2.4c). Thus, the cycling kinetics of the LOV domain are the primary determinant of the off rate of optogenetic-induced Rho1 activity. This emphasizes that there are rapid and robust mechanisms for shutting off Rho1 activity in vivo; furthermore, it suggests that cells continually activate Rho1 during cellular and developmental processes that require sustained Rho1 activation. The wildtype LOV domain is used for the remainder of the experiments presented, as the rapid recovery was not essential to address the questions answered here.

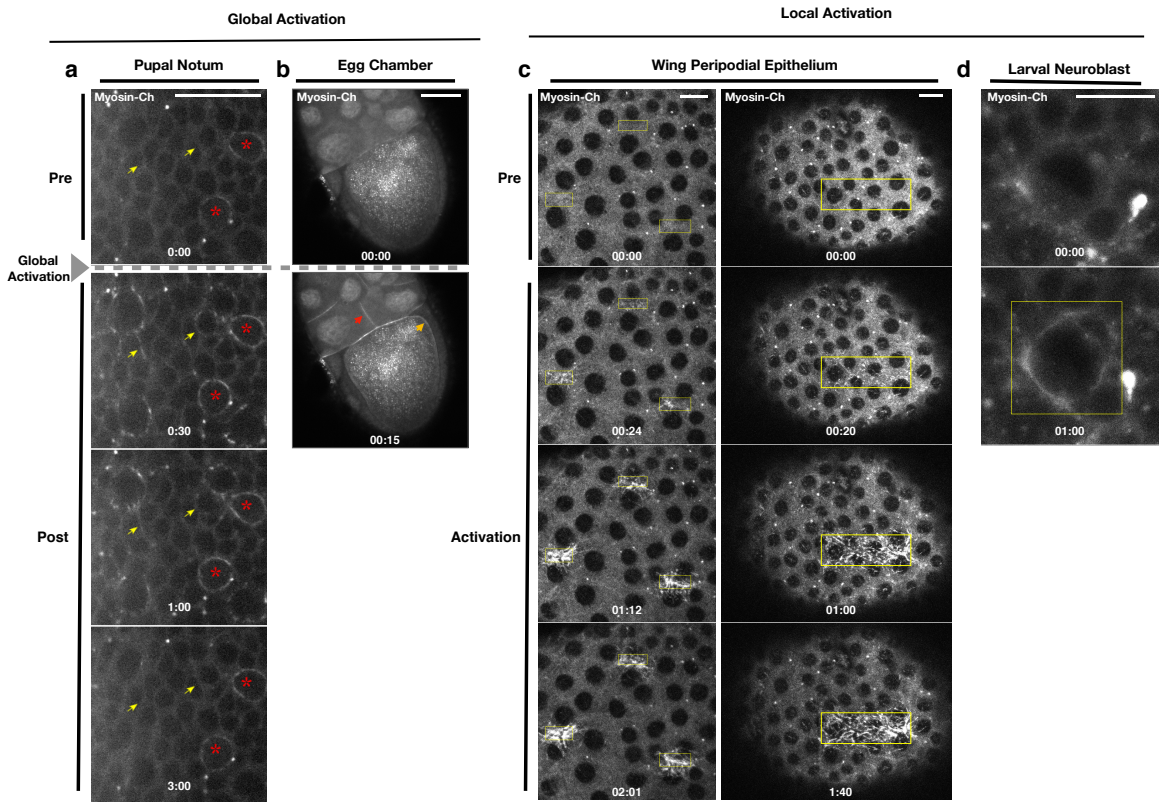

Figure 2.2: **Recruitment of PR-GEF activates Rho1 in all tissues tested.**
a) Pupal Notum expressing the optogenetic probes. Myosin-Ch is shown before and after global photoactivation. Yellow arrow indicates the same cell junction over time. Asterisks indicate mitotic cells. Data representative of 2/2 pupae. b) Egg chambers expressing the optogenetic probes. Myosin-Ch is shown before and after global photoactivation. Nurse cell junctions (red arrow) and the oocyte cortex (yellow arrow) are indicated. Data representative of 4/4 egg chambers. c-d) Larval wing imaginal discs (c) and larval neuroblast (d) expressing the optogenetic probes. Rho1 was locally photoactivated within the yellow boxes. Myosin-Ch is shown before and during activation. Myosin-Ch accumulates with sub-cellular precision in the peripodial epithelium, consisting of squamous cells (c, left). Data representative of 5/5 wing discs (c, left), 3/3 wing discs (c, right), and 6/6 neuroblasts from 2 central nervous systems (d). Time zero indicates the first pulse of blue light activation. Scale bars are 10 µm.

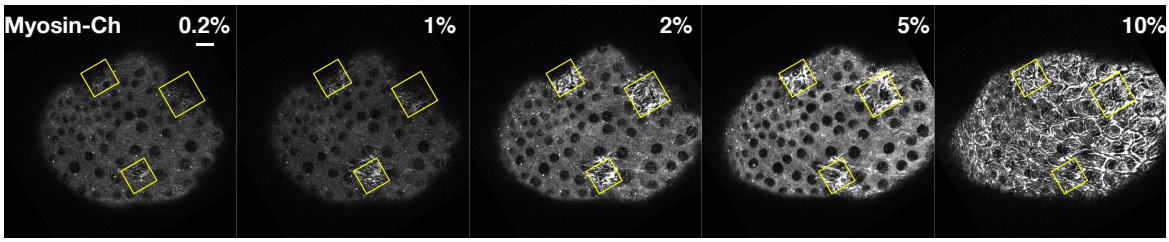

Figure 2.3: **Ectopic Rho1 activation is sensitive to light dose.**
Larval wing peripodial epithelia expressing the optogenetic components and Myosin-Ch. Rho1 was optogenetically activated in the yellow boxes. Laser power was attenuated to the indicated percent transmittance using an acusto-optical tunable filter. 10% transmittance induces substantial Rho1 activation outside of the activation zone. Lowering the laser transmittance yields decreasing amounts of myosin accumulation. Photoactivation lasted 2 min 20 sec for each % transmittance. Data representative of 4/4 wing imaginal discs. Scale bars are 10 µm.

2.3.2 Rho1 activation is sufficient to induce reversible invaginations in the Drosophila embryonic epithelium

After validating that this system reversibly activates Rho1 in the early *Drosophila* embryo, we asked whether an asymmetric zone of Rho1 activation is sufficient to induce an ectopic invagination in the embryonic dorsal epithelium just after cellularization. Ectopic Rho1 activation induces apical myosin accumulation and is sufficient to induce an ectopic invagination (Figure 2.5a). Importantly, the size of the invaginated region closely mirrors the size of the photoactivated zone, demonstrating the spatial precision of this approach and emphasizing that this deformation is light-dependent. (Rho1 is activated in asymmetric zones of the same dimensions throughout this work, except where explicitly stated.) This is consistent with recently published work [Izquierdo et al., 2018].

Local Rho1 activation also induces ectopic invaginations in the ventral embryonic epithelium prior to the onset of ventral furrowing (Figure 2.5b). The ectopic invaginations induced in either the dorsal or ventral epithelium recover to their pre-activation state within four minutes of cessation of optogenetic Rho1 activation (Figure 2.6). These recovery kinetics are

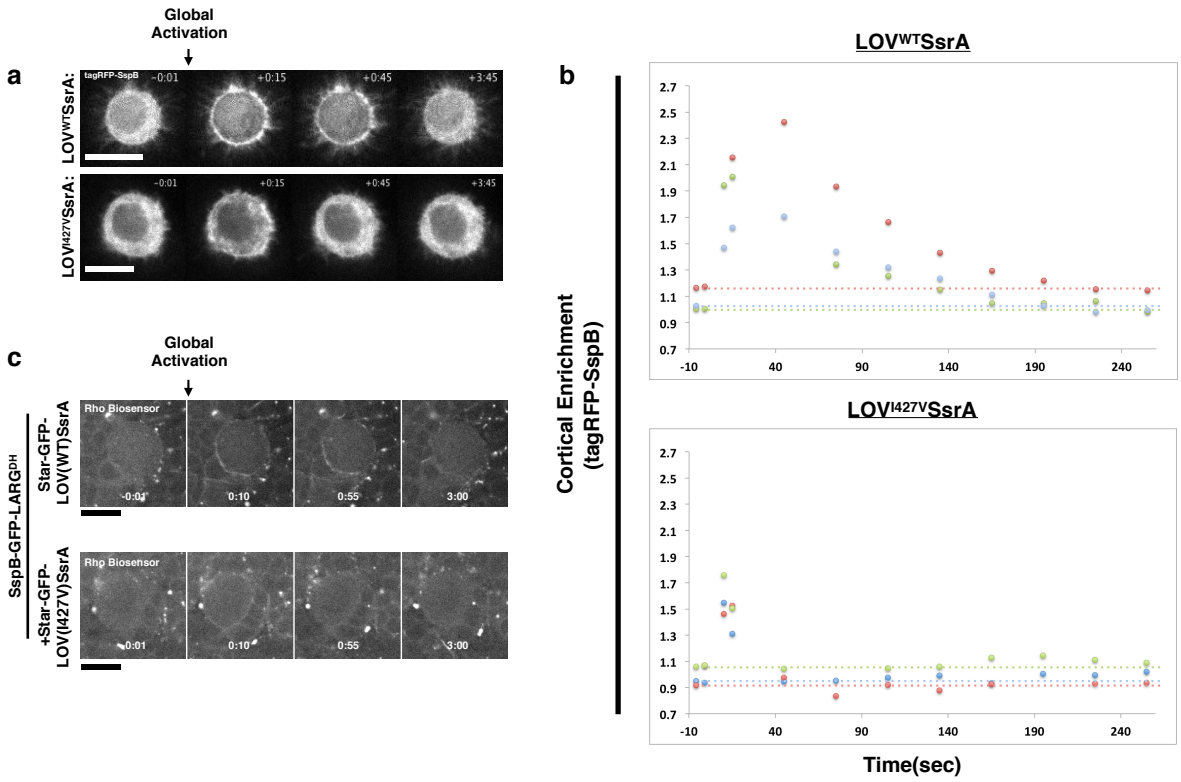

Figure 2.4: **Inactivation kinetics of the LOV domain dictate the off rate of optogenetic-induced Rho1 activity.**
a) S2 cells transiently transfected with recruitable tagRFP-SspB and a membrane localized WT LOV domain (top) or fast-cycling (I427V) LOV domain (bottom). Representative cells are shown before and after global photoactivation. b) Quantification of the cortical enrichment (membrane/cytoplasm) of SspB-tagRFP following global optogenetic Rho1 activation. c) Larval neuroblasts expressing PR-GEF, Rho-biosensor, and WT (top) or fast-cycling (bottom) membrane-localized LOV domain shown before and after global photoactivation. Scale bars are 5 µm. Rho-biosensor consists of the Rho binding domain of Anillin, a RhoA effector, fused to mCherry [Munjal et al., 2015, Piekny and Glotzer, 2008]. Data representative of 16 neuroblasts from 3 brains (top) and 19 neuroblasts from 4 brains (bottom).

slightly longer than the cycling kinetics of the WT LOV domain (Figure 2.1d & 2.4d). Thus, while ectopic Rho1 activation induces ectopic deformations, the downstream consequences of optogenetic Rho1 activation are rapidly and robustly inactivated in the absence of continued photoactivation.

2.3.3 Rho1 activation induces distinct apical constriction in the dorsal and ventral epithelium

To determine whether dorsal and ventral cells respond similarly to spatially and temporally identical zones of Rho1 activation, we locally activated Rho1 in the dorsal or ventral epithelium of embryos expressing the optogenetic components and the membrane marker Gap43-mCh and subsequently segmented tissues, tracked individual cells, and quantified the area of the apical-most surface of dorsal or ventral cells before and after optogenetic Rho1 activation [Aigouy et al., 2010]. We also quantified the anisotropy of apical constriction by measuring the extent of elongation of the apical-most surfaces of cells before and after photoactivation [Aigouy et al., 2010]. Local Rho1 activation in individual cells in the dorsal embryonic epithelium induced apical constriction (Figure 2.7a); optogenetic activation of Rho1 in a collection of dorsal cells also induced apical constriction (Figure 2.7b-c). Unlike cells of the endogenous ventral furrow, which exhibit strongly anisotropic apical constriction (Figure 2.8), optogenetically activated dorsal cells constrict isotropically (Figure 2.7d-bottom panel, 2.9, & 2.10). Thus, an asymmetric, rectangular zone of Rho1 activation via this probe is not sufficient to fully recapitulate the cell shape changes associated with endogenous ventral furrowing. This result differs from previous work (See Discussion) [Izquierdo et al., 2018].

We next tested whether optogenetic Rho1 activation has a different effect on ventral cells, which express ventral-specific genes. We activated ventral cells before they exhibited any overt signs of apical constriction. Optogenetic activation of Rho1 in a collection of ventral

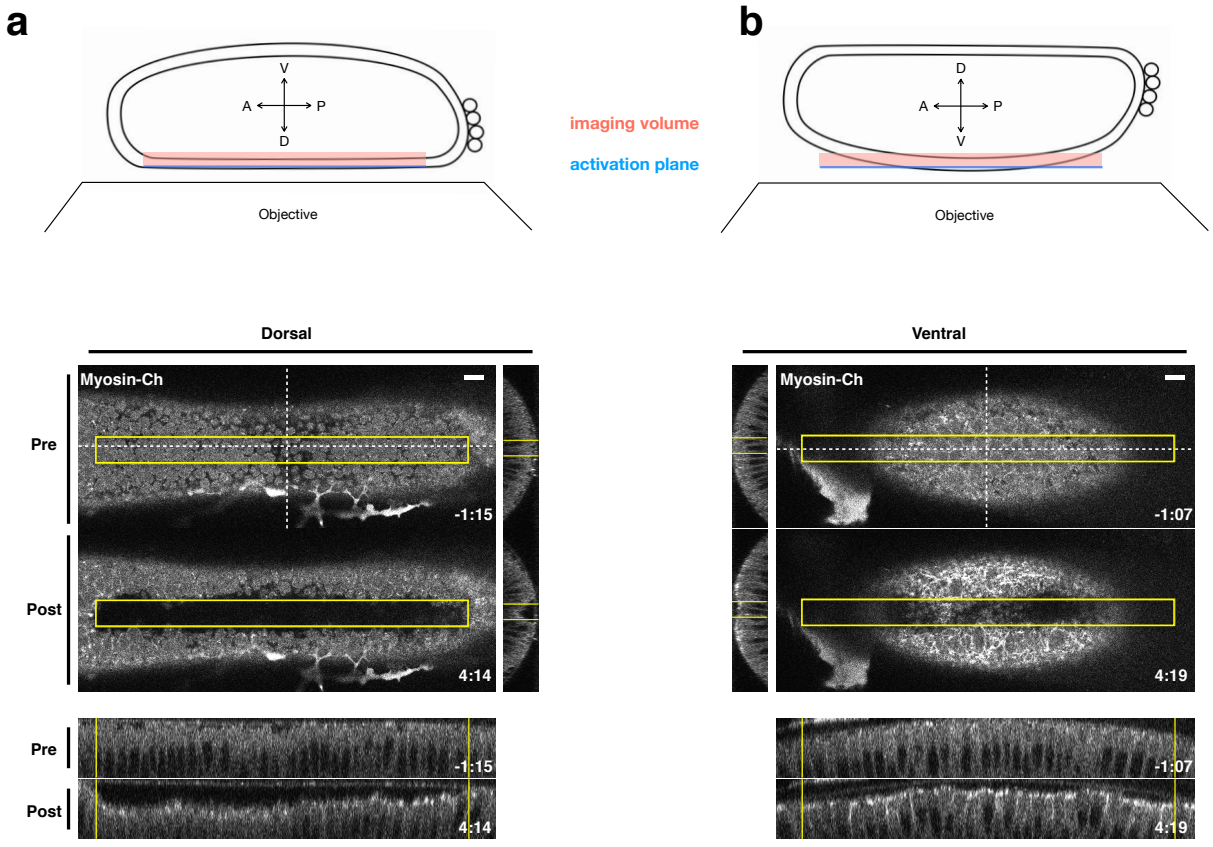

Figure 2.5: **Local Rho1 activation is sufficient to induce ectopic invaginations in the embryonic epithelium.**
a,b) Top: Schematic of local activation set up. Bottom: Embryos expressing the optogenetic components and Myosin-Ch at the onset of gastrulation were optogenetically activated in a single apical plane within the yellow box. Ectopic invaginations and Myosin-Ch accumulation are shown in the dorsal (a) and ventral (b) epithelium. Myosin-Ch accumulates both within and outside the region of optogenetic Rho1 activation in the ventral epithelium (b, YZ projection, Right; XZ projection, Bottom). This is due to endogenous gastrulation. Data representative of 7/7 (a) and 5/5 (b) embryos. Time zero indicates the first pulse of blue light activation. Scale bars are 10 µm.

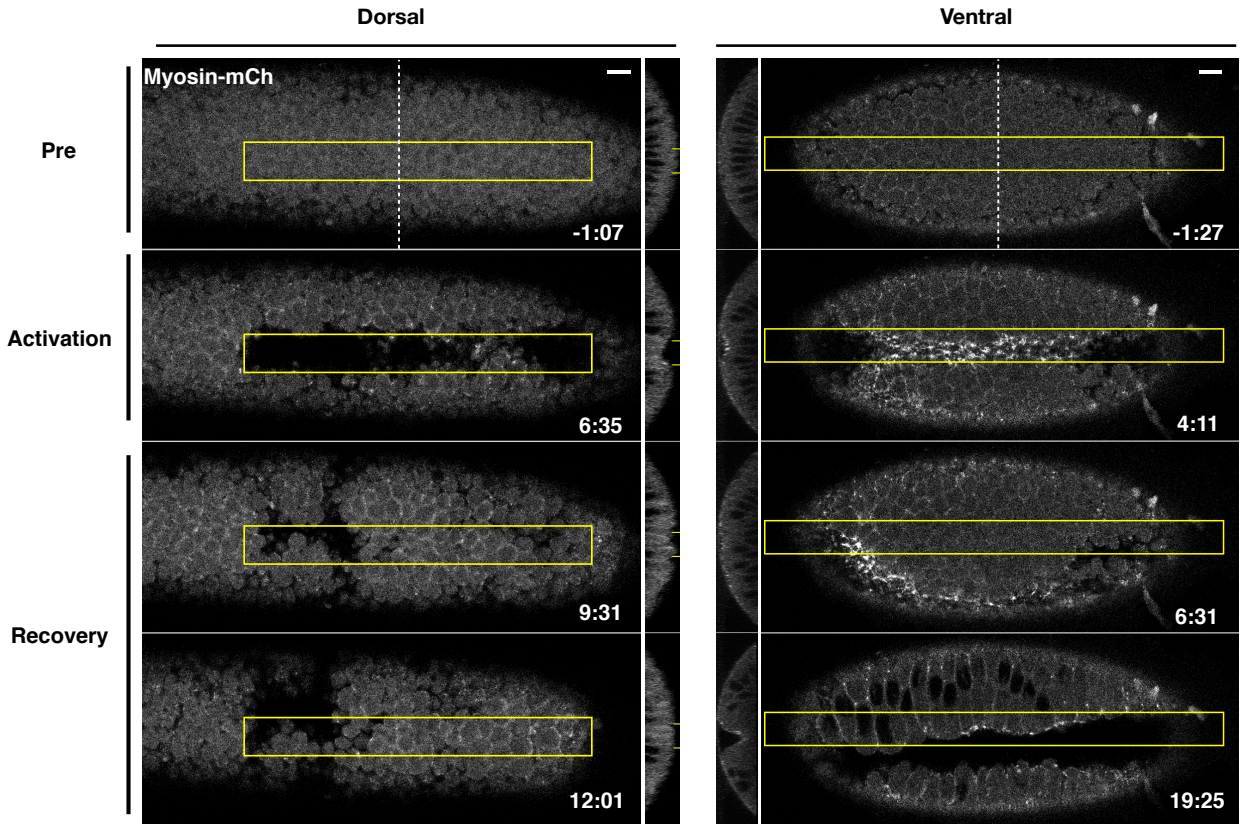

Figure 2.6: **Optogenetic-induced invaginations revert following cessation of Rho1 activation.**
Dorsal (left) or ventral (right) epithelium of *Drosophila* embryos expressing the optogenetic components and Myosin-Ch before, during, and after local Rho1 activation within the yellow boxes. Note that some cells in the dorsal epithelium remain invaginated after the recovery period. These sustained pockets of invagination are sometimes seen where the dorsal transverse folds form. Data representative of 5/5 dorsal and 4/4 ventral embryos. Time zero indicates the first pulse of blue light activation. Scale bars are 10 µm.

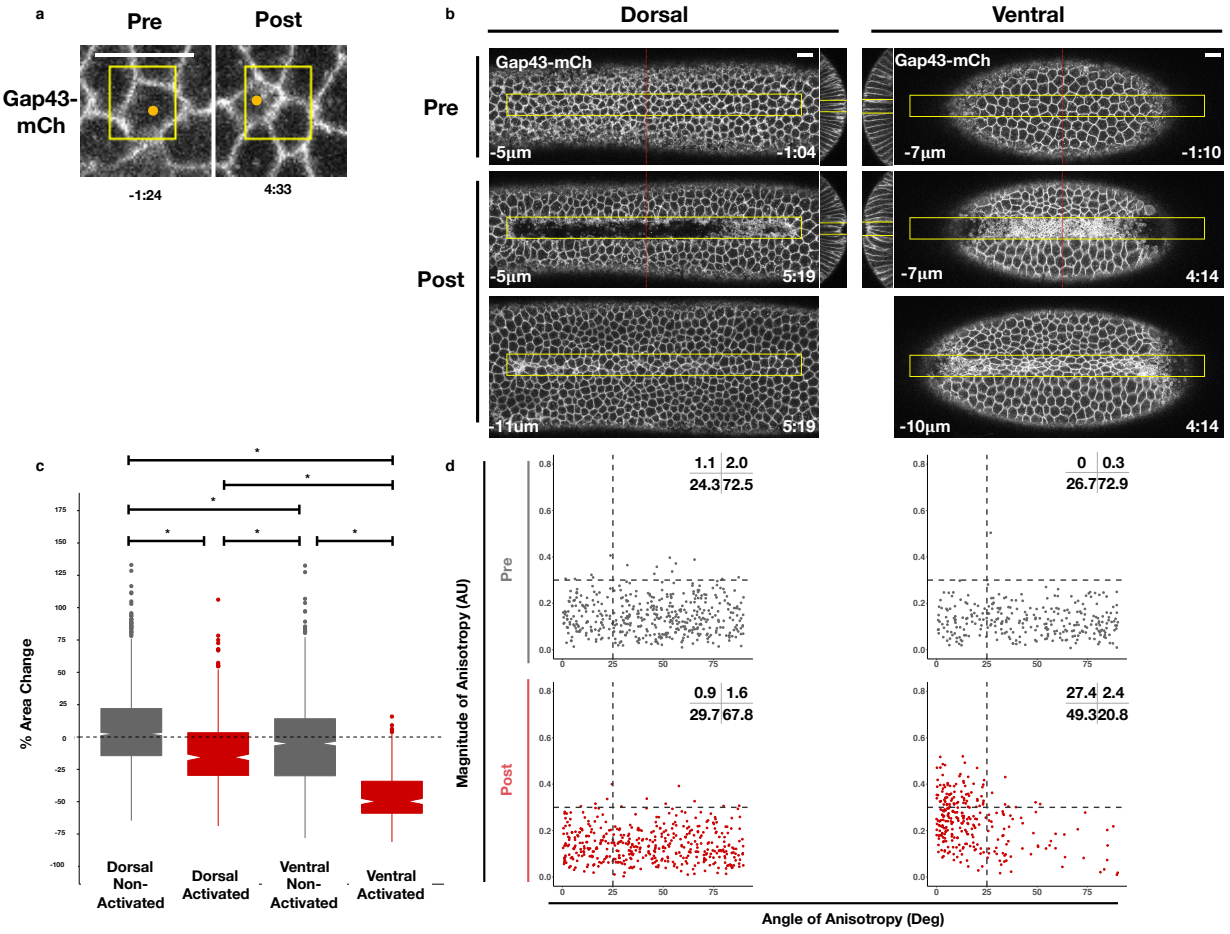

Figure 2.7: **Rho1 activation induces distinct apical constriction in dorsal and ventral epithelial cells.**
a) Dorsal cells from an embryo expressing the optogenetic components and Gap43-mCh at the onset of gastrulation before and after photoactivation within the yellow box. Z-slices shown represent the apical-most view of the activated cell (orange dot). Data representative of 7/8 cells from 2 embryos. b) Dorsal (left) and ventral (right) epithelium of embryos expressing the optogenetic components and Gap43-mCh at the onset of gastrulation. Rho1 was activated in the yellow box. Images shown in bottom panels were chosen to show the apical surfaces of activated cells. Red lines in (b) indicate position of each YZ slice. Data are representative of 4/4 (a) and 4/4 (b) embryos. Time zero indicates the first pulse of blue light activation. Scale bars are 10 µm. c) Quantification of apical area change induced by optogenetic Rho1 activation. Gray columns represent non-activated cells (cells outside the yellow box in (b)). Red columns represent activated cells (cells within the yellow box in (b)). Statistical Analysis: Kruskal-Wallis test, $Chi^2 = 691.6$, df=3, $p<2.2x10^{-}16$; Pairwise comparisons with Wilcoxon signed rank text, using BH method to adjust for multiple comparisons. * indicates $p < 0.05$.

Figure 2.7: (continued) **Rho1 activation induces distinct apical constriction in dorsal and ventral epithelial cells**
d) Anisotropy scatter plots: Each dot represents an activated dorsal (left) or ventral (right) cell before (top) or after (bottom) optogenetic activation of Rho1. The magnitude of anisotropy is plotted on the y-axis; the orientation of anisotropy, relative to the anterior-posterior axis of the embryo, is plotted on the x-axis. Dotted lines are provided to facilitate comparisons. Insets show percentage of cells in each quadrant. Cells in the upper left quadrant exhibit highly aligned, anisotropic apical constriction. 444 dorsal cells from 4 embryos and 288 ventral cells from 4 embryos were analyzed. See Figure 2.9 for plots of the changes in anisotropy of individual cells. See Figure 2.10 for statistical analysis of data in d.

cells also induced apical constriction within the zone of Rho1 activation (Figure 2.7b,c). However, the apical surfaces of activated ventral cells were elongated, indicating anisotropic apical constriction. This anisotropy was strongly aligned with the anterior-posterior axis (Figure 2.7d, 2.9, & 2.10). Notably, this light-induced, anisotropic apical constriction occurs within a 4 minute activation period (Figure 2.7d). In contrast, similar changes in anisotropy occur over a 15-20 minute period in non-activated embryos (Figure 2.8). Furthermore, a smaller, asymmetric zone of Rho1 activation also induces anisotropic apical constriction in activated ventral cells but not their non-activated neighbors (Figure 2.11), confirming that our optogenetic experiments recapitulate the cell shape changes seen during endogenous ventral furrow but induce these cell shape changes to occur earlier and faster than they normally would. Thus, in contrast to the isotropic apical constriction induced in activated cells within the dorsal epithelium, optogenetic Rho1 activation in cells within the ventral epithelium induces precocious, anisotropic apical constriction that strongly resemble the anisotropic apical constrictions seen during endogenous ventral furrow formation (Figure 2.8).

2.3.4 Genetic requirements for ventral-specific responses

The finding that an asymmetric zone of Rho1 activation induces differential responses in the dorsal and ventral epithelia suggests that ventral patterning may influence the response to

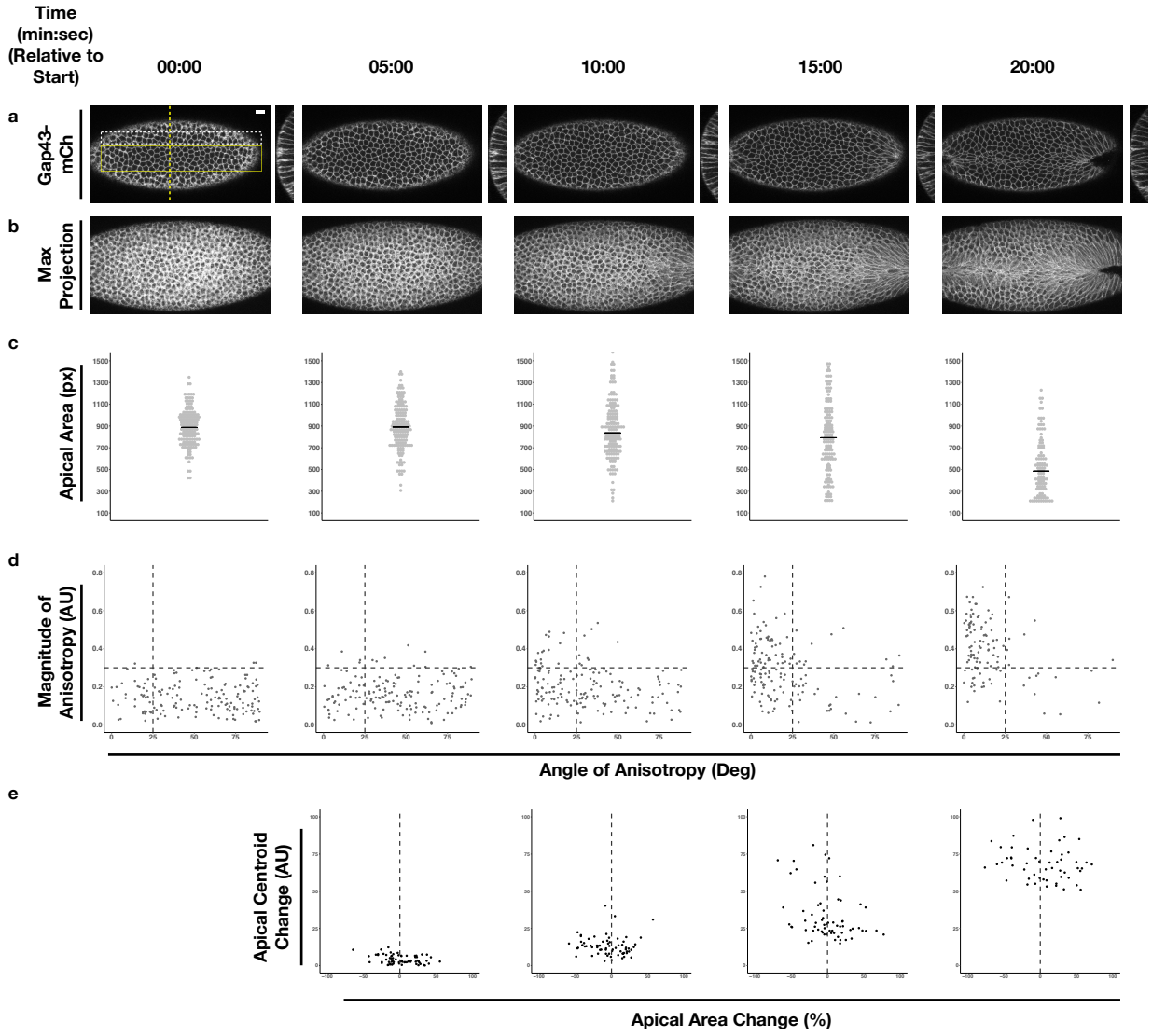

Figure 2.8: **Quantification of endogenous ventral furrow formation.**
a-b) Single plane (a) and maximum projection (b) images of a non-activated embryo expressing the optogenetic components and Gap43-mCh. c-d) Plot of apical area (c) or anisotropy (d) of cells in the endogenous ventral furrow (yellow box in a) at indicated time points. Black lines in (c) represent median. e) Plot of centroid change, relative to time 00:00, along the Y axis for cells neighboring the ventral furrow (white box in a). Data representative of 3/3 embryos. Scale bars are 10 µm.

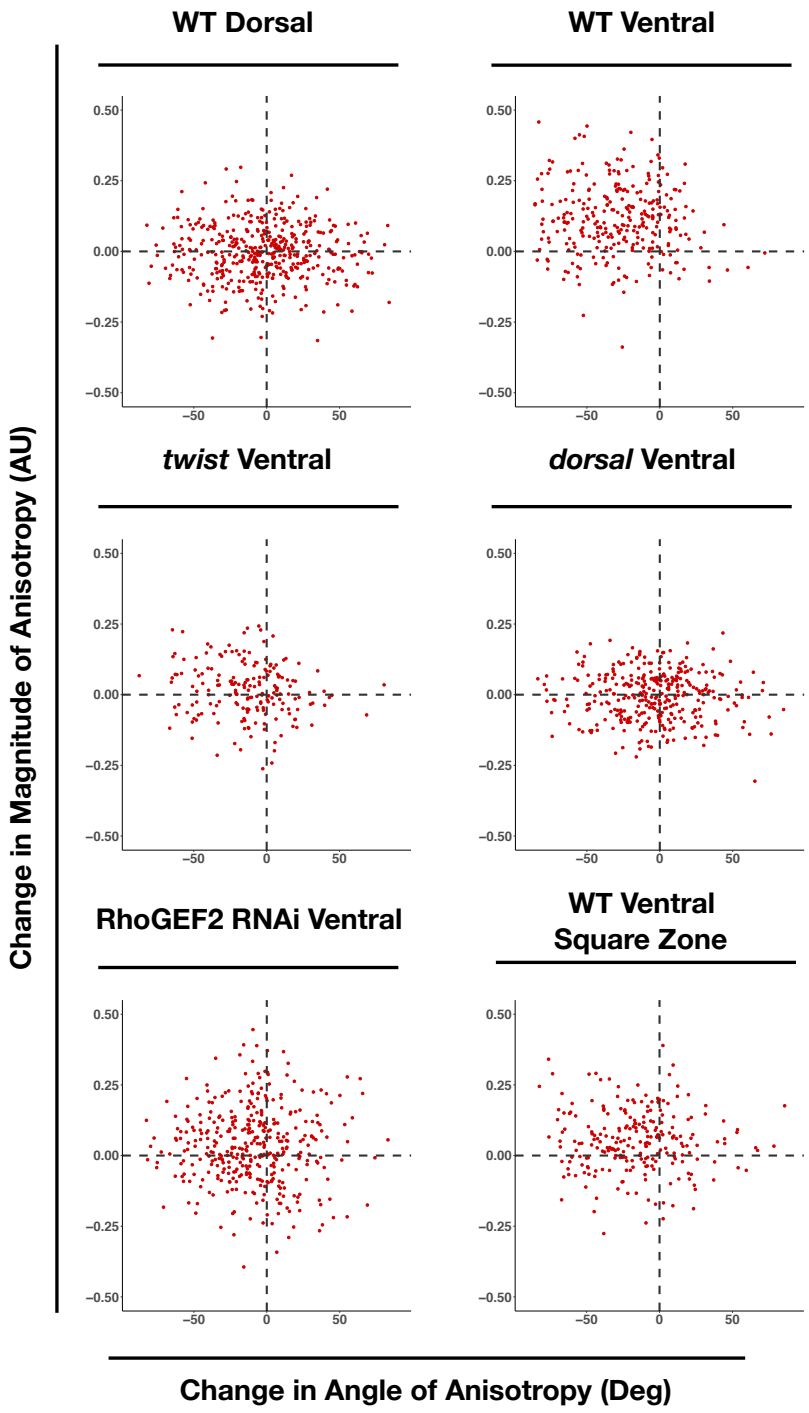

Figure 2.9: **WT ventral, but not dorsal, cells exhibit large changes in the magnitude and alignment of anisotropy in response to Rho1 activation.**
X and Y axes show the changes in anisotropy angle (X) and magnitude (Y) for each cell over the course of optogenetic activation. Angle change was calculated as end angle (in degrees) minus start angle (in degrees).

Figure 2.9: (continued) **WT ventral, but not dorsal, cells exhibit large changes in the magnitude and alignment of anisotropy in response to Rho1 activation.** Magnitude change was calculated as end magnitude minus start magnitude. 444 cells from 4 wildtype dorsally oriented, 288 cells from 4 wildtype ventrally oriented, 343 cells from 4 *dorsal* embryos, 189 cells from 3 *twist* embryos, 375 cells from 5 RhoGEF2 depleted embryos, and 239 cells from 5 square zone embryos were analyzed.

Rho1 activation. Ventral-specific factors, such as those downstream of Dorsal, Twist, and/or Snail, may cooperate with an asymmetric zone of Rho1 activation during endogenous ventral furrow formation to drive strong, anisotropic apical constriction. To test this hypothesis, we locally activated Rho1 in ventral cells lacking Dorsal protein, a factor required for ventral identity. Optogenetic Rho1 activation in embryos derived from females homozygous for a null *dorsal* allele still induced apical constriction, but these apical constrictions were weaker than those of WT ventral cells and were no longer anisotropic (Figure 2.12, 2.9, & 2.10). Indeed, in the absence of the Dorsal protein, the response of ventral cells to Rho1 activation is similar to the response of wildtype cells in the dorsal epithelium (Figure 2.12c v. Figure 2.7d-Activated Dorsal, 2.9, & 2.10). Thus, Dorsal is required to predispose ventral cells to constrict anisotropically along the anterior-posterior axis of the embryo.

The transcription factor Twist is downstream of Dorsal activity in ventral cells. We optogenetically activated Rho1 in ventral cells of embryos homozygous for a null allele of *twist*. These mutant cells exhibited apical constriction following ectopic Rho1 activation (Figure 2.12b), but the amount of constriction, magnitude of anisotropy, and the degree of alignment with the anterior-posterior axis was less than that of wildtype ventral cells (Figure 2.12c v. Figure 2.7d-Activated Ventral; Figure 2.9 & 2.10). Thus, Twist promotes the predisposition of ventral cells to constrict anisotropically along the anterior-posterior axis of the embryo. However, we note that ventral cells lacking Twist exhibit more aligned apical constriction than ventral cells lacking Dorsal (Figure 2.12c, 2.9, & 2.10). These distinct responses suggest that there is a Twist-independent mechanism downstream of Dorsal that

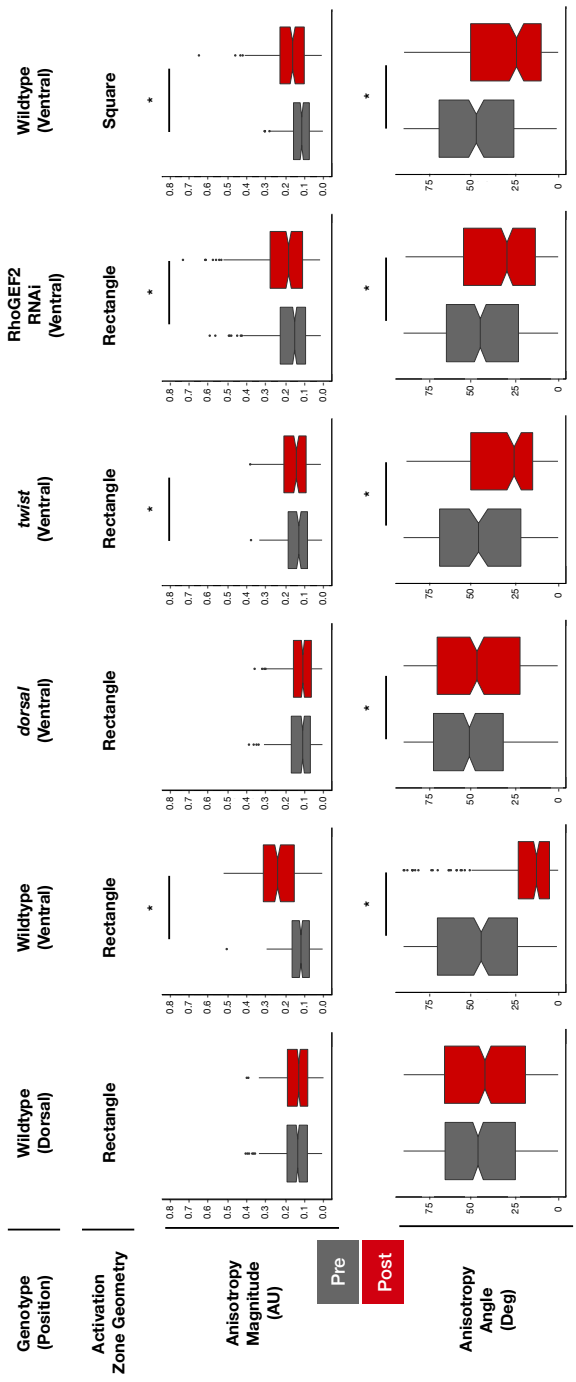

Genotype	Position of Activation Region	Time of measurement	Anisotropy angle		P value	Anisotropy magnitude		P value
			Average (deg)	Standard Deviation (+/-)		Average (AU)	Standard Deviation	
Wildtype	Dorsal	Pre-activation	45.0	25.4	0.1372	0.14	0.08	0.396
		Post-activation	42.9	26.5		0.14	0.07	
Wildtype	Ventral	Pre-activation	46.1	27.1	< 2.2E-16	0.13	0.07	< 2.2E-16
		Post-activation	18.1	18.8		0.24	0.11	
dorsal	Ventral	Pre-activation	49.9	25.4	0.01	0.12	0.07	0.311
		Post-activation	45.8	27.0		0.12	0.17	
twist	Ventral	Pre-activation	46.2	25.4	1.1E-09	0.14	0.07	0.02
		Post-activation	33.2	24.1		0.15	0.08	
RhoGEF2 (RNAi)	Ventral	Pre-activation	44.9	24.9	6.6E-10	0.17	0.10	3E-06
		Post-activation	35.3	25.2		0.21	0.12	
Wildtype Square region	Ventral	Pre-activation	47.2	25.5	2.5E-13	0.12	0.06	5.4E-12
		Post-activation	31.5	25.6		0.18	0.09	

Figure 2.10: **Comparisons of angle and magnitude of anisotropy before and after optogenetic Rho1 activation.**

Figure 2.10: (continued) **Comparisons of Angle and Magnitude of Anisotropy before and after optogenetic Rho1 activation.**
Top: Box plots showing the angle and magnitude of anisotropy before (gray) and after (red) optogenetic Rho1 activation for indicated genotypes. These data correspond to the X and Y axes of the scatter plots shown in (Figure 2.7d) and (Figure 2.12d). Statistical analysis: Wilcoxon signed rank test. * indicates $p<0.05$, indicating a statistically significant change in angle or magnitude in response to optogenetic Rho1 activation. Bottom: Table containing the mean, standard deviation, and p-value for the graphs above.

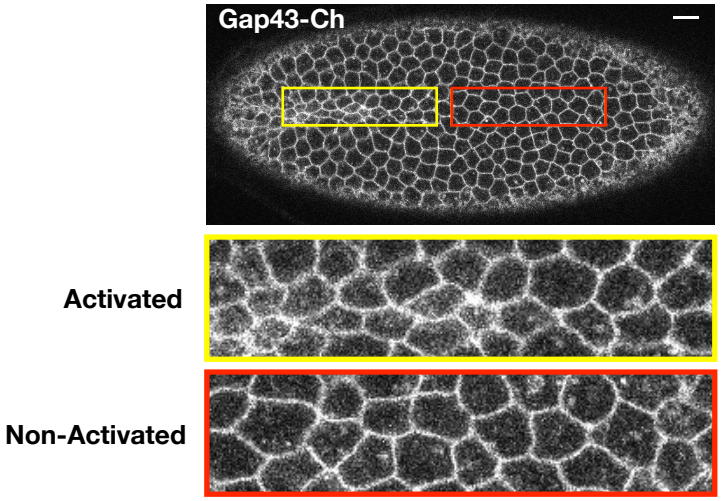

Figure 2.11: **Optogenetic activation of Rho1 induces precocious cell shape changes in the ventral epithelium.**
Ventral surface of an embryo expressing the optogenetic components and Gap43-Ch. Rho1 was activated within the yellow box. Zoomed images of activated (yellow) and non-activated (red) cells are shown. Data representative of 4/4 embryos. Scale bars are 10 µm.

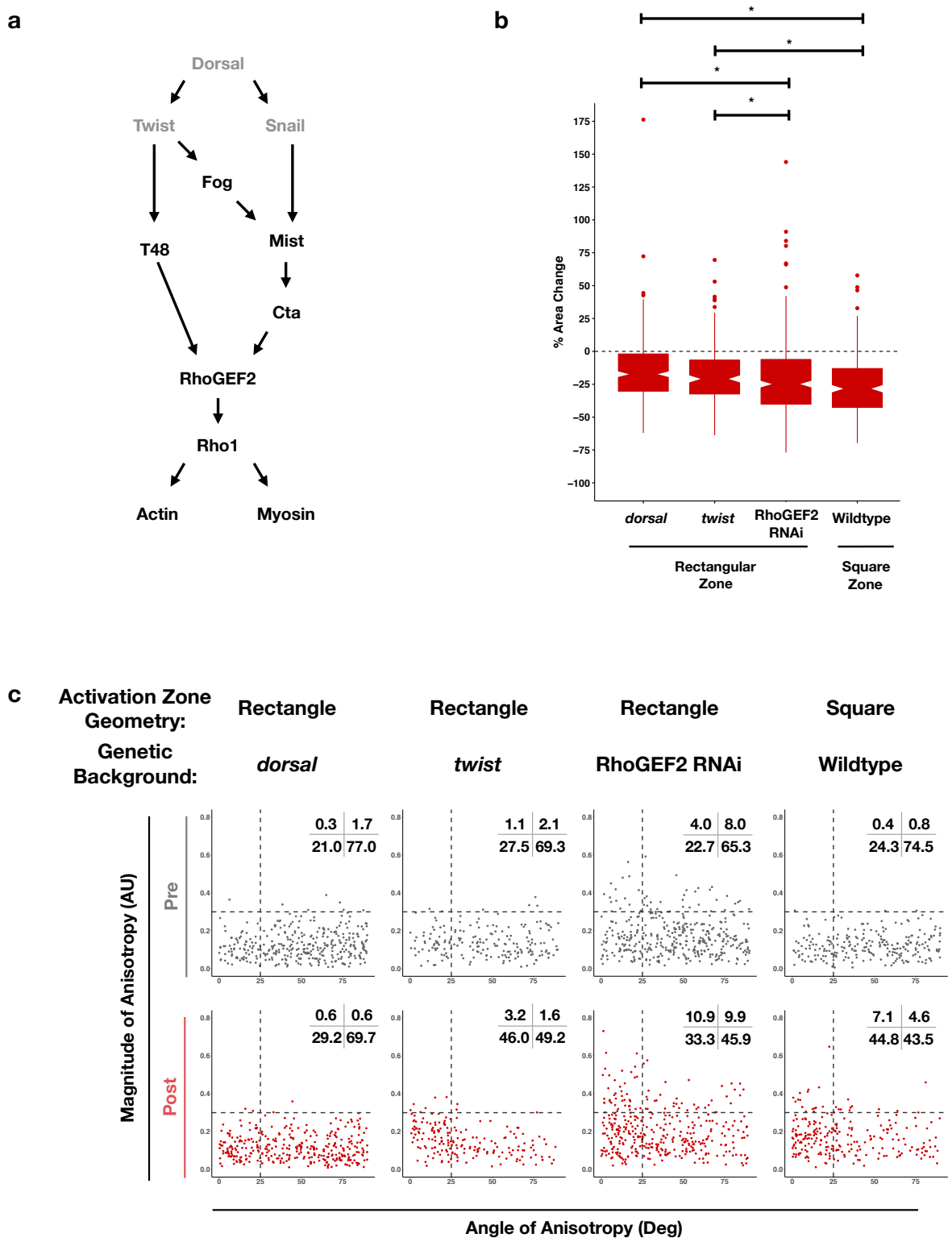

Figure 2.12: **Dorsal is required for and Twist promotes aligned, anisotropic apical constriction in response to ectopic Rho1 activation.**

Figure 2.12: (continued) **Dorsal is required for and Twist promotes aligned, anisotropic apical constriction in response to ectopic Rho1 activation.**
a) Schematic of genetic logic for ventral cell identity. Gray text indicates transcription factors.
b) Quantification of apical area change induced by optogenetic Rho1 activation in wildtype and mutant backgrounds. Statistical analysis: Kruskal-Wallis test, $Chi^2 = 37.3$, df=3, p=4.0x10$^-$8; Pairwise comparisons with Wilcoxon signed rank text, using BH method to adjust for multiple comparisons. * indicates $p < 0.05$.
c) Anisotropy scatter plots, as in Figure 2.7d, for wildtype embryos subjected to a square region of ectopic Rho1 activation or specified mutant embryos subjected to a rectangular zone of activation. Insets show percentage of cells in each quadrant. Cells in the upper left quadrant exhibit highly aligned, anisotropic apical constriction. See Figure 2.9 for plots of the changes in anisotropy of individual cells. See Figure 2.10 for statistical analysis of data in c. 343 cells from 4 *dorsal* embryos, 189 cells from 3 *twist* embryos, 375 from 5 RhoGEF2 depleted embryos, and 239 cells from 5 square zone embryos were analyzed.

promotes aligned anisotropic apical constriction in response to Rho1 activation. We speculate that Snail is responsible for this Twist-independent behavior, but repeated attempts to combine a null *snail* allele with our optogenetic components failed, so we were not able to test this hypothesis.

Dorsal is required for and Twist promotes ventral cells to respond to ectopic Rho1 activation with strong, aligned anisotropic apical constriction. This may reflect that the transcriptional targets of Dorsal and Twist are required for Rho1 activation during endogenous ventral furrow formation [Martin et al., 2009]. Thus, to determine whether Dorsal and Twist contribute to anisotropic apical constriction by regulating the expression of Rho1 activators or by regulating the expression of factors that cooperate with Rho1 activators, we optogenetically activated Rho1 in ventral cells depleted of RhoGEF2, the endogenous activator of actomyosin contractility during ventral furrow formation. RhoGEF2 is required for proper organization of the actomyosin cytoskeleton during cellularization, and embryos lacking RhoGEF2 have some cellularization defects, contributing to irregularities in the epithelium [Padash Barmchi et al., 2005]. Thus, prior to optogenetic activation, a subset of cells depleted of RhoGEF2 are anisotropic, though randomly aligned (Figure 2.12c). Despite the

non-uniformity in these epithelia, optogenetic activation of Rho1 in ventral cells depleted of RhoGEF2 increased the extent of aligned, anisotropic apical constriction (Figure 2.12, 2.9, & 2.10). Ectopic invaginations induced in the ventral or dorsal epithelium of embryos lacking RhoGEF2 failed to revert following cessation of optogenetic activation, in contrast to the rapid reversion of ectopic deformations in otherwise wildtype tissues. This suggests RhoGEF2 makes a significant contribution to the tension in the epithelium, likely through its role in organizing the actomyosin cytoskeleton. These results suggest ventral cells can respond to optogenetic Rho1 activation with anisotropic apical constriction in the absence of endogenous Rho1 activity. However, elevated Rho1 levels may contribute to strong, aligned, anisotropic apical constriction during endogenous ventral furrow formation.

Our experiments in the dorsal epithelium suggest that an asymmetric zone of Rho1 activation is not always sufficient to generate aligned, anisotropic apical constriction. However, we wondered whether an asymmetric zone of Rho1 activation might contribute to the cell shape changes seen in ventral epithelial cells during ventral furrow formation. To address this question, we locally activated Rho1 in a square region in ventral cells before any obvious apical constriction. Rectangular activation regions result in more highly anisotropic constrictions than square activation regions (Figure 2.12c v. Figure 2.7e-VentralPost, 2.9, & 2.10). Thus, even though an asymmetric zone of Rho1 activation is not sufficient to induce anisotropic apical constriction in the dorsal epithelium, the asymmetry of the zone of Rho1 activation promotes the highly aligned anisotropic apical constriction in the ventral epithelium.

Taken together, these results suggest that an asymmetric zone of Rho1 activation and ventral-specific factors, genetically downstream of Dorsal and Twist, both independently contribute to the ability of ventral cells to respond to ectopic Rho1 activation with aligned, anisotropic apical constriction.

2.3.5 Spreading of deformations within the endogenous ventral furrow region

Thus far, we have focused on the dorsal or ventral epithelium before the endogenous ventral furrow begins invaginating. We next asked whether optogenetic Rho1 activation would affect an already invaginating ventral furrow. Activation of Rho1 in a subset of cells locally accelerates their invagination (Figure 2.13a). This suggests Rho1 activity is rate-limiting during the invagination of the endogenous ventral furrow. Notably, the invagination of neighboring ventral furrow cells, outside of the defined activation region is also accelerated (Figure 2.13a-red arrow). Furthermore, optogenetic activation of Rho1 in the ventral epithelium prior to the onset of invagination frequently induces the invagination of both cells inside and neighboring the activation region (Figure 2.13b-red arrow). These non-autonomous cellular responses are not observed in the dorsal epithelium (Figure 2.13c). This ventral-specific response occurs in less than a minute, a time scale that is consistent with mechanical, rather than mechanochemical, transmission of forces. Thus, cells within the ventral and dorsal epithelia may exhibit differential mechanical properties.

2.3.6 Differential responses of cells flanking the Rho1 activation zone in the dorsal and ventral epithelium

Collectively, the results presented here suggest that ventral and dorsal cells exist in distinct mechanical environments. To further explore this possibility, we generated ectopic zones of Rho1 activation and focused on the behavior of cells adjacent to these zones. In the ventral epithelium, we observed extensive bending of non-activated cells towards optogenetically-induced invaginations (Figure 2.14b, filled arrowheads). This bending is readily visualized in maximum projections of the ventral surface post optogenetic activation, and it routinely extends several rows outside of the zone of photoactivation (Figure 2.14b, filled arrowheads). In contrast, long-range bending toward the ectopic invagination is not observed in the dorsal

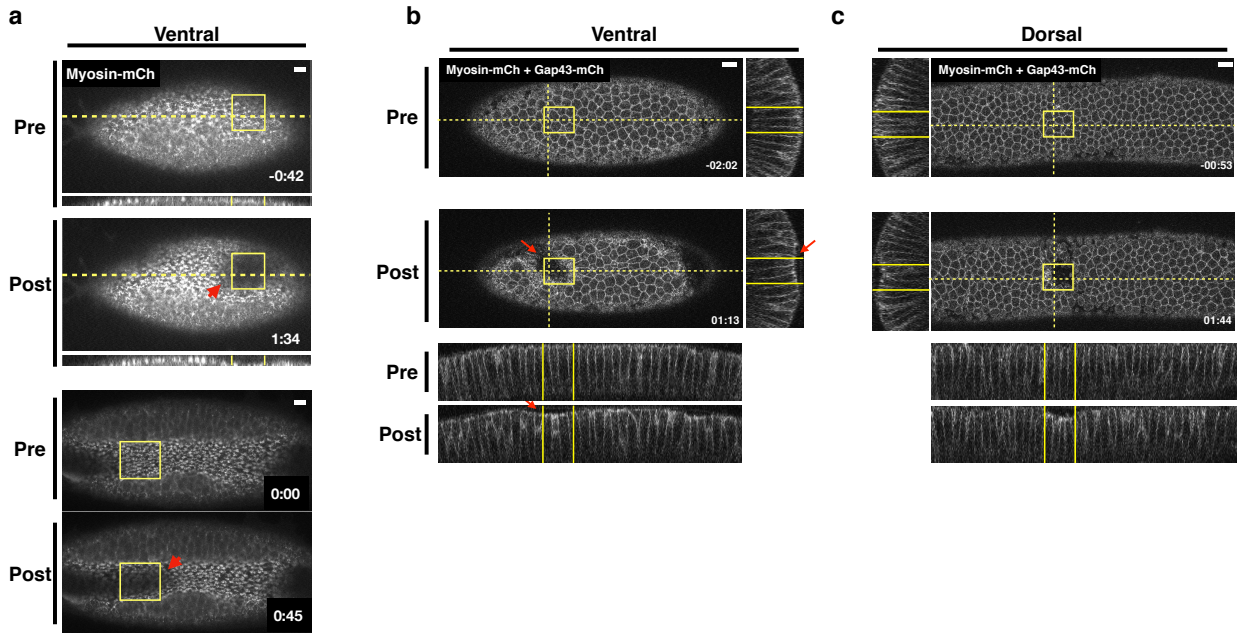

Figure 2.13: **Optogenetic Rho1 activation specifically induces cell non-autonomous responses in the ventral epithelium.**
a) Ventral epithelium of an embryos expressing the optogenetic components and Myosin-Ch and exhibiting an established furrow. Ectopic Rho1 activity accelerates the invagination of the endogenous ventral furrow. This acceleration extends outside of the zone of Rho1 activation (red arrow). Data representative of 3/5 embryos. b-c) Ventral (b) and dorsal (c) epithelium of an embryo expressing LOVSsrA, PR-GEF, Gap43-mCh, and Myosin-Ch at the onset of gastrulation. Optogenetic activation of Rho1 within the yellow box induces an ectopic invagination. This ectopic invagination extends outside the defined activation region in the ventral (b, red arrow) but not dorsal (c) epithelium. Data representative of 5/8 ventral and 4/4 dorsal embryos. Scale bars are 10 µm.

epithelium. Rather, the cells immediately adjacent to ectopic dorsal invaginations exhibit substantial stretching of their apical surfaces (Figure 2.14a, open arrowheads).

We quantified the bending of non-activated cells towards ectopic invaginations by measuring the change in the position of their apical centroids along the dorsal-ventral axis during the induction of the ectopic invaginations. Consistent with our visual observations, the centroids of the apical surface of non-activated ventral cells move substantially during the invagination of the photoactivated region, while the centroids of the apical surface of non-activated dorsal cells exhibit little movement during the comparable time (Figure 2.14c). Notably, dorsal cells neighboring ectopic invaginations are strongly biased towards expanding their apical surfaces, while the majority of ventral cells exhibit contraction of apical surfaces. Thus, not only do activated ventral and dorsal cells respond distinctly to optogenetic activation of Rho1, but the ventral and dorsal cells neighboring these regions of ectopic Rho1 activation respond distinctly to ectopic invaginations. These differential responses both within and adjacent to the activation zones suggest that the two epithelia exhibit differential mechanical properties.

2.4 Discussion

Given the extensive evidence implicating Rho1 activation in ventral furrow formation, we assessed whether an asymmetric zone of Rho1 activity is sufficient to initiate this morphogenetic process in the *Drosophila* embryo. Optogenetic activation of Rho1 in the dorsal epithelium does not recapitulate all cell- and tissue-level aspects of ventral furrow formation. However, Rho1 activation in the ventral epithelium induces cell- and tissue-level shape changes highly reminiscent of endogenous ventral furrow formation. Importantly, these changes are induced to occur earlier and more rapidly than they normally would. We propose that this context-dependent response to ectopic Rho1 activation arises from distinct material properties of the dorsal and ventral epithelia.

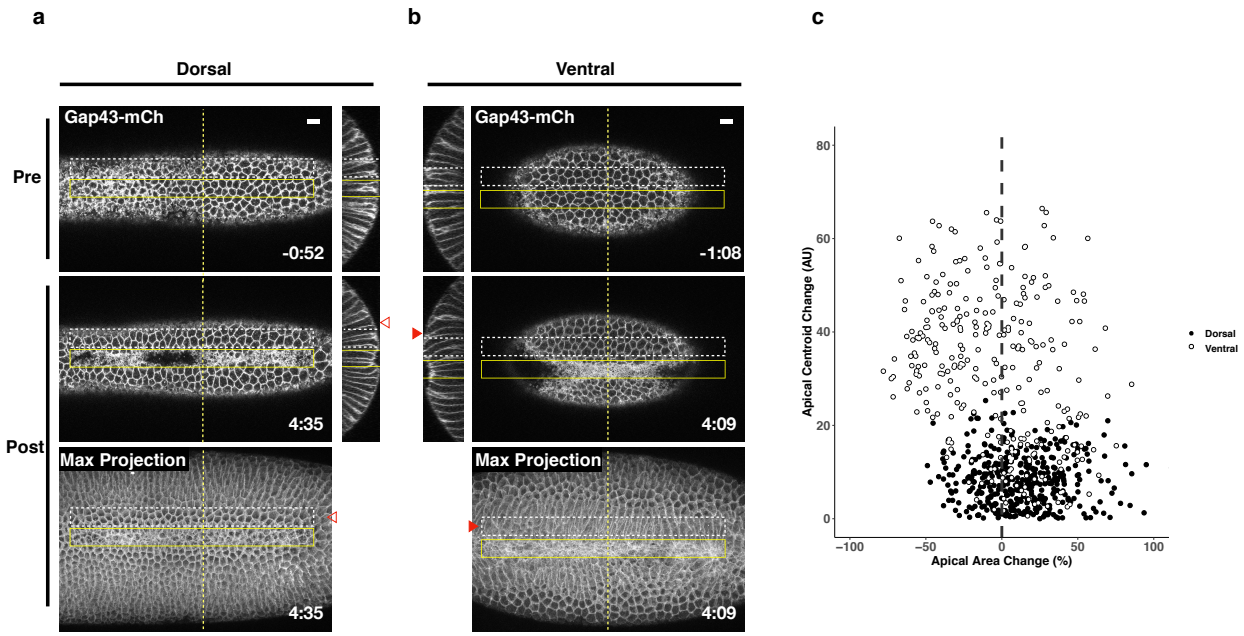

Figure 2.14: **Non-activated cells bend towards ectopic invaginations specifically in the ventral epithelium.**
a-b) Dorsal (a) and ventral (b) epithelium of embryos expressing the optogenetic components and Gap43-mCh at the onset of gastrulation. Local Rho1 activation within the yellow box induces ectopic invaginations in both the dorsal and ventral epithelium. Bottom panels: Maximum intensity projections of the indicated time point. Data representative of 4/4 dorsal and 4/4 ventral embryos. c) Quantification of cell shape changes exhibited by cells neighboring ectopic invaginations. X axis is the percent apical area change; Y axis is the change in position of the centroid of the apical cell surface along the dorsal-ventral axis. 407 dorsal cells from 4 embryos and 298 ventral cells from 4 embryos were quantified. The white dashed boxes in a and b indicate the "neighbor" cells that were quantified for these two embryos. Filled arrowheads indicate long-range bending of ventral cells; open arrowheads indicate the corresponding cells in the dorsal epithelium. Dorsal cells at the periphery are not perpendicular to the imaging plane before or after photoactivation and therefore do not appear as hexagons in the maximum projection images. Time zero indicates the first pulse of blue light activation. Scale bars are 10 µm.

2.4.1 A robust, ubiquitously expressed optogenetic system for use in Drosophila

The LOV-domain based optogenetic probe generated in this study is expressed ubiquitously throughout the *Drosophila* lifecycle. This ubiquitous and non-perturbing expression allows Rho1 activation to be readily controlled in any *Drosophila* tissue without the need to combine the probe with tissue-specific drivers. This probe acts rapidly, inducing Rho1 activity within a minute of photoactivation. Precise spatial control of Rho1 activation can be induced using a range of standard fluorescent imaging methods. Ectopic deformations induced by optogenetic Rho1 activation in the dorsal embryonic epithelium are limited to the zone of optogenetic Rho1 activation, and, in the wing peripodial epithelium, Rho1 can be activated with subcellular precision.

2.4.2 Optogenetically-induced invaginations are reversible

Using this optogenetic approach, we demonstrate that ectopic Rho1 activation is sufficient to induce ectopic, tissue-level shape changes throughout the embryonic epithelium at the onset of gastrulation. The cell shape changes induced by optogenetic Rho1 activation in ventral cells closely mirror those seen during endogenous ventral furrow formation, and ectopic Rho1 activation can modulate endogenous ventral furrow formation. This suggests that the potency of optogenetic activation of Rho1 via the LOV probe is on par with endogenous Rho1 activation during ventral furrowing.

Deformations induced by optogenetic activation of Rho1 persist through the duration of optogenetic activation. However, invaginated cells rapidly revert to their pre-activation positions and expand their apical areas following cessation of photoactivation, concurrent with rapid dissipation of optogenetically-induced myosin. Similar reversibilty occurs in the other tissues we examined as well as in cultured cells [Wagner and Glotzer, 2016, Oakes

et al., 2017]. This reveals the existence of potent, widespread mechanisms for inactivating Rho1 and its effectors. We infer that ventral furrow formation is driven by sustained Rho1 activation that overcomes this global inhibition.

2.4.3 PR-GEF and RhoGEF2-CRY2 induce distinct cellular responses

Our results are partially consistent with previous work, which activated Rho1 via membrane recruitment of a light-responsive RhoGEF2-CRY2 fusion protein [Izquierdo et al., 2018]. Both optogenetic systems induce ectopic deformations in the dorsal embryonic epithelium, but only RhoGEF2-CRY2 induces pulsatile Rho1 activity and anisotropic apical constriction in the dorsal epithelium.

The two systems use different RhoA/Rho1-specific GEFs, and this may underlie the differing results; LOV recruits LARG(DH) while CRY2 is fused to RhoGEF2(DHPH). Despite LARG being an extremely potent RhoA activator *in vitro* [Jaiswal et al., 2013], the transgene expressing LARG(DH) is well tolerated (Table 2.6), suggesting this recruitable GEF is non-perturbing. To directly compare LARG and RhoGEF2, we generated flies expressing SspB-GFP-RhoGEF2(DHPH) from the same genomic location as PR-GEF. This transgene does not readily homozygose even in the absence of the LOVSsrA membrane anchor (Table 2.6), suggesting it has significant light-independent activity. PH domains of the GEF subfamily that includes RhoGEF2 and LARG bind RhoA-GTP, and, *in vitro*, the interaction between the PH domain and membrane-bound RhoA-GTP potentiates GEF activity by up to 40 fold [Chen et al., 2010, Medina et al., 2013]. Introducing two point mutations (F1044A, I1046E) into the PH domain of RhoGEF2, which are predicted to disrupt its binding to RhoA-GTP, allows the resultant transgene to readily homozygose (Table 2.6). These observations are consistent with RhoGEF2-CRY2 acting via a feedforward mechanism where it can be recruited by Rho1-GTP via its PH domain and thereby amplify Rho1-GTP. The ability of RhoGEF2-CRY2 to amplify both endogenous and light-induced Rho1 activity

would be predicted to be particularly potent when it is overexpressed from a UAS promoter via Gal4. Feedforward activation via RhoGEF2-CRY2 may combine with the aforementioned mechanisms for Rho1 inactivation to generate the pulsatile Rho1 activity observed with RhoGEF2-CRY2 [Izquierdo et al., 2018]. Amplification of endogenous Rho1 activity by RhoGEF2-CRY2 could also explain the anisotropic apical constrictions induced when this probe is optogenetically activated in the dorsal epithelium. Activated cells in this epithelium would need to deform against increased resistive forces exerted by their neighbors as a result of chronic Rho1 activation.

Although the GEF domain of RhoGEF2 is perturbing when over-expressed as an isolated domain, in the context of the full length protein, its ability to generate positive feedback via its PH domain may contribute to the Rho1 activity pulses observed during ventral furrow formation [Martin et al., 2009, Mason et al., 2016].

2.4.4 Requirements for ventral-specific responses to Rho1 activation

Despite the ability of asymmetric zones of Rho1 activation to induce deformations in both dorsal and ventral embryonic epithelia, they only induced strong, aligned, anisotropic apical constriction in the ventral epithelium. Dorsal is required for and Twist promotes this ventral-specific response, consistent with the idea that this property is a consequence of the gene expression differences that result from dorsal-ventral patterning. Twist is required to stabilize Rho1-driven apical constriction [Martin et al., 2009]. Here, Twist promotes anisotropic apical constriction induced by sustained Rho1 activation. While it is possible that these two defects result from loss of the expression of a single Twist target gene, it is perhaps more likely that Twist controls the expression of multiple genes that independently contribute to ventral furrow formation. Notably, ventral cells lacking the Dorsal protein behave nearly identically to dorsal cells in wildtype embryos, while ventral cells lacking Twist exhibit weakly aligned, anisotropic apical constriction. Thus, a Twist-independent mechanism for generating aligned,

anisotropic apical constriction must also exist. We speculate that Snail may also contribute to ventral-specific behavior.

Alternatively, Dorsal and/or Twist may be required for anisotropic apical constriction because each factor promotes Rho1 activation by RhoGEF2. However, ventral cells depleted of RhoGEF2 exhibit an increase in magnitude and alignment of anisotropy following ectopic Rho1 activation; thus, elevated Rho1 activity alone does not explain this ventral-specific response. The muted change in anisotropy of ventral cells lacking RhoGEF2 compared to wildtype ventral cells can be explained by the fact that cells depleted of RhoGEF2 exhibit higher degrees of anisotropy prior to optogenetic activation of Rho1, most likely because the epithelium is disorganized due to defects in cytoskeletal organization and cellularization [Padash Barmchi et al., 2005]. Future work should identify the molecular targets of Dorsal and Twist that mediate anisotropic apical constriction. Two candidates of particular interest are Rap1 and its GEF Dzy; ventral cells lacking either of these proteins exhibit more isotropic apical constriction than wildtype ventral cells [Sawyer et al., 2009, Spahn et al., 2012].

2.4.5 Ventral and dorsal epithelia exhibit different material properties

The response of embryonic epithelial cells to optogenetic Rho1 activation depends on their location within the epithelium. Specifically, ventral, but not dorsal, cells constrict anisotropically, ventral deformations spread outside the activated regions, and several rows of epithelial cells bend toward activated ventral regions. Thus, the differences seen upon Rho1 activation are not limited to the response of the activated cells to Rho1 activation.

We propose that these ventral-specific behaviors arise as a consequence of dorsoventral patterning that endows the ventral epithelium with material properties that are distinct from those of the dorsal epithelium. These material properties (e.g. stiffness, deformability) likely result from differential organization and dynamics of the cytoskeleton and the junctions linking the cytoskeletons of neighboring cells. This dorsoventral patterning appears to specify

the length scale over which forces are transmitted through the tissue. Importantly, these properties do not solely result from Rho1 activation in ventral cells, as RhoGEF2-depleted cells retain some ventral characteristics. We suggest that these material properties shape the reciprocal interactions between Rho1-activated cells and their neighbors, influencing the response both within and outside the Rho1 activated region.

The molecules responsible for ventral-specific material properties are not known, but it may include regulated cell-cell adhesion and the associated cytoskeletal networks. During ventral furrow formation, E-cadherin molecules in ventral cells reorganize from a sub-apical position to an apical position and become more densely packed [Weng and Wieschaus, 2016]. These junctional rearrangements may contribute to efficient transmission of intracellular contractility throughout the ventral epithelium. Junctions transmit these forces through interactions with the actomyosin cytoskeleton which in turn influence the behavior of adherens junctions [Weng and Wieschaus, 2016]. These interactions ultimately generate the supracellular actomyosin network observed during ventral furrow formation [Martin et al., 2010, Yevick et al., 2019]. In our experiments, ectopic Rho1 activation was not sufficient to induce such networks in the dorsal epithelium, indicating a requirement for ventral-specific factors in their assembly.

The cellular behaviors observed during light-induced invaginations are remarkably similar to those that occur during endogenous ventral furrowing [Costa et al., 1994, Leptin et al., 1992, Leptin and Grunewald, 1990, Sweeton et al., 1991]. These shape changes were widely thought to occur as a direct consequence of the transcriptional induction of Rho1-dependent contractility in the ventral epithelium. By comparing identical patterns and intensity of Rho1 activation in wildtype and mutant tissues, we have shown that dorsoventral patterning has additional relevant targets beyond Rho1 activation.

2.4.6 Conclusion

In summary, this work shows that, despite inducing ectopic deformations, Rho1 activation alone is not sufficient to recapitulate the cell- and tissue-level behaviors observed during ventral furrow formation. Thus, a model of ventral furrow formation where Rho1 activity is the sole driver of cell and tissue behavior is incomplete. We propose that ventral-specific behaviors may arise from expression of factors that modulate the cytoskeleton and its connection to adherens junctions as well as promote strong intercellular coupling among cells of the ventral epithelium.

2.5 Methods and Materials

2.5.1 Plasmids

Plasmids used in this studied are listed in Table 2.1. pUbi-stop-mCD8GFP containing an attB site and pUbi>mEGFP-Anillin(RBD) were gifts from T. Lecuit. Plasmids created for this study were generated using SLiCE [Zhang et al., 2012] or one-step isothermal *in vitro* recombination [Gibson et al., 2009]. Stargazin-GFP-LOVpep and PDZx2-mCherry-LARG(DH) plasmids were published previously [Wagner and Glotzer, 2016]. Venus-iLID-CAAX and tgRFPt-SspB WT were obtained from Addgene (60411, 60415). pMT>Gal4 [Klueg et al., 2002] was obtained from the Drosophila Genomics Resource Center.

2.5.2 Fly stocks

Drosophila melanogaster was cultured using standard techniques at 25°C. Both male and female animals were used. Stocks used in this study include *pUbi>Gap43-mCherry/TM3*, generated by P-element insertion and was a gift from A. Martin; *pSqh>Sqh-mCherry* [Martin et al., 2009]; Δ *halo AJ* $twist^{EY53R12}$/CyO, a gift from M. Leptin; dl^{1} cn^{1} sca^{1}/CyO (BID:

3236); *UAS>RhoGEF2 shRNA* (BID: 76255); *P(mat-tub-Gal4)mat67* (BID: 7062).

Transgenic flies were generated by PhiC31-directed integration (GenetiVision). Transgenic lines generated for this study include: *Ubi>Stargazin-GFP*-LOVSsrA (attP2), Ubi>Stargazin-GFP*-LOV(I427V)SsrA (attP2), Ubi>SspB-GFP-LARG(DH) (VK37), Ubi>SspB-GFP-LARG(DH) (VK31), Ubi>SspB-GFP- RhoGEF2(DHPH) (VK37), Ubi>SspB-GFP-RhoGEF2(DHPH-F1044A, I1046E) (VK37), Ubi>SspB-mScarlet (VK37), Ubi>mCherry-Anillin(RBD) (attP40).*

Genotypes of flies used in each experiment are listed in Table 2.3 and Table 2.4.

2.5.3 S2 cells

3.1 x 10^6 S2 cells were transfected with 100 ng pMT>tagRFP-SspB and 250 ng pMT>Stargazin-GFP*-LOVSsrA or 250ng pMT>Stargazin-GFP*-LOV(I427V)SsrA using dimethyldioctadecyl-ammonium bromide (Sigma) [Han, 1996] at 250 ug/mL in six well plates. Expression from the pMT promoter was induced 2 days after transfection by addition of 0.35 mM $CuSO_4$. Cells were imaged live 24 hrs after $CuSO_4$ induction. 50 µL of the S2 cell culture was plated on a glass slide and covered with a coverslip. Clay feet were used as spacers between the slide and coverslip. See Table 2.5 for activation protocol details.

2.5.4 Preparation of Drosophila tissues for live imaging

Drosophila embryos were collected on apple juice agar plates for 90 min and aged for 90-120 min at 25°C such that a majority of embryos were completing cellularization at the time of mounting. Embryos were dechorionated in 30% bleach for 1 min, rinsed in water, aligned on an apple juice agar pad, and mounted on a coverslip with embryo glue (adhesive from double sided tape dissolved in heptane). The imaged surface (dorsal or ventral) was mounted on the coverslip. This coverslip was affixed via petroleum jelly to a metal slide with a hole in the center. Embryos were covered with halocarbon oil 200 immediately after mounting; they

were not compressed.

Central nervous systems were dissected from wandering third instar larvae in Schneider's *Drosophila* Medium (Sigma) supplemented with 10% Fetal Bovine Serum (Thermo Fisher Scientific). Central nervous systems were imaged in a chamber comprising a coverslip affixed with petroleum jelly to a metal slide with a hole in the center. Following dissection, central nervous systems were mounted in the chamber such that their dorsal side contacted the coverslip. The chamber was flooded with Chan and Gerhing's balanced solution [Chan and Gehring, 1971] to completely cover the central nervous system, and a gas-permeable membrane (YSI: 5793) was placed over the chamber to limit evaporation. These chambers were imaged on an inverted microscope.

Wing imaginal discs were dissected from wandering third instar larvae in S2 cell media supplemented with 10% FBS. Wing discs were mounted between a slide and glass coverslip in 50uL Chan and Gehring's balanced solution. Clay feet were used as spacers between the slide and coverslip.

To prepare pupal nota, whole pupae were extracted from their pupal cases 18 hours post pupariation and mounted on a glass slide in a humid chamber, as described previously [Zitserman and Roegiers, 2011]. Pupal nota were imaged on an upright microscope.

To image egg chambers, ovaries were dissected from 3-5 day old females aged on yeast. Individual stage 10 egg chambers were isolated and mounted between a coverslip and a slide. Clay feet were used as a spacer between the slide and coverslip.

2.5.5 Live imaging and optogenetic experiments

Global activation experiments were performed on a 63x/1.4 numerical aperture (NA) oil immersion lens on a Zeiss Axiovert 200M equipped with a Yokogawa CSU-10 spinning disk unit (McBain) and illuminated with 50-mW, 473-nm and 20- mW, 561-nm lasers (Cobolt) or on a Zeiss Axioimager M1 equipped with a Yokogawa CSU-X1 spinning disk unit (Solamere)

and illuminated with 50-mW, 488-nm and 50-mW, 561-nm lasers (Coherent). Images were captured on a Cascade 1K electron microscope (EM) CCD camera, a Cascade 512BT (Photometrics), or a Prime 95B (Photometrics) controlled by MetaMorph (Molecular Devices). Photoactivation was accomplished by illuminating the sample with 488 nm light for the indicated exposure times (Table 2.5.

Local activation experiments were performed on a inverted Zeiss LSM880 laser scanning confocal microscope with a 40X/1.4 numerical aperture (NA) objective. mCherry or mScarlet fluorescence was excited using the 561 nM solid state laser and was detected via a GaAsP spectral detector. Activation regions, indicated with yellow boxes throughout this manuscript, were defined in the "Bleaching" module. Pixels within the defined activation zone were exposed to 488nm light attenuated to 0.01 or 0.1 percent laser transmittance, using an Acousto-optic tunable filter, for 15 iterations every 20 seconds for the duration of the activation period. In general, we acquired a "pre" Z-Series of Gap43-mCh or Sqh-mCh, activated the defined region with 488nm light in a single Z-plane, and acquired a "post" Z-Series of Gap43-mCh or Sqh-mCh. See Table 2.5 for specific activation protocols for each experiment.

2.5.6 Image processing and cell shape analysis

All images were processed with FIJI [Schindelin et al., 2012]. TissueAnalyzer [Aigouy et al., 2010], a FIJI plugin, was used to segment the embryonic epithelium and track cells for quantification of apical area, apical cell anisotropy, and apical cell centroid. "Pre" and "Post" Z-stacks were tracked separately in TissueAnalyzer, and data for the apical area, apical cell elongation (a proxy for anisotropy), and apical cell centroid were extracted from each timepoint and concatenated into a master database

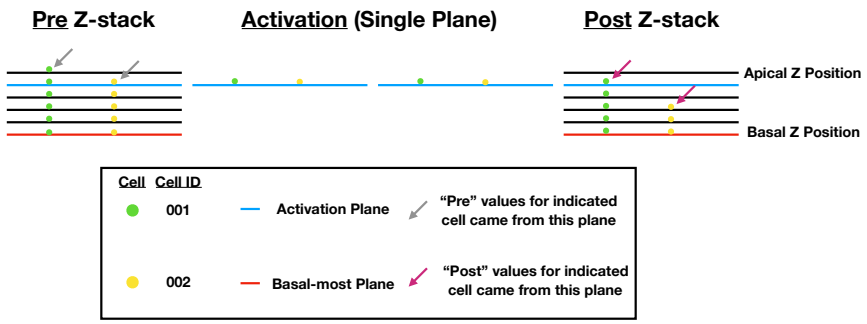

Figure 2.15: **Schematic of data collection and analysis for local activation experiments**

2.5.7 Statistics

Kruskal-Wallis rank sum tests and Wilcoxon signed rank tests were used as noted. All statistical tests were performed in R Studio.

2.6 Acknowledgements

This work was supported by R01GM085087, R35GM12709, and a France and Chicago Collaborating through the Sciences grant (M.G.), R01NS034783 (R.G.F), and NIH T32 GM007183 and NSF GRFP DGE-1144082; DGE-1746045 (A.R). We thank Ed Munro, Angika Basant, and Yu Chung Tse for helpful comments on this manuscript. We thank Ed Munro, Sally Horne-Badovinac, Thomas Lecuit, M.G. lab members, and R.G.F. lab members for helpful discussions and support. Alyssa Harker provide assitance with SQL. Benoit Aigouy provided assistance with TissueAnalyzer. Audrey Williams helped with oocyte dissections. We thank the Glick, Martin, Leptin, and Lecuit labs for generous sharing of reagents. We thank Ben Glick for access to the SnapGene molecular biology software (http://www.snapgene.com). Stocks obtained from the Bloomington *Drosophila* Stock Center (NIH P40OD018537) were used in this study. Reagents obtained from *Drosophila* Genomics Resource Center, supported by NIH grant 2P40OD010949 were used in this study.

Table 2.1: Chapter 2 Plasmids Used

Plasmid Generated	Fragment Source	Backbone Source
pMT>Stargazin-GFP*-LOVSsrA (* represents inactivation of fluorphore with Y66C mutation.)	Stargazin-GFP amplified from Stargazin-GFP-LOVpep [Wagner and Glotzer, 2016] LOVSsrA amplified from Venus-iLID-CAAX [Guntas et al., 2015] (Addgene: 60411) GFP silenced by site-directed mutagenesis (Y66C)	pMT>Gal4 [Klueg et al., 2002]
pMT>Stargazin-GFP*-LOV(I427V)SsrA	N/A	pMT>Stargazin-GFP* -LOVSsrAw/ site directed mutagenesis
pUbi>Stargazin-GFP*-LOVSsrA	Stargazin-GFP*-LOVSsrA amplified from pMT>Stargazin-GFP*-LOVSsrA	pUbi-stop-mCD8GFP (Contains attB site)
pUbi>Stargazin-GFP*-LOV(I427V)SsrA	Stargazin-GFP*-LOV(I427V)SsrA amplified from pMT>Stargazin-GFP*-LOV(I427V)SsrA	pUbi-stop-mCD8GFP (Contains attB site)
pUbi>SspB-GFP-LARG(DH)	LARG(DH) amplified from PDZx2-mCherry-LARG(DH) [Wagner and Glotzer, 2016] SspB amplified from tgRFPt-SspB(WT) [Guntas et al., 2015] (Addgene: 60415)	pUbi-stop-mCD8GFP (Contains attB site)
pMT>tagRFP-SspB	SspB amplified from tgRFPt-SspB(WT) [Guntas et al., 2015] (Addgene: 60415)	pMT>Gal4
pUbi>SspB-mScar	SspB amplified from pMT>tagRFP-SspB mScar amplified from pmScarlet-C1 (Addgene: 85042)	pUbi-stop-mCD8GFP (Contains attB site)

Table 2.2: Chapter 2 Plasmids Used (Cont.)

Plasmid Generated	Fragment Source	Backbone Source
pUbi>SspB-GFP-RhoGEF2(DHPH)	RhoGEF2(DHPH) amplified from genomic prep of Sp/CyO; UASp>RFP-RhoGEF2/TM3 [Wenzl et al., 2010]	pUbi-SspB-GFP-LARG(DH) (Replace LARG(DH)) (Contains attB site)
pUbi>SspB-GFP-RhoGEF2(DHPH-F1044A,I1046E)	N/A	pUbi>SspB-GFP-RhoGEF2(DHPH) w/ site directed mutagenesis
pUbi>mCherry-Anillin(RBD)	Anillin(RBD) amplified from pUbi>mEGFP-Anillin(RBD) [Munjal et al., 2015] mCherry amplified from pm-Cherry2B (F. Valbuena and B. Glick, manuscript in preparation)	pUbi-stop-mCD8GFP (Contains attB site)

Table 2.3: Chapter 2 Genotypes and Reproducibility

Figure	Genotype	Replicates
2.1b	*SspB-mScarlet ; Stargazin-GFP*-LOVSsrA*	4/4 embryos
2.1d	*SspB-GFP-LARG(DH) ; Stargazin-GFP*-LOVSsrA, Sqh-mCherry / Stargazin-GFP*-LOVSsrA*	5/5 embryos
2.2a	*SspB-GFP-LARG(DH); Stargazin-GFP*-LOVSsrA, Sqh-mCherry*	2/2 pupae
2.2b		4/4 egg chambers
2.2c		5/5 (left), 3/3 (right) wing discs
2.2d		2 CNSs ; 6 Neuroblasts
2.3	*SspB-GFP-LARG(DH); Stargazin-GFP*-LOVSsrA, Sqh-mCherry*	3/3 wing discs
2.4a-top	Transfection: tagRFP-SspB + Stargazin-GFP*-LOVSsrA	3/3 cells
2.4a-bottom	Transfection: tagRFP-SspB + Stargazin-GFP*-LOV(I427V)SsrA	3/3 cells
2.4c-top	*SspB-GFP-LARG(DH) Ubi>mCherry-Anillin(RB); Stargazin-GFP*-LOVSsrA*	3 brains ; 16 neuroblasts
2.4c-bottom	*SspB-GFP-LARG(DH) Ubi>mCherry-Anillin(RB); Stargazin-GFP*-LOV(I427V)SsrA*	4 brains ; 19 neuroblasts
2.5	*SspB-GFP-LARG(DH) ; Stargazin-GFP*-LOVSsrA, Sqh-mCherry/ Stargazin-GFP*-LOVSsrA*	7/7 embryos (a) 5/5 embryos (b)
2.6	*SspB-GFP-LARG(DH) ; Stargazin-GFP*-LOVSsrA, Sqh-Ch/ Stargazin-GFP*-LOVSsrA*	5/5 embryos (dorsal) 4/4 embryos (ventral)
2.7	*SspB-GFP-LARG(DH); Stargazin-GFP*-LOVSsrA, Gap43-mCherry*	2/2 embryos; 7/8 cells (a) 4/4 embryos; 444 cells (b) 4/4 embryos; 288 cells (c)
2.8	*SspB-GFP-LARG(DH) ; Stargazin-GFP*-LOVSsrA, Gap43-Ch*	3/3 embryos
2.9	see Fig. 3 & 4	see Fig. 3 & 4
2.10	see Fig. 3 & 4	see Fig. 3 & 4
2.11	*SspB-GFP-LARG(DH) ; Stargazin-GFP*-LOVSsrA, Gap43-Ch*	4/4 embryos

Table 2.4: Chapter 2 Genotypes and Reproducibility (Cont.)

Figure	Genotype	Replicates
2.12	1) Δ *halo AJ twist*^{EY53R12} *; SspB-GFP-LARG(DH), Stargazin-GFP*-LOVSsrA, Gap43-mCherry* 2) *dl*^{1} *cn*^{1} *sca*^{1} *; SspB-GFP-LARG(DH), Stargazin-GFP*-LOVSsrA, Gap43-mCherry* 3) *P(mat-tub-Gal4)mat67 / SspB-GFP-LARG(DH); SspB-GFP-LARG(DH), Stargazin-GFP*-LOVSsrA, Gap43-mCherry / Stargazin-GFP*-LOVSsrA UAS>RhoGEF2 shRNA* 4) *SspB-GFP-LARG(DH);Stargazin-GFP*-LOVSsrA, Gap43-mCherry (square zone)*	1) 3/3 embryos ; 189 cells 2) 4/4 embryos ; 343 cells 3) 5/5 embryos ; 375 cells 4) 5/5 embryos ; 239 cells
2.13a	*SspB-GFP-LARG(DH) ; Stargazin-GFP*-LOVSsrA, Sqh-Ch*	3/5 embryos
2.13b-c	*SspB-GFP-LARG(DH) ; Stargazin-GFP*-LOVSsrA, Gap43-mCherry / Stargazin-GFP*-LOVSsrA, Sqh-mCherry*	5/8 embryos (ventral, b) 4/4 embryos(dorsal, c)
2.14	*SspB-GFP-LARG(DH); Stargazin-GFP*-LOVSsrA, Gap43-mCherry*	4/4 embryos (a) 4/4 embryos (b) 407 cells, dorsal (c) 298 cells, ventral (c)

Table 2.5: Chapter 2 Activation Protocols

Figure	Microscope, Wavelength	Activation Protocol	Total Activation Time
2.1b	LSM880, 488nm	Every 20 sec	1 min 40 sec
2.1d	Spinning Disc, 488nm	Global (1000ms) every 20 sec	1 min
2.2a	Spinning Disc, 488nm	Global every 15 sec	30 sec
2.2b	Spinning Disc, 488nm	Global every 5 sec	15 sec
2.2c	LSM880, 488nm	Every 20 sec	2:01 min (left) 1:40 (right)
2.2d	LSM880, 488nm	Every 20 sec	1 min
2.3	LSM880, 405nm	Every 20 sec (See indicated percent transmittance)	2 min 20 sec
2.4a-b	Spinning Disc, 488nm	Global every 5 sec	5 sec
2.4c	Spinning Disc, 488nm	Global every 5 sec	20 sec
2.5a-b	LSM880, 488nm	Every 20 sec	4min
2.6	LSM880, 488nm	Every 20 sec	6 min 35 sec (left) 4 min 11 sec (right)
2.7a-b	LSM880, 488nm	Every 20 sec	4 min
2.11	LSM880, 488nm	Every 20 sec	1 min 40 sec
2.12	LSM880, 488nm	Every 20 sec	4 min
2.13a	LSM880, 488nm	Every 20 sec	1 min 20 sec
2.13b	LSM880, 488nm	Every 20 sec	1 min 20 sec
2.13c	LSM880, 488nm	Every 20 sec	1 min 40 sec
2.14a-b	LSM880, 488nm	Every 20 sec	4 min

Table 2.6: Recruitable GEF Viability Tests

Cross Scored	Possible Genotype	Observed	Expected	Chi²
SspB-GFP-LARG(DH)/CyO x SspB-GFP-LARG(DH)/CyO	1) LARG (DH)/CyO 2) LARG(DH)/LARG(DH)	379 165	362.7 181.3	2.198
SspB-GFP-RhoGEF2(DHPH)/CyO x SspB-GFP-RhoGEF2(DHPH)/CyO	1) RhoGEF2(DHPH)/CyO 2) RhoGEF2(DHPH)/RhoGEF2(DHPH)	318 54	248 124	59.27
SspB-GFP-RhoGEF2 (DHPH-F1044A,I1046E)/CyO x SspB-GFP-RhoGEF2 (DHPH-F1044A,I1046E)/CyO	1) RhoGEF2(DHPH*)/CyO 2) RhoGEF2(DHPH*)/RhoGEF2(DHPH*)	430 192	414.7 207.3	1.694

CHAPTER 3

OPTOGENETIC DISSECTION OF *DROSOPHILA* NEUROBLAST POLARIZATION

3.1 Abstract

The *Drosophila* neuroblast, the precursor of the central nervous system, is a well-studied example of cell polarization. At the onset of mitosis, polarity factors and cell fate determinants polarize into distinct apical and basal crescents, ultimately driving a stem cell-like asymmetric cell division. PAR proteins, including Bazooka, aPKC, Par6, and Cdc42, are key regulators of neuroblast polarization, but the mechanisms by which these polarity factors rapidly reorganize during neuroblast polarization are poorly understood. For example, Cdc42, a conserved polarity regulator, is required during neuroblast polarization, but when and where does Cdc42 act during this polarization? Furthermore, what minimal set of factors is needed to nucleate an apical crescent? Answering these and related questions necessitates tools that can characterize and manipulate protein activity with high spatial and temporal resolution. Toward this end, we report the development of a Cdc42 biosensor that detects active Cdc42 in *Drosophila* tissues. Furthermore, we developed optogenetic probes to control the activity of Cdc42 as well as the localization of aPKC and a fragment of Bazooka (Par3) in the *Drosophila* central nervous system. These tools promise to deepen our understanding of PAR protein dynamics during *Drosophila* neuroblast polarization. Finally, we provide evidence of a novel interaction between aPKC and a fragment of Par6 containing only the CRIB and PDZ domains, emphasizing that there is still much to discover about the molecular interactions governing neuroblast polarization.

3.2 Introduction

Polarization generates cellular domains of distinct morphology, size, and/or molecular identity [St Johnston and Ahringer, 2010]. The biological implications of polarization varies in different contexts: Polarization underlies directed cell migration and is essential for epithelia formation, maintenance, and function. Furthermore, polarization enables asymmetric cell divisions, such as stem cell divisions, that generate diverse cell types. To fully understand how cells accomplish these diverse cellular processes, we must delineate the mechanism(s) by which cells polarize.

Drosophila neuroblasts, the precursors of the *Drosophila* central nervous system, are a well-studied model of cell polarization. Neuroblasts delaminate from the embryonic ventral neuroectoderm and undergo repeated rounds of asymmetric division along the apicobasal axis to produce a larger, apical, self-renewing neuroblast and a smaller, basal, differentiating ganglion mother cell [Hartenstein and Wodarz, 2013]. Polarization of PAR proteins precedes and enables the asymmetric division of *Drosophila* neuroblasts. This group of proteins includes aPKC/PKC-3, Bazooka/PAR-3, Par6, Cdc42, Par1, and Lgl. These proteins are highly conserved and establish cell polarity in many organisms and cell types [Suzuki and Ohno, 2006]. Prior to each asymmetric neuroblast division, PAR proteins, including Bazooka, Par6, and aPKC, accumulate at the apical cortex; this apical complex segregates into the neuroblast stem cell during cell division [Rolls et al., 2003, Petronczki and Knoblich, 2001, Schober et al., 1999]. In contrast, cell fate determinants, including Prospero (Pros), Brain Tumor (Brat), and Numb, and their adaptor proteins, including Partner of Numb (Pon) and Miranda (Mira), accumulate at the basal cortex of mitotic neuroblasts and segregate into the differentiating ganglion mother cell (GMC) [Betschinger et al., 2006, Bello et al., 2006, Lee et al., 2006a,c, Wang et al., 2006, Lu et al., 1998, Ikeshima-Kataoka et al., 1997, Shen et al., 1997]. Notably, this cortical polarity is re-established at the onset of prophase, prior to

each neuroblast division [Prehoda, 2009, Siegrist and Doe, 2006]. The molecular interactions among PAR proteins were discussed in Chapter 1.2.

aPKC is a key effector of neuroblast polarization. This kinase phosphorylates basal factors, including Numb and Mira, neutralizing positively charged membrane binding motifs in these proteins and antagonizing their association at the apical cortex [Bailey and Prehoda, 2015, Atwood and Prehoda, 2009, Smith et al., 2007]. Larval neuroblasts lacking aPKC exhibit uniformly cortical Mira, demonstrating the importance of aPKC in neuroblast polarization [Rolls et al., 2003]. Notably Bazooka localization is unperturbed in neuroblasts lacking aPKC; thus, aPKC functions downstream of Bazooka [Rolls et al., 2003]. Overexpression of membrane-targeted aPKC (aPKC-CAAX) displaces Mira from the entire neuroblast cortex [Lee et al., 2006b], suggesting aPKC may be sufficient to polarize basal factors in neuroblasts. Despite this central role of aPKC in neuroblast polarization, it is not clear whether aPKC is sufficient *in vivo* to restrict the localization of cell fate determinants and adaptors in neuronal precursors. Moreover, the dynamics of aPKC activity have not been investigated: How rapidly do cell fate determinants and adaptor proteins re-associate with the cortex following silencing of aPKC activity? Is there cell cycle regulation of cell fate determinants' or adaptor proteins' ability to respond to aPKC activity?

In contrast to the well studied role of aPKC in neuroblast polarization, the role of Cdc42, a Rho family GTPase, remains unclear. Cdc42 is a conserved regulator of polarization; it mediates symmetry breaking and bud site selection in budding yeast [Bi and Park, 2012] and maintains PAR polarization in the C. elegans zygote [Motegi and Sugimoto, 2006]. Larval neuroblasts lacking Cdc42 do not accumulate aPKC or Par6 on their cortex and exhibit uniformly cortical Mira [Atwood et al., 2007]. Additionally, Cdc42 binding activates the PDZ domain of Par6 [Peterson et al., 2004]. Taken together, these data suggest that Cdc42 may play a role in initiating and/or maintaining cell polarization in *Drosophila* neuroblasts. Antibody staining suggests that Cdc42 is apically enriched in mitotic neuroblasts [Atwood et al.,

2007], but the activity profile of Cdc42 during neuroblast polarization has not been characterized. Furthermore, it is unclear how Cdc42 becomes active in *Drosophila* neuroblasts, as no Cdc42 GEFs have been found to be required for neuroblast polarization. Finally, the possibility that Cdc42 activity is sufficient to polarize neuroblasts has not been investigated.

While genetic and biochemical approaches have generated a detailed model of neuroblast polarization, the open questions posed above remain open because they necessitate methods that can rapidly and sensitively detect protein activity in real time as well as tools that can acutely manipulate Cdc42 and aPKC activity *in vivo*. Here, we describe the development of two biosensors that detect Cdc42 activity in S2 cells and in *Drosophila* tissues. Furthermore, we generate optogenetic probes that manipulate Cdc42 activity, Baz localization, and aPKC activity *in vitro* and *in vivo*.

3.3 Results

3.3.1 Detecting endogenous Cdc42 activity

Characterizing the endogenous pattern of Cdc42 activity during neuroblast polarization necessitates the development of a robust biosensor for Cdc42 activity. One successful approach for generating biosensors is to fuse the Cdc42-GTP binding domain of a GTPase effector to a fluorescent protein [Kumfer et al., 2010, Tong et al., 2007]. In this vein, we fused tagRFP to the GTPase binding region of two *Drosophila* proteins known to bind Cdc42-GTP: WASp and Par6 [Peterson et al., 2004, Ben-Yaacov et al., 2001]. When expressed in S2 cells, tagRFP-WASp^{GBD} and tagRFP-Par6$^{CRIB-PDZ}$ are cytoplasmic and nuclear (Figure 3.1). Co-expression of wildtype Cdc42 induced cortical accumulation of tagRFP-WASp^{GBD} and tagRFP-Par6$^{CRIB-PDZ}$ in a subset of S2 cells (Figure 3.1). Co-expression of constitutively active Cdc42 induced cortical accumulation of tagRFP-WASp^{GBD} in a larger proportion of S2 cells (Figure 3.1). These results suggest both biosensors can detect

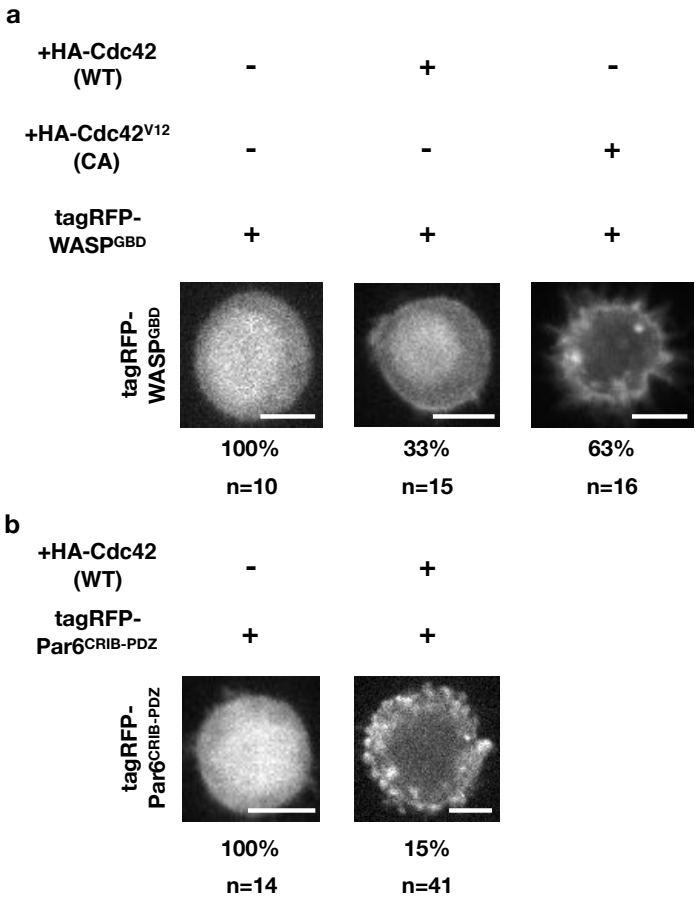

Figure 3.1: **Putative Cdc42 biosensors respond to Cdc42 overexpression in S2 cells.**
S2 cells expressing tagRFP-WASp^{GBD} (a) or tagRFP-Par6$^{CRIB-PDZ}$ (b) alone, or with overexpression of wildtype Cdc42, or with overexpression of constitutively active Cdc42, as indicated. n indicates number of cells scored; percentages below image indicate percent of cells displaying that phenotype. Scale bars are 5 µm.

Cdc42-GTP.

We generated transgenetic flies expressing tagRFP-WASp^{GBD} or tagRFP-Par6$^{CRIB-PDZ}$ from a Ubiquitin promoter. Ubi>tagRFP-WASp^{GBD} expression was extremely weak, so we focused on Ubi>tagRFP-Par6$^{CRIB-PDZ}$ in flies. We also generated UAS>tagRFP-Par6$^{CRIB-\ PDZ}$. Both Ubi and UAS driven tagRFP-Par6$^{CRIB-PDZ}$ are well tolerated and express in the *Drosophila* larval central nervous system and larval wing imaginal disc (Figure 3.2a,c). Ubi>tagRFP-Par6$^{CRIB-PDZ}$ is mostly diffuse throughout the cytoplasm

of *Drosophila* neuroblasts, and overexpression of constitutively active Cdc42 greatly enhances the cortical accumulation of this transgene (Figure 3.2a,b). Notably, Ubi>tagRFP-Par6$^{CRIB-PDZ}$ exhibits cortical accumulation in the neuroepithelium (Figure 3.2a-red arrow). This is likely due to the fact that this probe retains the ability to interact with aPKC and Bazooka (see below).

Worniu-Gal4 driven UAS>tagRFP-Par6$^{CRIB-PDZ}$ exhibits higher cortical accumulation than Ubi>tagRFP-Par6$^{CRIB-PDZ}$ (Figure 3.2a,c), suggesting higher expression levels of tagRFP-Par6$^{CRIB-PDZ}$ may more effectively report on Cdc42 activity. Depletion of Cdc42 in the central nervous system or wing imaginal disc dramatically reduces the cortical accumulation of tagRFP-Par6$^{CRIB-PDZ}$ (Figure 3.2c-e). Collectively, these results suggest tagRFP-Par6$^{CRIB-PDZ}$ detects Cdc42 activity *in vivo*.

We attempted to characterize the endogenous pattern of Cdc42 activity during neuroblast polarization by combining Ubi>tagRFP-Par6$^{CRIB-PDZ}$ with Histone-GFP, as a marker for cell cycle stage. In a few instances we observed increased biosensor signal at the apical cortex during prophase, but Ubi>tagRFP-Par6$^{CRIB-PDZ}$ exhibited a low signal to noise ratio and was sensitive to photobleaching. Thus, we were unable to map the endogenous pattern of Cdc42 activity in *Drosophila* neuroblasts (see discussion).

3.3.2 Optogenetic manipulation of Cdc42 activity

Determining whether Cdc42 activity is sufficient to instruct neuroblast polarization requires a method for acutely activating Cdc42 *in vivo*. Toward this end, we adapted an optogenetic probe to activate Cdc42 in *Drosophila* [Guntas et al., 2015, Strickland et al., 2012]. This probe compromises a membrane localized LOV domain fused to an SsrA peptide and the SspB protein fused to GFP and the Dbl homology (DH) and pleckstrin homology (PH) domains of Intersectin, a Cdc42-specific GEF (Figure 3.3a) [Guntas et al., 2015, Jaiswal et al., 2013]. (Intersectin-GFP-SspB is hereafter called Cdc42GEF.) Blue light induces a

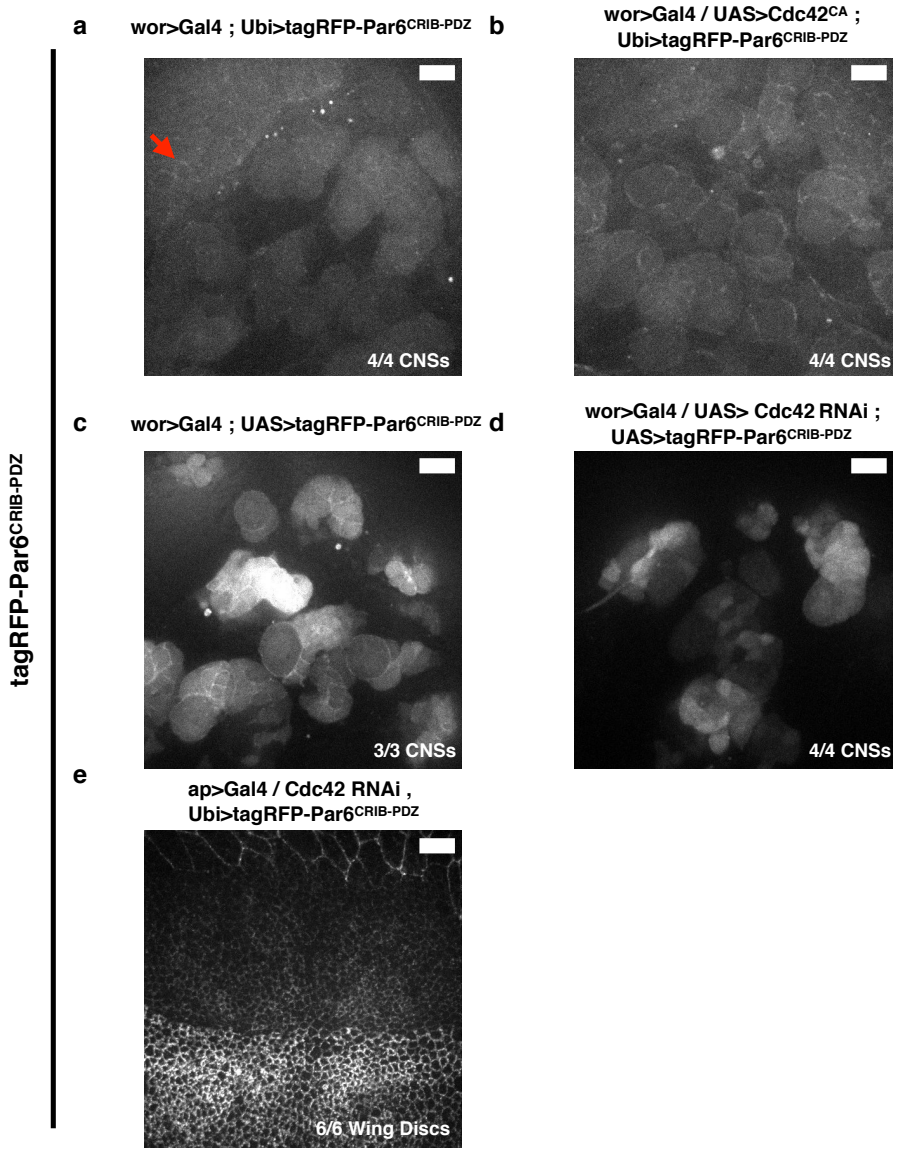

Figure 3.2: **tagRFP-Par6$^{CRIB-PDZ}$ responds to Cdc42 activity *in vivo*.**
a-b: Larval central nervous systems expressing Ubi>tagRFP-Par6$^{CRIB-PDZ}$ without (a) or with (b) overexpression of Cdc42-CA. Red arrow indicating coritcal accumulation in the neuroepithelium.
c-d: Larval central nervous systems expressing worniu>Gal4 and UAS>tagRFP-Par6$^{CRIB-PDZ}$ without (c) or with (d) Cdc42 RNAi expression.
e: Larval wing imaginal disc expressing Ubi>tagRFP-Par6$^{CRIB-PDZ}$ and ap>Gal4 driven Cdc42 RNAi.
Genotypes are indicated at the top of each image. Scale bars are 10 µm.

conformational change in the LOV domain, allowing SsrA to recruit Cdc42GEF to the plasma membrane and activate Cdc42.

We tested whether this optogenetic probe activates Cdc42 in S2 cells. Recruitment of Cdc42GEF to membrane-localized LOVSsrA induced cortical accumulation of both tagRFP-WASp^{GBD} and tagRFP-Par6$^{CRIB-PDZ}$ (Figure 3.3b,c). Importantly, expression of Cdc42 GEF without co-expression of LOVSsrA did not induce cortical accumulation of tagRFP-WASp^{GBD}, and recruitment of GFP-SspB to LOVSsrA did not induce cortical accumulation of tagRFP-Par6$^{CRIB-\ PDZ}$ (Figure 3.3b,c). Furthermore, introducing two point mutations into tagRFP-Par6$^{CRIB\ -PDZ}$, which are known to abolish its binding to Cdc42 [Atwood et al., 2007], eliminates its ability to respond to Cdc42GEF recruitment (Figure 3.3c). These results confirm that this optogenetic probe activates Cdc42 in S2 cells; furthermore, they show that tagRFP-WASp^{GBD} and tagRFP-Par6$^{CRIB-PDZ}$ detect active Cdc42.

To determine whether this optogenetic probe activates Cdc42 in *Drosophila* tissues, we generated transgenic flies expressing both optogenetic components and combined the optogenetic probe with the Cdc42 biosensor, Ubi>tagRFP-Par6$^{CRIB-PDZ}$. Global activation with 488nm light induced robust recruitment of Cdc42GEF to the neuroblast plasma membrane (Figure 3.3d). Moreover, light-mediated recruitment of Cdc42GEF induced accumulation of Ubi>tagRFP-Par6$^{CRIB-PDZ}$ at the plasma membrane, suggesting that this optogenetic probe rapidly activates Cdc42 in *Drosophila* (Figure 3.3d).

As a preliminary test of Cdc42's ability to influence neuroblast polarization, we monitored the effect of global Cdc42GEF recruitment on larval neuroblast asymmetric division. Previous studies indicated that overexpression of constitutively active Cdc42 caused apical polarity factors to spread uniformly around the embryonic neuroblast cortex and ultimately resulted in symmetric neuroblast divisions [Atwood et al., 2007]. We reasoned that globally and persistently recruiting Cdc42GEF to the neuroblast cortex should constitutively activate Cdc42 and could cause symmetric neuroblast divisions. However, global recruitment of

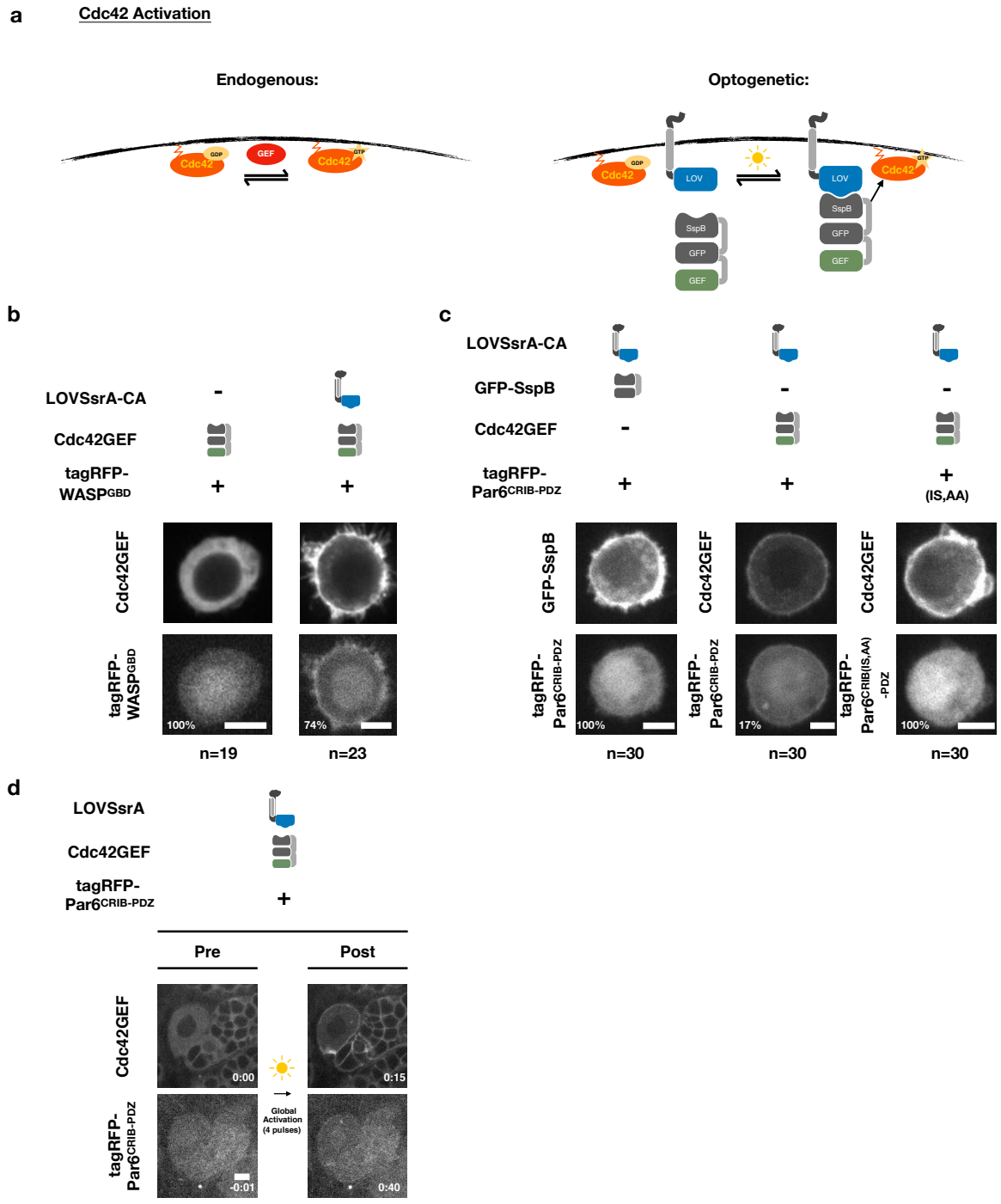

Figure 3.3: **Optogenetic control of Cdc42 in *Drosophila*.**
a: Schematic of endogenous (left) and optogenetic (right) mechanisms for Cdc42 activation. b: S2 cells transiently transfected to express tagRFP-WASp^{GBD} (bottom) and Cdc42GEF (ITSN-GFP-SspB) (top) without (left) or with (right) constitutively active, membrane localized LOVSsrA (not shown).

Figure 3.3: (continued) c: S2 cells transiently transfected to express tagRFP-Par6$^{CRIB-PDZ}$ (left-bottom, middle-bottom) or tagRFP-Par6$^{CRIB(IS,AA)-PDZ}$ (right-bottom) and constitutively active, membrane-localized LOVSsrA (not shown). These cells were also transfected to transiently express GFP-SspB (left-top) or Cdc42GEF (middle-top, right-top).
b-c: n indicates number of cells scored in each condition; percentages in image indicate percent of cells displaying that phenotype.
d: Larval neuroblasts expressing membrane localized LOVSsrA, Cdc42GEF, and Ubi>tagRFP-Par6$^{CRIB-PDZ}$.
Scale bars are 5 µm.

Cdc42GEF to the neuroblast cortex for over 40 minutes affected neither larval neuroblasts' asymmetric division nor the timing of their progression through mitosis. In contrast, 4 of 9 isolated embryonic neuroblasts subjected to global, optogenetic activation of Cdc42 divided symmetrically. This preliminary observation suggests Cdc42 activity may have a stronger influence on the polarization of embryonic versus larval neuroblasts.

3.3.3 Optogenetic control of Bazooka

It is possible that Cdc42 activity is not sufficient to induce neuroblast polarization. If this is the case, we reasoned that developing a photorecruitable version of Bazooka (PR-Baz), which is one of the most upstream regulators of neuroblast polarity, could be an alternative approach to manipulating and thereby dynamically studying neuroblast polarity. We eliminated Bazooka's N-terminal oligomerization domain [Benton and St Johnston, 2003a] and its C-terminal membrane binding domain [Krahn et al., 2010] so that PR-Baz accumulates at the cell cortex only upon photoactivation (Figure 3.4a). Thus, PR-Baz primarily comprises three PDZ domains; these PDZ domains have been implicated in binding Par6 and aPKC [Holly et al., 2020, Li et al., 2010b, Morais-de Sa et al., 2010, Lin et al., 2000, Wodarz et al., 2000].

PR-Baz is rapidly and robustly recruited to the S2 cell and neuroblast plasma membrane following global photoactivation (Figure 3.4b,c). PR-Baz weakly recruits aPKC to the S2

plasma membrane when these two proteins are co-expressed with a membrane-localized, constitutively activated LOVSsrA (LOVSsrA-CA) (Figure 3.4d). Co-expression of full-length Par6 greatly enhances the ability of Baz(PDZs) to recruit aPKC. Thus, recruitable Baz(PDZs) can nucleate a polarity complex in S2 cells (Figure 3.4d). Though PR-Baz is photosensitive in the *Drosophila* central nervous system, we have not yet rigorously tested whether global PR-Baz recruitment affects asymmetric cell division, nor have we assayed whether PR-Baz recruitment to the plasma membrane affects the localization of other polarity factors.

3.3.4 Optogenetic control of aPKC

aPKC is thought to be a linchpin of neuroblast polarization. Upstream apical polarity factors, including Bazooka and Par6, cooperate to localize and activate aPKC at the apical plasma membrane [Rolls et al., 2003]; aPKC, in turn, phosphorylates and excludes basal adaptor proteins and cell fate determinants, including Miranda and Numb, ultimately segregating them to the basal cortex and into the ganglion mother cell [Bailey and Prehoda, 2015, Atwood and Prehoda, 2009, Smith et al., 2007]. To directly test the model whereby the kinase activity of aPKC is sufficient to polarize a neuroblast, we generated photorecruitable aPKC (PR-aPKC) by fusing aPKC to GFP and SspB (Figure 3.5a).

PR-aPKC is recruited to membrane-localized LOVSsrA in both S2 cells and larval neuroblasts (Figure 3.5a-c). PR-aPKC co-recruits Par6 to the S2 cell plasma membrane, indicating that it is still capable of protein-protein interactions (Figure 3.5a-b). Moreover, constitutive recruitment of aPKC to the S2 cell cortex strongly reduces the accumulation of cortical Numb, a known aPKC phospho-target (Figure 3.5d). Thus, PR-aPKC maintains its kinase activity. We performed preliminary experiments to assay the activity of PR-aPKC in *Drosophila* neuroblasts; specifically, we expressed PR-aPKC, the membrane-localized LOV domain, and worniu>Gal4 driven UAS>Lgl-mCh or UAS>Mira-mCh. However, persistent,

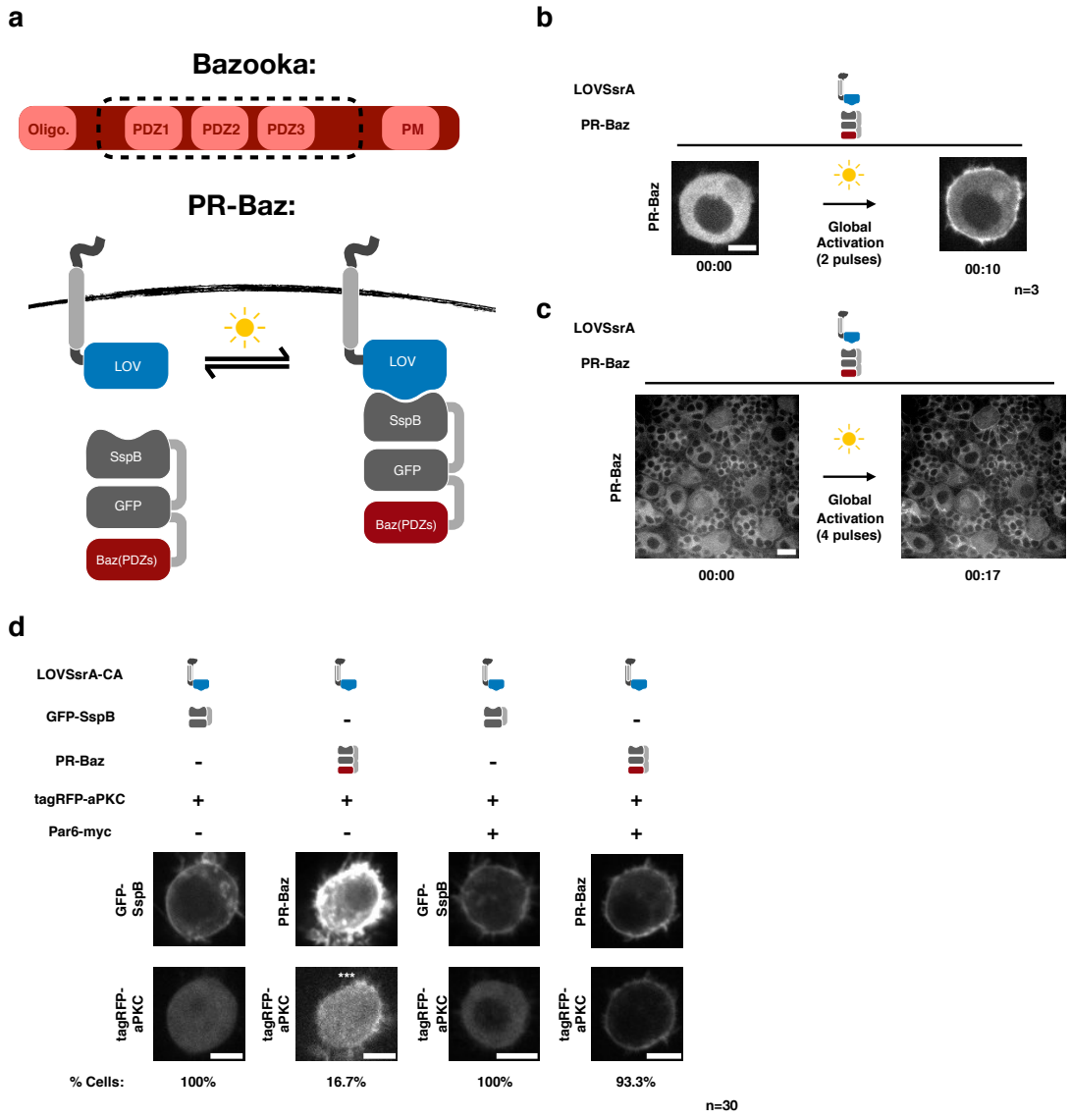

Figure 3.4: **PR-Baz is photosensitive and nucleates a complex with aPKC and Par6.**
a: Schematic showing Bazooka domain structure (top) and photorecruitable(PR)-Baz (bottom). Dashed box indicates region of Bazooka included in PR-Baz.
b: S2 cell transiently transfected with PR-Baz and membrane-localized LOVSsrA. Global activation consisted of 2 pulses of 488nm light every 5 sec.
c: Larval central nervous system expressing PR-Baz and non-fluorescent, membrane-localized LOVSsrA. Global activation consisted of 4 pulses of 488nm light every 5 sec.
d: S2 cells transiently transfected with the indicated constructs. n indicates number of cells scored in each condition; percentages below image indicate percent of cells displaying that phenotype.
All time stamps are min:sec. Scale bars are 5 µm.

global recruitment of PR-aPKC to the neuroblast cortex did not obviously alter Lgl or Mira localization in interphase or mitosis in these neuroblasts. Thus, the potency of PR-aPKC *in vivo* is unclear.

In the course of these experiments, we discovered that PR-aPKC can co-recruit a fragment of Par6 that contains only the CRIB and PDZ domains to the plasma membrane, suggesting that aPKC may interact, directly or indirectly, with this fragment of Par6 (Figure 3.6a). This is surprising, as aPKC and Par6 are thought to interact mainly through their PB1 domains [Lang and Munro, 2017, Prehoda, 2009]. PR-aPKC lacking its kinase activity or containing only its kinase domain does not co-recruit tagRFP-Par6$^{CRIB-PDZ}$ (Figure 3.6a). Thus, while aPKC can co-recruit Par6$^{CRIB-PDZ}$, this co-recruitment does not appear to be solely through aPKC's kinase domain; it does, however, require aPKC's kinase activity.

Cdc42 is a known binding partner of Par6$^{CRIB-PDZ}$ [Peterson et al., 2004, Joberty et al., 2000, Lin et al., 2000, Gotta et al., 2001]. We tested whether the ability of PR-aPKC to co-recruit Par6$^{CRIB-PDZ}$ depends on the ability of Par6$^{CRIB-PDZ}$ to interact with Cdc42. Par6$^{CRIB(IS,AA)-PDZ}$, which cannot interact with Cdc42, is still co-recruited to the cell cortex with PR-aPKC. However, this co-recruitment is dampened: Fewer cells expressing Par6$^{CRIB(IS,AA)-PDZ}$ exhibit cortical accumulation than cells expressing Par6$^{CRIB(WT)-PDZ}$, and the cortical accumulation is weaker when present (Figure 3.6b). Thus, the ability of Par6$^{CRIB-PDZ}$ to interact with Cdc42 promotes its co-recruitment with PR-aPKC.

3.4 Discussion

Cdc42 is required for proper PAR protein polarization in the *Drosophila* neuroblast [Atwood et al., 2007]. However, the molecular function of Cdc42 in this process is unclear. As a first step towards better understanding the role of Cdc42 in neuroblast polarity, we adapted a biosensor to detect its activity in *Drosophila*. This biosensor, tagRFP-Par6$^{CRIB-PDZ}$,

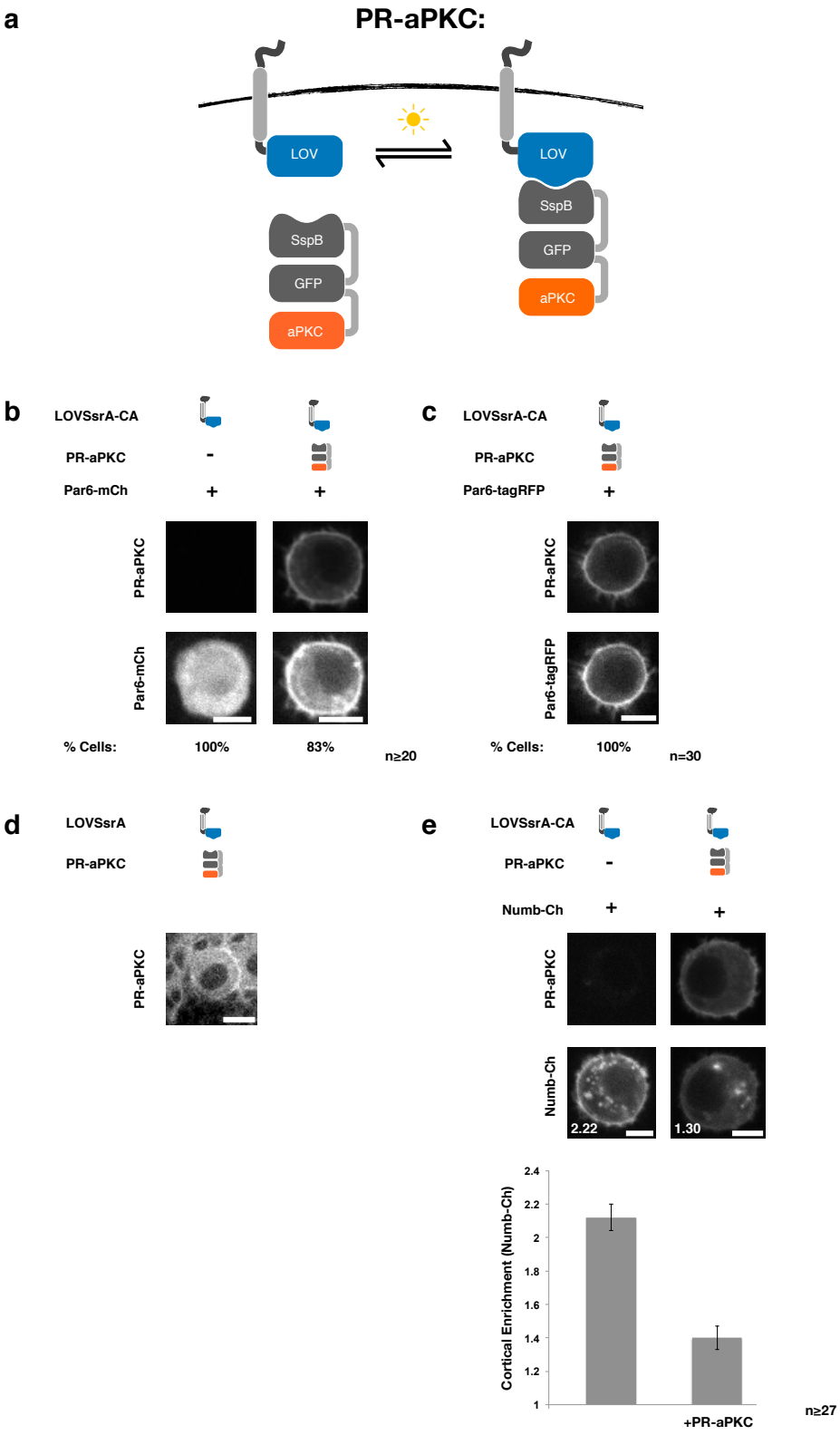

Figure 3.5: **PR-aPKC co-recruits Par6 and displaces Numb.**

Figure 3.5: (continued)
a: Schematic of optogenetic recruitment of aPKC.
b-c: S2 cells transiently transfected with PR-aPKC, constitutively active, membrane-localized LOVSsrA, and Par6-mCherry (a) or Par6-tagRFP (b). n indicates number of cells scored in each condition; percentages below image indicate percent of cells displaying that phenotype.
d: Larval neuroblast expressing PR-aPKC and membrane localized LOVSsrA. Image is a still following global activation with 488nm light.
e-top: S2 cells transiently transfected with constitutively active, membrane localized LOVSsrA, Numb-mCherry, and -/+ PR-aPKC.
e-bottom: Average cortical enrichment of Numb-Ch (membrane/cytoplasm) in the absence (left) or presence (right) of constitutively recruited PR-aPKC. Numbers in e-top indicate the cortical enrichment value for Numb-Ch in the two cells shown. Cortical enrichment was measured in at least 27 cells for each condition. Errors bars represent standard error. Scale bars are 5 µm.

detects Cdc42 activity *in vitro* and *in vivo*, as overexpression of constitutively active Cdc42 or optogenetic recruitment of a Cdc42 GEF increases the cortical accumulation of this sensor. We attempted to use Ubi>tagRFP-Par6$^{CRIB-PDZ}$ to characterize the activity profile of Cdc42 during neuroblast polarization, but we found that Ubi>tagRFP-Par6$^{CRIB-PDZ}$ exhibited a low signal to noise ratio and was sensitive to photobleaching. Thus, live imaging of this biosensor with better spatial and temporal resolution is needed to definitively characterize Cdc42 activity during neuroblast polarization. UAS>tagRFP-Par6$^{CRIB-PDZ}$ expresses at higher levels than Ubi>tagRFP-Par6$^{CRIB-PDZ}$, and it is possible that careful titration of wor>Gal4 driven expression of UAS>tagRFP-Par6$^{CRIB-PDZ}$ could overcome the limitations of Ubi>tagRFP-Par6$^{CRIB-PDZ}$.

Despite being unable to image Ubi>tagRFP-Par6$^{CRIB-PDZ}$ long term, our initial observations of this biosensor suggest that it exhibits weak, uniformly cortical association throughout the neuroblast cell cycle. This is particularly noticeable when the biosensor is expressed from the UAS promoter. This is somewhat surprising, as Cdc42 is traditionally thought to be an apical polarity factor in neuroblasts [Atwood et al., 2007]. If our preliminary observations hold true, it may indicate that Cdc42 is active at low levels throughout the

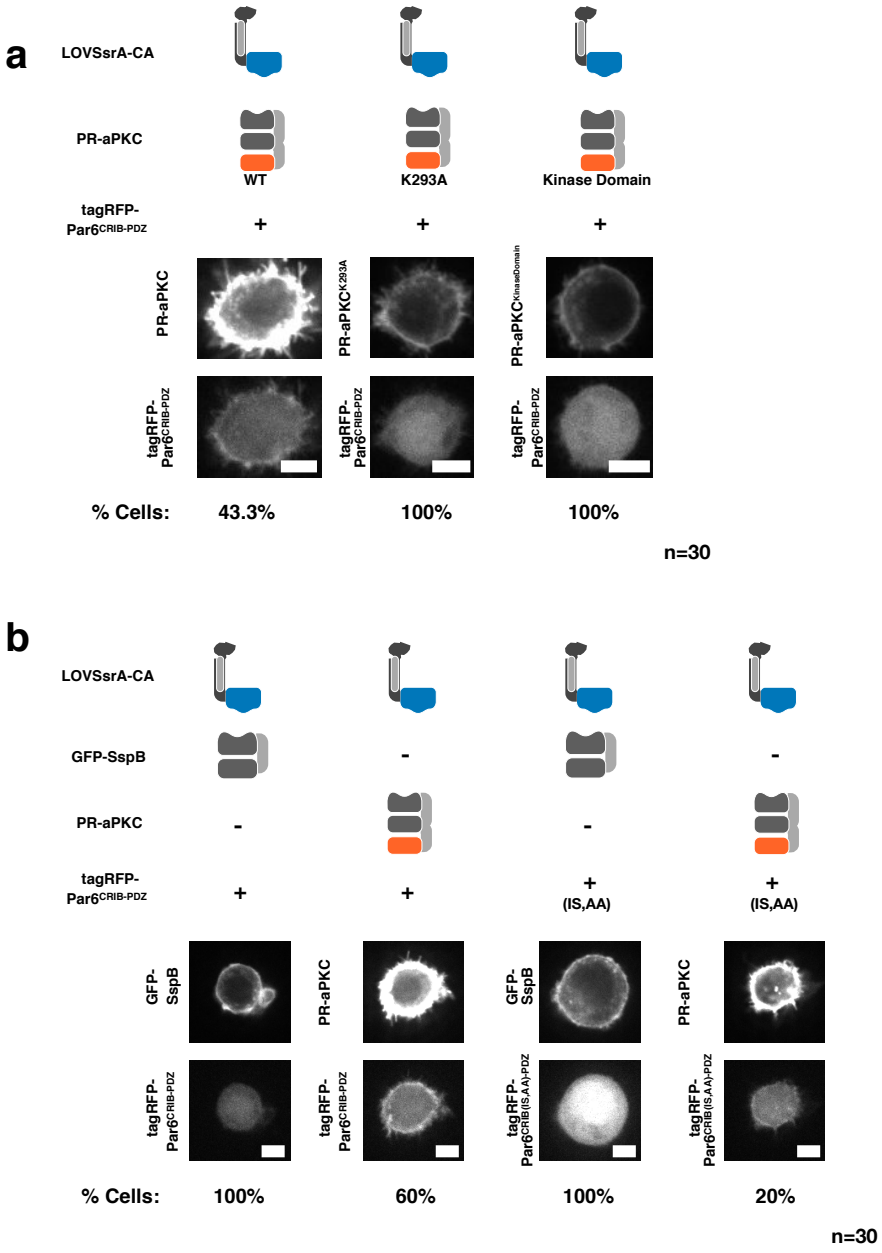

Figure 3.6: **PR-aPKC co-recruits a fragment of Par6.**
a) S2 cells transiently transfected with indicated aPKC construct (top), tagRFP-Par6$^{CRIB-PDZ}$ (bottom), and constitutively active, membrane-localized LOVSsrA (not shown).
b) S2 cells transiently transfected with PR-aPKC or GFP-SspB (top), WT or CRIB mutant tagRFP-Par6$^{CRIB-PDZ}$ (bottom), and constitutively active, membrane-localized LOVSsrA (not shown).
n indicates number of cells scored in each condition; percentages below images indicate percent of cells displaying the documented phenotype. Scale bars are 5 µm.

neuroblast cortex. Furthermore, this may suggest that Cdc42 activity plays a permissive, rather than instructive, role in neuroblast polarization. Specifically, apical polarity crescents form where Cdc42 activity overlaps with a nucleator of apical polarity, such as Bazooka, and permits this nucleator to build an apical polarity crescent.

Consistent with Cdc42 being permissive, rather than instructive, for neuroblast polarization, continuous global optogenetic activation of Cdc42 did not affect the asymmetric division of larval neuroblasts in explanted central nervous systems. Importantly, we demonstrated that the optogenetic probe for activating Cdc42 works in tissue culture and tissues. The fact that global optogenetic activation of Cdc42 did not induce symmetric neuroblast divisions contrasts with previous work, which demonstrated that chronic overexpression of constitutively active Cdc42 could induce neuroblasts to divide symmetrically [Atwood et al., 2007]. This difference may reflect the acute versus chronic nature of optogenetic and constitutive genetic activation, respectively. In the optogenetic experiments, Cdc42 expression is maintained at endogenous levels, and Cdc42 is acutely activated after neuroblasts assume their stem cell-like fate. In the genetic overexpression experiments, constitutively active Cdc42 is expressed well above the endogenous level of Cdc42, and this gross overexpression may titrate away other polarity factors, such as Par6 or aPKC, inhibiting their normal functions. If this is the case, constitutively active Cdc42 compromises the asymmetric division of neuroblasts indirectly, not because it is instructive for neuroblast polarization. Moreover, asymmetric cell division is the downstream-most readout of neuroblast polarity. It is possible that optogenetic activation of Cdc42 is sufficient to drive upstream polarization events, such as Par6 accumulation, without affecting asymmetric cell division. It will be important to assay how upstream polarity factors, such as Par6 and aPKC, are affected by acute Cdc42 activation.

Another possible explanation for the result that optogenetic activation of Cdc42 does not induce symmetric cell division is that Cdc42 may act redundantly with a parallel pathway to

polarize *Drosophila* neuroblasts. Notably, centrioles are required for maintaining the polarity axis across mitoses in larval neuroblasts [Januschke and Gonzalez, 2010], and this centriole-derived cue may override optogenetic Cdc42 activity. Additionally, embryonic neuroblasts that have been isolated from their overlying ectoderm cells exhibit a randomized axis of polarity [Siegrist and Doe, 2006]. Perhaps, in these sensitized backgrounds, Cdc42 activity would be sufficient to induce neuroblast polarization. Notably, in our hands, approximately half of isolated embryonic neuroblasts divided symmetrically when subjected to persistent global optogenetic activation of Cdc42.

In short, our results raise the possiblity that Cdc42 activity is not sufficient to instruct neuroblast polarization. However, Cdc42 is required for proper neuroblast polarization [Atwood et al., 2007], so what is its function in this cellular process? One intriguing hypothesis is that Cdc42 might act as a switch to promote the kinase activity of membrane-localized aPKC. In support of this hypothesis, recent work in *C. elegans* showed that a version of PKC-3(aPKC) that can be artificially tethered to the plasma membrane even in the absence of PAR-3 (Bazooka) antagonizes PAR-1, a PKC-3 substrate, from localizing at the plasma membrane. This displacement of PAR-1 by membrane-tethered PKC-3 occurs in the absence of PAR-3(Bazooka) but not in the absence of CDC-42 [Rodriguez et al., 2017]. Thus, in the *C. elegans* zygote, CDC-42 promotes PKC-3's kinase activity. Additionally, this work showed that PKC-3/PAR-6 complexes associated with CDC-42 are more diffuse, while PKC-3/PAR-6 complexes associated with PAR-3 are more punctate [Rodriguez et al., 2017]. This finding is consistent with earlier work that demonstrated PAR6/PKC-3 complexes can associate with CDC-42 independent of PAR-3 in certain genetic backgrounds [Beers and Kemphues, 2006]. Collectively, these results support a model in which PAR-3 functions with PKC-3/PAR-6 complexes to recruit them to the plasma membrane, while CDC-42 functions to release PKC-3/PAR-6 complexes from PAR-3 and promote PKC-3's kinase activity. Whether Cdc42 plays such roles in the *Drosophila* neuroblast could be tested by determining

whether optogenetic activation of Cdc42 affects the diffusivity of Par6/aPKC complexes in neuroblasts.

In addition to optogenetically controlling Cdc42 activity, we also generated a probe that could ectopically recruit the PDZ domains of Baz to the neuroblast cortex. The second PDZ domain of Bazooka was recently shown to interact with a C-terminal PDZ binding motif in aPKC [Holly et al., 2020]. This interaction was required for aPKC to form an apical crescent in mitotic neuroblasts. Thus, ectopic crescents of PR-Baz should be effective at generating ectopic domains of aPKC activity, and this optogenetic probe should be effective in manipulating neuroblast polarity. It will be especially interesting to assay the ability of PR-Baz to nucleate and/or disrupt neuroblast polarity at different phases of mitosis.

The final optogenetic probe we developed is PR-aPKC. We used full length aPKC; thus this photosensitive protein should retain all the protein-protein interactions of endogenous aPKC as well as its kinase activity. Indeed, recruitment of PR-aPKC to the S2 cell cortex substantially reduced the amount of Numb-Ch, a substrate of aPKC, on the S2 cell plasma membrane. However, global persistent recruitment of PR-aPKC to the cortex of neuroblasts expressing Mira-Ch or Lgl-Ch did not alter Mira or Lgl localization, despite the fact that previous work has shown that aPKC localized to the neuroblast cortex via a CAAX box is sufficient to displace Mira from the neuroblast cortex [Lee et al., 2006b]. This may reflect that PR-aPKC is not enzymatically active *in vivo*. Notably, GFP and SspB are fused to the C-terminus of aPKC, close to the kinase domain. Engineering a PR-aPKC that has a free C-terminus may increase its kinase activity. Alternatively, this preliminary result may simply reflect an imbalance in expression levels of Mira/Lgl, which are expressed from the UAS promoter, and PR-aPKC, which is expressed, at lower levels, from a Ubi promoter. It will be interesting to assay how PR-aPKC recruitment affects endogenously tagged Mira-Ch localization [Hannaford et al., 2018].

In the course of validating PR-aPKC in S2 cells, we made the unexpected discovery that a

small fragment of Par6, containing only the CRIB and PDZ domains of Par6, is co-recruited to the plasma membrane with PR-aPKC. This raises the possibility that aPKC interacts with this fragment of Par6. The biological significance of this potential protein-protein interaction is unknown. It will be important to identify the precise residues in aPKC and Par6 that mediate this co-recruitment so that these residues can be specifically disrupted and the significance of the potential interaction can be tested *in vivo*. Towards this end, we found that the kinase domain alone of aPKC does not co-recruit this fragment of Par6, suggesting the N-terminal portion of aPKC may mediate this potential interaction. It is also notable that this fragment of Par6 accumulates apically in polarized epithelia, including that of the larval wing imaginal disc and the neuroepithelia, indicating that this Par6 fragment retains its ability to interact with PAR polarity factors in vivo. Within the last few months, a novel interaction between PDZ2 of Bazooka and the C-terminus of aPKC was identified [Holly et al., 2020]. This published work together with our unpublished work emphasizes that there is still much to discover about the molecular interactions governing neuroblast polarization.

In addition to identifying new protein-protein interactions, such as that discovered by Holly et al. [2020], recent work in *Drosophia* neuroblasts has painted a very dynamic picture of this process. Live imaging of aPKC revealed that aPKC first appears as small punctae in the apical neuroblast cortex. These punctae coalesce to form an apical cap of aPKC in metaphase neuroblasts before later flowing toward the cleavage furrow [Oon and Prehoda, 2019]. Similar PAR polarization dynamics have been documented in *Drosophila* tissue culture [Kono et al., 2019]. Mira localization is also dynamic throughout the neuroblast cell cycle [Hannaford et al., 2018]: Mira is uniformly localized at the interphase neuroblast cortex, displaces at the onset of mitosis, and accumulates in a strong basal crescent by metaphase. These recent works argue that a complete understanding of this dynamic process necessitates the characterization of protein activity with subcellular precision. Furthermore, approaches

that permit acute manipulation of polarity factor localization and/or activity will be critical in testing the current models of neuroblast polarization as well as gaining further insight into this cell biological process.

Towards this end, the work presented here documents the development of a biosensor to detect Cdc42 activity in *Drosophila*. Furthermore, we generated several optogenetic probes for manipulating cell polarity in neuroblasts, and, presumably, other *Drosophila* tissue. We have only performed preliminary experiments to validate these tools both in *Drosophila* tissue culture cells and *Drosophila* tissues, but these tools promise to be effective in acutely perturbing cell polarity in a variety of *Drosophila* tissues.

3.5 Methods and Materials

3.5.1 Plasmids

Plasmids generated in this studied are listed in Table 3.1 and were generated using SLiCE [Zhang et al., 2012] or one-step isothermal *in vitro* recombination [Gibson et al., 2009]. pUbi-stop-mCD8GFP, containing an attB site, was a gift from T. Lecuit. GST-Par6 (JB133) and pCDNA3.1numb (AH085) were gifts from J. Knoblich. Baz cDNA (LD04932) was obtained from the Drosophila Genomics Resource Center. aPKC pAGW was from A. Wodarz. Stargazin-GFP-LOVpep and PDZx2-mCherry-LARG(DH) plasmids were published previously [Wagner and Glotzer, 2016]. pAHW-Cdc42 and pAHW-Cdc42(V12) were also previously published [Neisch et al., 2010]. Venus-iLID-CAAX, tgRFPt-SspB WT, and hITSN1-tgRFP-SspB(WT) were obtained from Addgene (60411, 60415, 60419). pMT>Gal4 [Klueg et al., 2002] was obtained from the Drosophila Genomics Resource Center.

3.5.2 Fly stocks

Drosophila melanogaster was cultured using standard techniques at 25°C. Both male and female animals were used. Flies expressing *worniu>Gal4* were a gift from C. Doe. *pUAS>Mira-Ch* and *pUAS>Lgl-Ch* were gifts from J. Knoblich. *w[1118]; Pw[+mC]=UAS-Cdc42.V12LL1* (BID: 4854), *y[1] sc[*] v[1] sev[21]; Py[+t7.7] v[+t1.8] =TRiP. HMS01502attP40* (BID: 35756), and *y[1] w[1118]; Pw[+mW.hs]=GawBap[md544]/CyO* (BID: 3041) were obtained from Bloomington Stock Center.

Transgenic flies were generated by PhiC31-directed integration (GenetiVision). Transgenic lines generated for this study include: *pUbi>tagRFP-Par6*$^{CRIB-PDZ}$, *pUAS>tagRFP-Par6*$^{CRIB-PDZ}$, *pUbi>ITSN(DHPH)-GFP-SspB*, *pUbi>Baz(PDZs)-GFP-SspB*, and *pUbi>aPKC-GFP-SspB*. Genotypes of flies used in each experiment are listed in Table 3.4.

3.5.3 S2 cells

3.1 x 10^6 S2 cells were transfected with the indicated constructs, using dimethyldioctadecylammonium bromide (Sigma) [Han, 1996] at 250 ug/mL in six well plates. Expression from the pMT promoter was induced 2 days after transfection by addition of 0.35 mM $CuSO_4$. Cells were imaged live 24 hrs after $CuSO_4$ induction. 50 µL of the S2 cell culture was plated on a glass slide and covered with a coverslip. Clay feet were used as spacers between the slide and coverslip.

3.5.4 Preparation of Drosophila tissues for live imaging

Central nervous systems were dissected from wandering third instar larvae in Schneider's *Drosophila* Medium (Sigma) supplemented with 10% Fetal Bovine Serum (Thermo Fisher Scientific). Central nervous systems were imaged in a chamber comprising a coverslip affixed with petroleum jelly to a metal slide with a hole in the center. Following dissection, central

nervous systems were mounted in the chamber such that their dorsal side contacted the coverslip. The chamber was flooded with Chan and Gerhing's balanced solution [Chan and Gehring, 1971] to completely cover the central nervous system, and a gas-permeable membrane (YSI: 5793) was placed over the chamber to limit evaporation. These chambers were imaged on an inverted microscope.

The protocol for isolating embryonic neuroblasts was adapted from Siegrist & Doe (2006). Embryos were collected for 2 hours at 25°C on apple juice agar plates and aged for 4.5 hours such that embryos were stage 10-11 at time of neuroblast isolation. Embryos were collected from apple juice plates with embryo wash (0.4% NaCl, 0.03% Triton X-100), rinsed with water, dechorinated in 30% bleach for 1 minute, and transferred to a dounce homogenizer containing 1.5 mL Chan & Gehring's Balanced Saline Solution supplemented with 2% FBS [Chan and Gehring, 1971]. Embryos were homogenized with 10 strokes of the dounce. The homogenized mixture was transfered to 0.6mL eppendorf tubes with a glass pipette, and cells were pelleted by 5 short (<5sec) spins at $<$ 4000 RMP. The supernatant was aspirated, and pellets were resuspended in 100-400 uL of fresh Chan & Gehring's Solution. Resuspended cells were plated in petri dishes fitted with glass coverslips for imaging. After 30 minutes, the dish was flooded with up to 2 additional mLs of Chan & Gehring's Solution before imaging on an inverted microscope.

Wing imaginal discs were dissected from wandering third instar larvae in S2 cell media supplemented with 10% FBS. Wing discs were mounted between a slide and glass coverslip in 50uL Chan and Gehring's balanced solution. Clay feet were used as spacers between the slide and coverslip.

3.5.5 Live imaging and optogenetic experiments

Global activation experiments were performed on a 63x/1.4 numerical aperture (NA) oil immersion lens on a Zeiss Axiovert 200M equipped with a Yokogawa CSU-10 spinning disk

unit (McBain) and illuminated with 50-mW, 473-nm and 20- mW, 561-nm lasers (Cobolt) or on a Zeiss Axioimager M1 equipped with a Yokogawa CSU-X1 spinning disk unit (Solamere) and illuminated with 50-mW, 488-nm and 50-mW, 561-nm lasers (Coherent). Images were captured on a Cascade 1K electron microscope (EM) CCD camera, a Cascade 512BT (Photometrics), or a Prime 95B (Photometrics) controlled by MetaMorph (Molecular Devices). Photoactivation was accomplished by illuminating the sample with 488 nm light for the indicated exposure times.

3.5.6 Image processing

All images were processed with FIJI [Schindelin et al., 2012]. Data in Figure 3.5 were plotted in Excel. Cortical enrichment was calculated by first thresholding images to define membrane and cytoplasm. Membranes were then straightened, and vertical lines, 10 px in height, were drawn along the horizontally-straightened membrane. The max pixel intensity along each vertical line was determined in FIJI, and the max pixels for all vertical lines for a given cell were averaged to determine the cortical intensity of Numb-Ch. A user defined circular region of 30 x 30 px was defined in the cytoplasm. The average pixel value from this cytoplasm ROI was used as the cytoplasmic intensisty. Background signal was defined as the average px intensity outside the region thresholded as membrane. Cortical enrichment, as plotted in 3.5e, was calculated as [Avg Cortical Intensity - Avg Background Intensity]/[Avg Cytoplasmic Intensity - Avg Background Intensity].

3.6 Acknowledgements

This work was supported by R01GM085087, R35GM12709, and a France and Chicago Collaborating through the Sciences grant (M.G.), and NIH T32 GM007183 and NSF GRFP DGE-1144082; DGE-1746045 (A.R). We thank Meaghan Griffin for help with molecular biology. We thank Richard Fehon, Ed Munro, Sally Horne-Badovinac, J.M. Philippe, M.G. lab

members, and R.G.F. lab members for helpful discussions and support. We thank the Fehon, Glick, Knoblich, and Lecuit labs for generous sharing of reagents. We thank Ben Glick for access to the SnapGene molecular biology software (http://www.snapgene.com). Stocks obtained from the Bloomington *Drosophila* Stock Center (NIH P40OD018537) were used in this study. Reagents obtained from *Drosophila* Genomics Resource Center, supported by NIH grant 2P40OD010949 were used in this study.

Table 3.1: Chapter 3 Plasmids Generated

Plasmid Generated	Fragment Source	Backbone Source
pMT>Stargazin-GFP*-LOVSsrA (* represents inactivation of fluorphore with Y66C mutation.)	Stargazin-GFP amp. from Stargazin-GFP-LOVpep [Wagner and Glotzer, 2016] LOVSsrA amp. from Venus-iLID-CAAX [Guntas et al., 2015] (Addgene: 60411) GFP silenced by site-directed mutagenesis (Y66C)	pMT>Gal4 [Klueg et al., 2002]
pMT>Stargazin-GFP*-LOVSsrA-CA (Constitutively active)	NA	pMT>Stargazin-GFP*-LOVSsrA w/ site directed mutagenesis to delete K533 in LOV
pUbi>Stargazin-GFP*-LOVSsrA	Stargazin-GFP*-LOVSsrA amp. from pMT>Stargazin-GFP*-LOVSsrA	pUbi-stop-mCD8GFP (Contains attB site)
pMT>tagRFP-WASp^{GBD}	tagRFP amp. from tgRFPt-SspB(WT) [Guntas et al., 2015] (Addgene: 60415) WASp amp. from genomic prep of w1118	pMT>Gal4 [Klueg et al., 2002]
pMT>tagRFP-Par6$^{CRIB-PDZ}$	tagRFP amp. from tgRFPt-SspB(WT) [Guntas et al., 2015] (Addgene: 60415) Par6$^{CRIB-PDZ}$ amp. from GST-Par6 (J. Knoblich)	pMT>Gal4 [Klueg et al., 2002]
pUbi>tagRFP-Par6$^{CRIB-PDZ}$	pMT>tagRFP-Par6$^{CRIB-PDZ}$	pUbi-stop-mCD8GFP (Contains attB site)
pMT>ITSN(DHPH)-GFP-SspB	ITSN and SspB amp. from hITSN1-tgRFPt-SspB(WT) [Guntas et al., 2015] (Addgene: 60419)	pMT>Gal4 [Klueg et al., 2002]
pUbi>ITSN(DHPH)-GFP-SspB	pMT>ITSN(DHPH)-GFP-SspB	pUbi-stop-mCD8GFP (Contains attB site)

Table 3.2: Chapter 3 Plasmids Generated (Cont.)

Plasmid Generated	Fragment Source	Backbone Source
pMT>GFP-SspB	GFP-SspB from pMT>ITSN(DHPH)-GFP-SspB	pMT>Gal4 [Klueg et al., 2002]
pMT>tagRFP-Par6$^{CRIB(IS,AA)-PDZ}$	NA	pMT>tagRFP-Par6$^{CRIB(IS,AA)-PDZ}$ w/ site directed mutagenesis to mutate IS -> AA in CRIB
UAS>tagRFP-Par6$^{CRIB-PDZ}$	pMT>tagRFP-Par6$^{CRIB-PDZ}$	pUASTattB
pMT>Baz(PDZs)-GFP-SspB	Baz cDNA (DRGC)	pMT>Gal4 [Klueg et al., 2002]
pUbi>Baz(PDZs)-GFP-SspB	pMT>Baz(PDZs)-GFP-SspB	pUbi-stop-mCD8GFP (Contains attB site)
pMT>Par6-myc	Par6 amp. from GST-Par6 (J. Knoblich) myc generated via annealed oligos	pMT>Gal4 [Klueg et al., 2002]
pMT>tagRFP-aPKC	tagRFP amp. from tgRFPt-SspB(WT) [Guntas et al., 2015] (Addgene: 60415) aPKC amp. from aPKC pAGW (A. Wodarz)	pMT>Gal4 [Klueg et al., 2002]
pMT>aPKC-GFP-SspB	pMT>tagRFP-aPKC	pMT>ITSN(DHPH)-GFP-SspB (ITSN excised)
pUbi>aPKC-GFP-SspB	pMT>aPKC-GFP-SspB	pUbi-stop-mCD8GFP (Contains attB site)
pMT>Par6-mCh	Par6 amp. from pMT>Par6-myc mCherry amp. from pm-Cherry2B (F. Valbuena and B. Glick, manuscript in preparation)	pMT>Gal4 [Klueg et al., 2002]
pMT>Par6-tagRFP	tagRFP amp. from tgRFPt-SspB(WT) [Guntas et al., 2015] (Addgene: 60415) Par6 amp. from pMT>Par6-myc	pMT>Gal4 [Klueg et al., 2002]

Table 3.3: Chapter 3 Plasmids Generated (Cont.)

Plasmid Generated	Fragment Source	Backbone Source
pMT>Numb-mCh	pCDNA3.1numb(AH085) (Knoblich lab) pm-Cherry2B (F. Valbuena and B. Glick, manuscript in preparation)	pMT>Gal4 [Klueg et al., 2002]
pMT>aPKC^{K293A}-GFP-SspB	NA	MT>aPKC^{K293A}-GFP-SspB p w/ site directed mutagenesis for K293A in aPKC
pMT>aPKC^{KinaseDomain}-GFP-SspB	aPKC^{KinaseDomain} amp. from pMT>aPKC-GFP-SspB	pMT>aPKC-GFP-SspB (aPKC(FL) excised)

Table 3.4: Chapter 3 Genotypes

Figure	Genotype
3.2a	*; wor>Gal4 ; Ubi>tagRFP-Par6$^{CRIB-PDZ}$*
3.2b	*; wor>Gal4 / UAS>Cdc42(CA) ; Ubi>tagRFP-Par6$^{CRIB-PDZ}$*
3.2c	*; wor>Gal4 ; UAS>tagRFP-Par6$^{CRIB-PDZ}$*
3.2d	*; wor>Gal4 / UAS>Cdc42RNAi ; UAS>tagRFP-Par6$^{CRIB-PDZ}$*
3.2e	*; ap>Gal4 / UAS>Cdc42RNAi ; Ubi>tagRFP-Par6$^{CRIB-PDZ}$*
3.3d	*Ubi>ITSN-GFP-SspB ; Ubi>tagRFP-Par6$^{CRIB-PDZ}$ Ubi>Stargazin-GFP*-LOVSsrA*
3.4c	*Ubi>Baz(PDZs)-GFP-SspB; Ubi>Stargazin-GFP*-LOVSsrA*
3.5d	*Ubi>aPKC-GFP-SspB; Ubi>Stargazin-GFP*-LOVSsrA*

CHAPTER 4

DISCUSSION AND FUTURE DIRECTIONS

4.1 Summary

Organismal development is a complex process. Understanding how a simple ball of cells transforms into a multi-layered adult with multiple cell types and tissues requires understanding how cells make decisions about fate, shape, and growth. Furthermore, development involves the coupling and coordinating of each of these decisions across cells within tissues. My thesis work was motivated by the desire to understand how cells within tissues generate subcellular asymmetries that segregate cellular contents unequally and drive cell- and tissue-level shape changes. Specifically, I sought to understand how two Rho family GTPases, Rho1 and Cdc42, drive tissue morphogenesis and cell polarization, respectively. Building upon previous work in the Glotzer lab, I adapted a LOV-domain based optogenetic system for use in *Drosophila*. The previous chapters demonstrate that this system controls both Rho1 and Cdc42 activity throughout *Drosophila* development. I further adapted this system to directly control two PAR proteins, Bazooka (Par3) and aPKC. Moreover, Chapter 2 demonstrates how optogenetic control of Rho1 activity enabled the testing of a longstanding model of ventral furrow formation. Our result, that ventral cells are primed to respond to Rho1 activity differently than dorsal cells, reveals that a ventral-specific factor cooperates with spatially patterned Rho1 activity to effect the cellular- and tissue-behaviors observed during endogenous ventral furrow formation. This work underscores the power of optogenetic approaches to test existing models as well as the feasibility of controlling Rho GTPase activity in *Drosophila*. However, this is only the first step in exploiting these optogenetic tools to gain new insight into ventral furrow formation and neuroblast polarization.

In the following sections, I discuss remaining outstanding questions in both Rho-1 mediated morphogenesis and Cdc42-mediated polarization, which can now be addressed with the

tools established here. This list of questions is not exhaustive, but it reflects the questions I find most interesting. I finish with thoughts about moving beyond Rho1 and Cdc42, offering my thoughts on developing additional probes for the *Drosophila* optogenteic toolkit.

4.2 Rho1 and morphogenesis in *Drosophila*

4.2.1 What protein activity enables ventral-specific responses to Rho1 activation?

The results discussed in Chapter 2 demonstrate that identical spatial patterns of Rho1 activation induce distinct cell and tissue-level responses in the dorsal and ventral epithelium. Most notably, ventral, but not dorsal, cells exhibit anisotropic apical constriction and coordinated cellular movements in response to Rho1 activation. These observations suggest that Rho1-centric models of ventral furrow formation are incomplete and reveal the existence of a ventral specific factor or activity that cooperates with Rho1 activity to drive cell and tissue-level shape changes during ventral furrow formation.

What is the identity of this ventral-specific factor? Several proteins, not considered to be canonical regulators of ventral furrow formation, are required for completion of this morphogenetic event, including the GTPase Rap1, its GEF Dizzy, and E-cadherin [Spahn et al., 2012, Haruta et al., 2010]. It is possible that one of these proteins cooperates with Rho1 to promote the ventral-specific behaviors identified by our experiments. Consistent with this possibility, embryos lacking Rap1 or its GEF Dizzy fail to complete ventral furrowing and exhibit uncoordinated apical constrictions during ventral furrow formation [Spahn et al., 2012]. However, while our experiments identified a ventral-specific, Rho1-independent activity, Rap1 activity is not restricted to the ventral epithelium during *Drosophila* gastrulation: Rap1 also modulates the depth of the dorsal transverse folds which initiate slightly later than the ventral furrow [Wang et al., 2013]. However, local regulation of Rap1 may promote

ventral-specific responses. Notably, Rap1 promotes the formation of apical adherens junction belts of E-cadherin in the early embryo [Spahn et al., 2012], and Rap1 acts through α-catenin to modulate the depth of dorsal folds [Wang et al., 2013]. It is possible that Rap1 similarly acts through E-cadherin and/or α-catenin in ventral cells to modulate their response to Rho1 activation.

E-cadherin is another candidate for promoting ventral cell-specific responses to Rho1 activation. Like embryos lacking Rap1, embryos expressing a mutant version of E-cadherin that lacks the membrane-proximal portion of its extracellular domain also exhibit uncoordinated apical constriction during ventral furrow formation [Haruta et al., 2010]. Furthermore, ventral furrows that form in this mutant background often regress, indicating an inability to sustain tissue-level shape changes. Like Rap1, E-cadherin function is not ventral-specific; this junctional protein acts throughout the embryo to promote cell-cell adhesion. However, this E-cadherin mutant, lacking a portion of its extracellular domain, is specifically defective in ventral furrow formation: Cellularization and posterior midgut invagination occur normally in embryos expressing this mutant E-cadherin as their sole source of E-cadherin. Perhaps the membrane-proximal extracellular region of E-cadherin participates in homo- or heterotypic extracellular interactions needed specifically during ventral furrowing, a rapid tissue-level shape change. Alternatively, this mutant E-cadherin is a hypomorph, and cells within the ventral furrow require higher levels of E-cadherin function than elsewhere in the embryonic epithelium. It will be interesting to assay the effect of Rho1 activation in ventral cells lacking Rap1 or expressing this mutant version of E-cadherin. If ventral cells from these mutant backgrounds do not exhibit anisotropic apical constriction or coordinated cell shape changes in response to optogenetic activation of Rho1, it will strongly support the idea that Rap1 or the extracellular region of E-cadherin promotes these ventral-specific responses to Rho1 activation.

Another interesting candidate for mediating these ventral specific behaviors is T48, a

transmembrane protein that promotes Rho1 activation during ventral furrow formation [Kölsch et al., 2007]. Ectopic expression of T48 in *Chironomus riparius* converts mesodermal internalization from individual cell ingressions to a coordinated invagination [Urbansky et al., 2016]. Thus, it is possible that T48 plays a Rho1-independent role in coordinating cellular behaviors across the ventral furrow. Notably, T48 is expressed specifically in ventral cells, and it is genetically downstream of Dorsal and Twist [Kölsch et al., 2007], consistent with our finding that Dorsal is required for and Twist promotes ventral-specific responses to ectopic Rho1 activation. T48 contains a C-terminal peptide sequence that can interact with PDZ domains [Kölsch et al., 2007]. Perhaps this peptide recruits a PDZ domain containing protein that promotes the ventral-specific responses to Rho1 activation. Alternatively, the extracellular domain of T48 may promote ventral specific responses, for example by modulating the organization of adherens junctions.

*4.2.2 How are tissue level shape changes **sustained** in vivo?*

The work presented here together with previously published work show that acute Rho1 activation generates on-demand morphogenesis [Izquierdo et al., 2018]. However, these tissue-level shape changes rapidly revert upon removal of ectopic Rho1 activity (Chapter 2). This begs the question: How are cell shape changes sustained long enough to enable morphogenesis during organismal development?

In the case of ventral furrowing, ventral cells apically constrict, invaginate, and undergo an epithelial to mesenchyme transition (EMT) before migrating dorsally [Leptin, 1999]. This EMT ensures that ventral furrowing is an irreversible tissue level shape change. Thus, the apical constrictions observed during ventral furrowing need not be maintained indefinitely, but they do need to be maintained over the course of ventral furrow invagination, which occurs over approximately 15 minutes [Sweeton et al., 1991, Turner and Mahowald, 1977]. Ratcheted, or sustained, apical constrictions are observed as early as 2 minutes after initiation

of ventral furrow formation [Martin et al., 2009]. Thus, what molecular mechanism sustains cell shape changes over the course of this morphogenetic event?

Reorganization of junctional proteins is one possible mechanism for sustaining apical constriction and tissue bending throughout ventral furrowing. Under such a model, cellular contractility would acutely and transiently alter cell shape. During this acute phase of cell-shape change, junctional proteins would rearrange, perhaps clustering together and/or engaging in homotypic interactions, to form a ratchet that prevents relaxation of the cell shape change even after dissipation of cellular contractility. Consistent with this observation, junctional proteins rearrange during both *Drosophila* mesoderm invagination and *C. elegans* endoderm internalization [Weng and Wieschaus, 2016, Marston et al., 2016, Kölsch et al., 2007].

Additionally, remodeling of the actin cytoskeleton may help sustain apical constriction. Rho1 mediated contractility could remodel the apical actin meshwork. Subsequent stabilization of this remodeled actin meshwork, for example through association with actin crosslinkers, could then ratchet the cell apex in a constricted state. Consistent with this hypothesis, blocking F-actin remodeling, via interference with cofilin activity, disrupts apical constriction in cells of the ventral furrow [Jodoin et al., 2015].

Membrane remodeling may also contribute to sustaining cell and tissue shape changes during *Drosophila* gastrulation. Depleting proteins required for endocytosis (Rab35, Sbf) compromises ventral furrow formation [Miao et al., 2019]. However, it is unlikely that reduction in membrane, alone, would sustain a cell- or tissue-level shape change, as membrane is fluid and unlikely to resist relaxation. Thus, membrane remodeling would likely work in concert with junctional and/or cytoskeletal rearrangements to stabilize cell and tissue shape change.

Recent optogenetic experiments support a model of sustained cell shape change that involves junctional reorganization and membrane endocytosis. Specifically, Cavanaugh et al.

[2020] induced junctional shortening by optogenetically activating RhoA in mammalian tissue culture cells. This junctional shortening was partially sustained, and it correlated with E-cadherin clustering. Moreover, endocytosis was required for the junctional shortening to be partially maintained. Importantly, these sustained cell shape changes took place over a much longer time scale (>20 minutes) than individual ratcheted apical constrictions occur during ventral furrow formation (1-2 minutes). Thus, whether a similar mechanism explains the sustained cell shape changes observed during ventral furrowing remains to be determined.

Alternatively, it is possible that sustained Rho1 activity itself is required for stabilization of Rho1-induced cell- and tissue-level shape changes. Consistent with this hypothesis, active Rho1 and its effector myosin are observed in ventral cells throughout ventral furrowing [Mason et al., 2016, Fox and Peifer, 2007, Dawes-Hoang et al., 2005, Nikolaidou and Barrett, 2004]. Furthermore, optogenetically induced tissue deformations persist as long as optogenetic activation of Rho1 is sustained but rapidly revert upon removal of the optogenetic stimulus (Chapter 2). In order to determine the mechanism by which cell and tissue shape changes are sustained during ventral furrowing, it will be important to assay whether junctional rearrangements, actin disassembly/reassembly, and/or endocytosis are induced by optogenetic activation of Rho1 in the *Drosophila* embryo. For example, if endocytosis does accompany ectopic, Rho1-induced tissue-level shape changes that are not sustained, it will indicated that endocytosis alone does not underlie the maintenance of cell and tissue shape changes during *Drosophila* gastrulation.

4.2.3 Is Rho1 activity sufficient to induce junctional rearrangements in Droso-phila?

Regardless of whether they act as the ratchet during apical constriction and tissue invagination, junctional proteins undoubtedly rearrange along the apical-basal axis over the course of ventral furrow formation [Weng and Wieschaus, 2016, Kölsch et al., 2007]. Specifically,

junctional proteins move from sub-apical to apical positions (Figure 4.1). Similarly, junctions concentrate at the apical-most region of lateral membranes in endodermal precursors before they invaginate [Marston et al., 2016]. Is myosin activity alone sufficient to drive these rearrangements? Notably, Fog or T48 overexpression, throughout the *Drosophila* embryo is sufficient to shift junctions apically [Weng and Wieschaus, 2016, Kölsch et al., 2007]. However, Fog and T48 may have other downstream targets, besides Rho1 activation and myosin-mediated contractility, which promote junctional rearrangements. This question could be readily addressed in *Drosophila* by live imaging fluorescently tagged junctional proteins, such as E-cadherin, while simultaneously optogenetically activating Rho1. Preliminary attempts at monitoring E-cadherin in the *Drosophila* embryonic epithelium while simultaneously optogenetically activating Rho1 were unsuccessful, chiefly because available versions of red fluorescently tagged E-cadherin rapidly photobleach and are incompatible with long-term living imaging. Generating E-cadherin endogenously tagged with more photostable red fluorescent proteins is a key hurdle in determining whether Rho1 activation is sufficient to induce junctional rearrangements in *Drosophila*. Alternatives to fluorescent proteins, such as SNAP- and Halo-tags, could also enable longer term imaging of E-cadherin during optogenetic experiments [Kohl et al., 2014]. Determining whether Rho1 activity is sufficient to induce junctional rearrangments *in vivo* would shed light on whether junctional rearrangements underlie sustained tissue level shape changes: If the same optogenetic activation of Rho1 that induces junctional rearrangements does not effect sustained tissue-level shape changes, it would be clear that junctional rearrangements alone are not sufficient to ratchet cell- and tissue-shape changes.

Notably, recent work in tissue culture cells showed that optogenetic activation of Rho1 along a junction induced E-cadherin clustering [Cavanaugh et al., 2020]. The junctional E-cadherin clustering induced in these experiments, which occurred perpendicular to the apicobasal axis of the cultured cells, is distinct from the junctional rearrangements observed

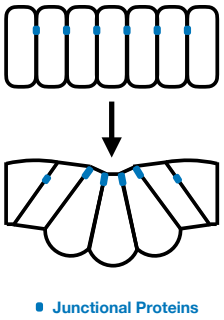

Figure 4.1: **Junctional proteins reorganize during ventral furrow formation.** Junctional proteins (blue) move from subapical to apical locations during ventral furrowing in the *Drosophila* embryo. A similar junctional rearrangement occurs during endoderm internalization in the *C. elegans* embryo.

during ventral furrow formation and endoderm invagination, which occur along the apicobasal axis. Nevertheless, this work demonstrates the feasibility of combining optogenetic activation of Rho1 with long-term imaging of E-cadherin.

4.2.4 What is the biological significance of pulsed contractility?

Both Rho1 and myosin exhibit pulsatile behavior in many systems. For example, as discussed in the introduction, pulsatile Rho1 and actomyosin precede ventral furrow formation and invagination in the *Drosophila* embryo [Roh-Johnson et al., 2012, Martin et al., 2009], and myosin pulses drive cortical flow and PAR protein polarization in the *C. elegans* zygote [Munro et al., 2004]. Furthermore, myosin pulses accompany the junctional rearrangements that drive germband extension in the *Drosophila* embryo. Notably, laser ablation of medial myosin pulses during germband extension caused junctions that had begun shrinking to relax (Rauzi 2010). However, are pulses of Rho1 and/or downstream effectors actually necessary to drive these developmental events? *C. elegans* zygotes still polarize their cortex in the absence of myosin pulses [Motegi et al., 2011, Zonies et al., 2010], and our optogenetic experiments induced tissue morphogenesis even though our activation protocols did not induce pulsatile Rho1 activity. These observations raise the possibility that pulses of Rho1 activity and

its effectors may be a consequence of the underlying biochemical network rather than a requirement for the cellular events with which they correlate. The importance of Rho1 and myosin pulses during ventral furrow formation can be readily tested in *Drosophila*, as different activation protocols that do or do not activate Rho1 in a pulsatile manner, while holding total Rho1 activation constant, could be applied to embryonic epithelia lacking endogenous contractility, such as in *dorsal* mutants. Would the cellular and molecular changes induced by pulsed Rho1 activation differ from those induced by sustained Rho1 activation?

4.2.5 Using optogenetic activation of Rho1 to delineate the contributions of distinct pools of actomyosin

During many morphogenetic events, such as ventral furrow formation and germ band extension, active Rho1 and actomyosin accumulates at multiple subcellular locations, including junctions and apical-medial regions (Figure 4.2) [Martin et al., 2009, Rauzi et al., 2010]. What is the contribution of each of these pools of Rho1 and actomyosin? This question cannot be addressed with traditional pharmacological approaches, as the same drug that eliminates Rho1 activity at the junction also eliminates Rho1 activity in the apical-medial region. In some cases, genetic manipulations can eliminate either the apical-medial or junctional pool of Rho1 activity [Garcia De Las Bayonas et al., 2019], but these genetic manipulations are chronic, requiring elimination or overexpression of a Rho1 activator over long periods of developmental time. In contrast, optogenetic approaches are well suited to tackle this problem. By activating Rho1 specifically and acutely at the junctions or apical-medial region, we could identify the consequences of contractility at each of these locations. For example, showing that Rho1 activation in the apical-medial, but not junctional, region of a cell drives junctional shortening during germband extension would be strong evidence that it is the apical-medial pool of Rho1 and actomyosin activity that are important for this cellular and developmental event. Furthermore, such experiments would reveal how the two pools

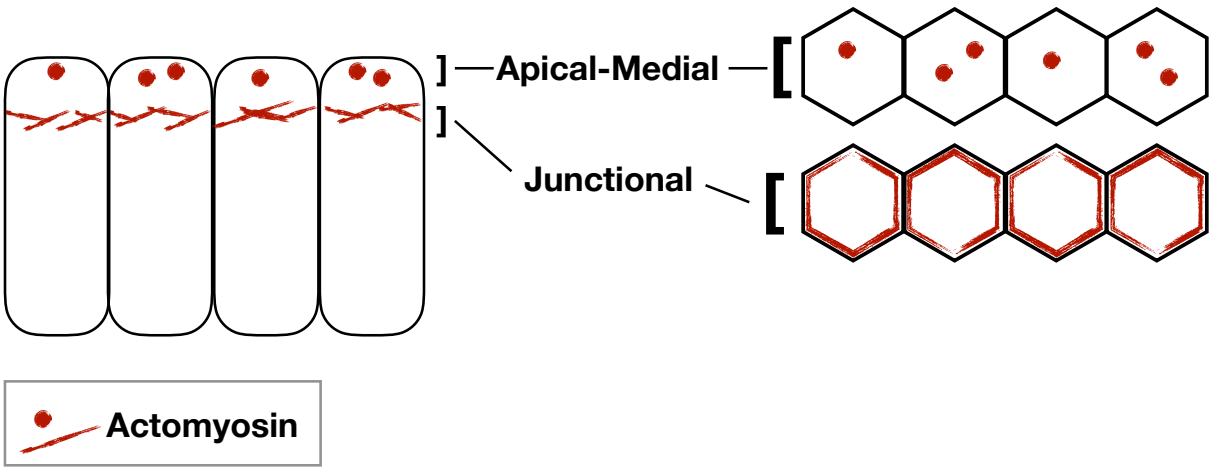

Figure 4.2: **Distinct pools of actomyosin exist during cell and tissue shape changes.** Which pool of actomyosin (red), apical-medial or junctional, drives cell and tissue-level shape changes? Do the two pools influence each other?

of Rho1 and actomyosin contractility interact during cell and tissue shape changes: Does Rho1 activation in the apical-medial region of a cell subsequently lead to Rho1 activity at the junctions? If so, this would be evidence of a feedforward mechanism for Rho1 activation within cells. In theory, these experiments would complement laser ablation experiments, which disrupt actomyosin structures with subcellular precision. However, unlike laser ablation, which can induce collateral damage, optogenetic activation of Rho1 would specifically affect contractility downstream of Rho1. Thus, similar to the way that we used optogenetic activation of Rho1 to reveal differences in the dorsal and ventral embryonic epithelia, optogenetics could be used to interrogate different functions of junctional versus apical-medial actomyosin within single cells.

4.3 What is the role of Cdc42 in neuroblast polarity?

Cdc42 is a critical regulator of cell polarization in many organisms. Cdc42 activity is required for symmetry breaking and bud site selection in budding yeast [Chiou et al., 2017, Bi and Park, 2012, Park and Bi, 2007], and Cdc42 activity maintains cortical polarity in the *C.*

elegans zygote [Kumfer et al., 2010, Motegi and Sugimoto, 2006, Aceto et al., 2006, Kay and Hunter, 2001, Jantsch-Plunger et al., 2000]. In both of these cases, the GEFs that activate Cdc42 activity are known. Cdc42 is required for the formation of apical crescents of Par6 and aPKC in *Drosophila* neuroblasts [Atwood et al., 2007], but the molecular mechanism by which Cdc42 promotes the formation of these apical crescents is unclear. Furthermore, unlike in *S. cerevisiae* and *C. elegans* zygotes, the GEF(s) that activate Cdc42 during neuroblast polarization have not been identified. Thus, there is much to understand about the role of Cdc42 during neuroblast polarization.

One possible function of Cdc42 during neuroblast polarization is that Cdc42 activity instructs the formation of apical polarity crescents. Optogenetic experiments in *S. cerevisae* demonstrated that Cdc42 activity is indeed sufficient to break symmetry in the budding yeast cell membrane and drive bud site selection [Witte et al., 2017]. This hypothesis is readily testable by optogenetics: If Cdc42 activity can instruct neuroblast polarization, local optogenetic activation of Cdc42 should drive ectopic accumulation of apical PAR proteins, including Par-6.

In opposition to this hypothesis, we have not obtained evidence of global Cdc42 activity affecting polarity factor localization or asymmetric cell division in *Drosophila* neuroblasts (see Chapter 3). Importantly, optogenetic activation of Cdc42 promotes the cortical association of Par-6 with the cell membrane in Drosophila S2 tissue culture cells and the recruitment of a Cdc42 biosensor in neuroblasts, confirming that our optogenetic probe does activate Cdc42 in *Drosophila*. It is possible that we are not activating Cdc42 to a high enough level to disrupt polarization in *Drosophila* neuroblasts. However, it is also possible that Cdc42 plays a permissive, rather than instructive, role in neuroblast polarization. In this case, Cdc42 may be required for apical polarity proteins, such as aPKC and Par6 to localize to and act at the apical plasma membrane; however, Cdc42 activity alone cannot mediate their recruitment. Instead, Cdc42 activity may need to overlap with a second factor that can

promote the association of aPKC and Par6 with the plasma membrane.

If Cdc42 activity cannot instruct neuroblast polarization, is there a protein activity that is sufficient to induce polarity in neuroblasts? Bazooka (Par3) lies genetically upstream of Cdc42 in neuroblast polarity [Atwood et al., 2007], and, as a scaffold, Bazooka binds many of the proteins that localize to the apical neuroblast cortex [Holly et al., 2020, Renschler et al., 2018, Morais-de Sa et al., 2010, Li et al., 2010b, Lin et al., 2000, Joberty et al., 2000, Wodarz et al., 2000]. Thus, Bazooka is an intriguing candidate for the neuroblast polarity inducer. Chapter 3 demonstrates the development of a photorecruitable version of Bazooka's PDZ domains, and it will be interesting to test whether PR-Baz can instruct the formation of a polarity crescent in neuroblasts. Alternatively, a combination of Cdc42 activity and Bazooka scaffolding may be the minimal unit for instructing polarization in the *Drosophila* neuroblast. This, too, could be readily tested by optogenetically activating Cdc42 and optogenetically recruiting Baz to a region of the neuroblast cortex. These experiments will be particularly informative in compromised backgrounds that remove endogenous polarity cues which could override and obscure the ability of an optogenetically activated or recruited protein to instruct polarization. For example, if Bazooka is indeed capable of instructing neuroblast polarization, PR-Baz may need to be recruited to the cortex of neuroblasts lacking endogenous Bazooka so that endogenous polarity crescents do not interfere with optogenetically induced polarization. Furthermore, larval neuroblasts lacking centrioles and embryonic neuroblasts isolated from their overlying ectoderm have both been shown to have randomized axes of polarity over subsequent asymmetric divisions, indicating that the memory of cortical polarity is lost in these two conditions [Januschke and Gonzalez, 2010, Siegrist and Doe, 2006]. Optogenetic recruitment of PR-Baz may be more potent in such neuroblasts.

It will be important to be mindful of potential cell cycle inputs on nucleators of neuroblast polarity. For example, Bem1, a scaffolding protein, can specify the site of bud site selection

when optogenetically recruited to the *S. cerevisiae* plasma membrane, but only after Cdk1 has become active. Bazooka, also a scaffolding protein, may be similarly dependent upon cell cycle stage to induce polarization. Indeed Bazooka crescents are first detectable in prophase [Wodarz et al., 2000, Schober et al., 1999, Wodarz et al., 1999]. Furthermore, PLK-1, a cell cycle regulator, negatively regulates the oligomerization of PAR-3 in the *C. elegans* zygote [Dickinson et al., 2017]. It would be quite interesting to discover that the ability of Bazooka to interact with other PAR proteins and/or the ability of Bazooka to oligomerize at the neuroblast plasma membrane is cell cycle-regulated. This possibility should be considered when experiments are designed to test the sufficiency of Bazooka to instruct neuroblast polarization.

In addition to playing a role in forming polarity crescents, Cdc42 may also tune the activity of aPKC during cell polarization. In the *C. elegans* zygote, both PAR-3 and CDC-42 are genetically required for the localization of PKC-3 and PAR-6 at the anterior cortex of the *C. elegans* zygote [Schonegg and Hyman, 2006, Kay and Hunter, 2001, Tabuse et al., 1998]. Recently, it was shown that a version of PKC-3 that is fused to a C1B domain can be ectopically forced to the plasma membrane via addition of a drug, PMA, bypassing the need for either PAR-3 or CDC-42 in membrane recruitment of PKC-3 [Rodriguez et al., 2017]. Using this pharmocological-sensitive PKC-3, it was shown that PKC-3 at the plasma membrane in embryos lacking PAR-3 can still displace PAR-1 from the plasma membrane, suggesting PAR-3 is not required to promote the kinase activity of PKC-3. In contrast, C1B-PKC-3 forced to the plasma membrane in the absence of CDC-42 no longer displaced PAR-1 from the membrane, suggesting that, unlike PAR-3, CDC-42 affects the kinase activity of PKC-3. Interestingly, RNAi against CDC-42 increases the clustering of PAR-6, while RNAi against PAR-3 decreases the clustering of PAR-6. Collectively, this work suggests a model whereby PAR-3 functions as a platform upon which PKC-3/PAR-6 complexes assemble and associate with the plasma membrane while CDC-42 promotes the kinase activity of PKC-

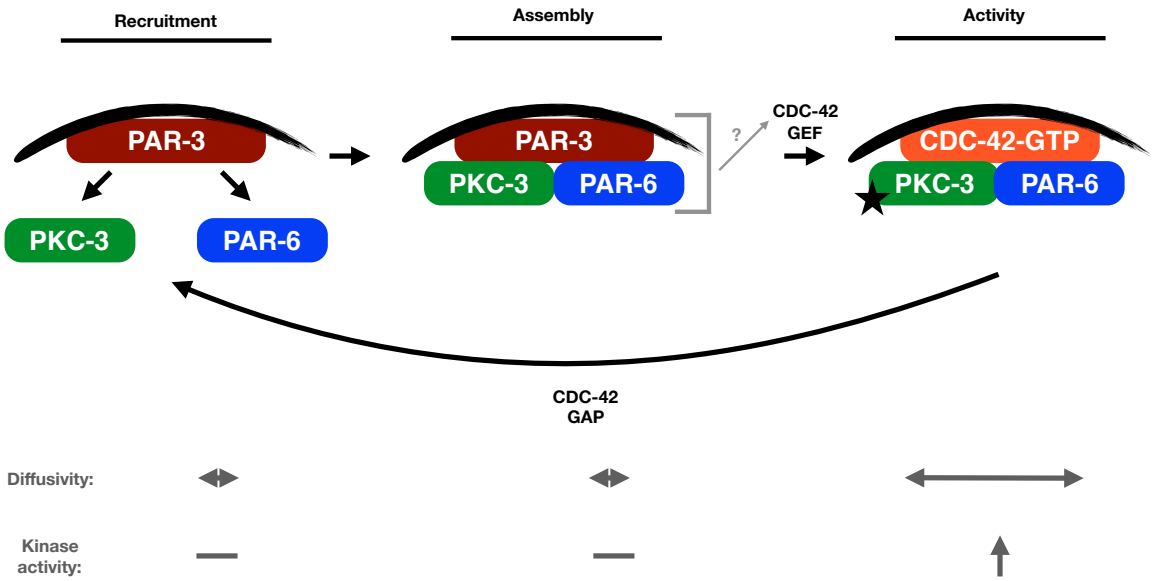

Figure 4.3: **Proposed model for Baz(PAR-3) and Cdc42 during polarization of the *Drosophila* neuroblast and *C. elegans* zygote.** PAR-3(Baz) recruits PKC-3(aPKC) and PAR-6 to the plasma membrane (left) and promotes the formation of a PAR-3/PKC-3/PAR-6 complex (middle). Active, GTP bound CDC-42 associates with PAR-6, releasing PKC-3/PAR-6 from PAR-3 (right). This promotes the diffusivity of PKC-3/PAR-6 as well as the kinase activity of PKC-3. Hydrolysis of GTP by CDC-42 leads to the disassembly of the PKC-3/PAR-6/CDC-42 complex and the return of PKC-3 and PAR-6 to the cytoplasm. PAR-3 and/or the PAR-3/PKC-3/PAR-6 complex may promote CDC-42 activity by recruiting a CDC-42 GEF (gray arrow). Star indicates kinase activity. Model based on the work of [Rodriguez et al., 2017, Sailer et al., 2015, Beers and Kemphues, 2006].

3/PAR-6 complexes. Furthermore, the RNAi data suggest that in addition to promoting kinase activity, CDC-42 association with PKC-3/PAR-6 complexes may promote their release from PAR-3 and increase their diffusion within the anterior cortex (Figure 4.3). These data are consistent with earlier work that identified distinct modes of membrane association for PAR-6: One mode involved binding to PAR-3. The other mode involved binding to CDC-42 in the absence of CDC-37 [Beers and Kemphues, 2006]. It is intriguing to speculate that PAR-3 or the PAR-3/PKC-3/PAR-6 complex could promote CDC-42 activity by recruiting a CDC-42 GEF (Figure 4.3).

This is an intriguing potential function for Cdc42 activity in the *Drosophila* neuroblast, and it could be readily tested with the optogenetic tools developed during my thesis

work. Specifically, does optogenetic activation of Cdc42 change the diffusivity of Par6 or aPKC within already formed PAR crescents? This would be indicative of Cdc42 activity influencing the oligomerization state of Par6 or aPKC. Does recruitable aPKC exhibit more kinase activity in neuroblasts expressing Cdc42 versus those depleted of Cdc42? Cdc42 acting to license aPKC's kinase activity could build in an intrinsic timer into the activity of Cdc42/aPKC/Par6 complexes. Cdc42, a GTPase, will eventually hydrolyze its GTP, and this hydrolysis event would likely disrupt the association of Cdc42 with an aPKC/Par6 complex as well as release the aPKC/Par6 complex from the plasma membrane. Thus, the licensing of aPKC kinase activity by Cdc42 would provide an additional layer of regulation over the formation of apical polarity crescents in *Drosophila* neuroblasts, ensuring that aPKC can only displace cell fate determinants from the apical-proximal cell cortex.

Another interesting set of questions involves the existence and importance of cortical flows for neuroblast polarity. Does Cdc42 activity generate cortical flows in neuroblasts? If so, do these flows contribute to cortical polarization? CDC-42, acting through MRCK-1 and myosin, promotes cortical flows during the maintenance phase of polarization in the *C. elegans* zygote [Sailer et al., 2015, Kumfer et al., 2010, Motegi and Sugimoto, 2006]. These flows contribute to maintaining the anterior and posterior PAR domains. Cortical myosin flows have been detected during cleavage furrow positioning and cytokinesis in neuroblasts [Roubinet et al., 2017]; thus, whether they also exist during and contribute to neuroblast polarization should also be investigated.

4.4 Technological hurdles limiting optogenetic control of Rho family GTPases

The work in this thesis and other publications establishes the feasibility of controlling Rho family GTPase activity via optogenetics in *Drosophila* [Izquierdo et al., 2018]. However, technical challenges remain that will need to be overcome to realize the full promise of

these optogenetic probes and to address the questions discussed above. For example, it will be critical to gain precise sub-cellular control over optogenetic activation of both Rho1 and Cdc42. To date, experiments designed to deliver light to a small proportion of the neuroblast cortex yielded uniformly cortical photorecruitable (PR)-probe recruitment and protein activation. Furthermore, while we have been able to restrict activation in the Z dimension in embryonic epithelial cells (along the apicobasal axis), PR-probes rapidly spread around the cell membrane in the X and Y dimensions (along the anterior-posterior axis), even when activation light is directed to a single junction. The fast cycling mutant LOV domain (Figure 2.4) may help overcome this technological hurdle, as this LOV domain recovers to its dark state in less than a minute. Fast cycling LOV domains that diffuse outside of the defined activation zone will rapidly revert to their dark state, increasing the precision of the light stimulus. Titrating down activation light doses is another promising solution. Furthermore, identification of membrane anchors that exhibit much less diffusion in the *Drosophila* plasma membrane could also improve the spatial precision of optogenetic activation in this organism. Endogenous proteins, such as the polarity factors discussed in Chapter 3, are capable of occupying subcellular domains within the plasma membrane. Thus, fusing the light-sensitive LOV domain to endogenous proteins, such as Bazooka or E-cadherin, is another potential solution to the problem of subcellular protein activation. Regardless of which approach solves this technical challenge, surmounting it is necessary to perturb cellular processes with sub-cellular precision.

Another technical hurdle that will improve the power of the optogenetic approaches developed here is the ability to combine local optogenetic activation with rapid 3D image acquisition. Morphogenesis, both endogenous and optogenetically induced, happens in three dimensions, and it is important to capture these cell and tissue movements throughout the volume of the tissue over time. The local activation experiments performed in this thesis were performed on a laser scanning confocal microscope. Thus, the time needed to image the

entire specimen volume was often incompatible with desired activation protocol. Performing these experiments on a spinning disc confocal microscope, which can acquire information in the z-dimension much faster will be an improvement. Combining the optogenetic probes developed here with less perturbing image acquisition setups, such as light sheet microscopy, will be even more fruitful. For example, the apical constrictions that occur during ventral furrowing are accompanied by cell lengthening along the apico-basal axis as well as expansion of the basal region of the cell [Gelbart et al., 2012]. Do the apical constrictions induced by optogenetic activation of Rho1 induce similar cell shape changes along the apicobasal axis? If not, why? What other protein activities are necessary to drive these additional cell shape changes?

4.5 Moving beyond optogenetic control of Rho1 and Cdc42 in *Drosophila*

The outstanding questions discussed above demonstrate that we have only begun deploying the optogenetic probes developed here to gain new insight into Rho1-mediated morphogenesis and Cdc42-mediated polarization in *Drosophila*. However, many questions in cell and developmental biology lie outside the reach of optogenetically controlled Rho1 or Cdc42. For example, the GTPase Rap1 plays roles in several morphogenetic events during *Drosophila* gastrulation, including the invagination of both the ventral furrow and the dorsal transverse folds [Wang et al., 2013, Spahn et al., 2012]. An optogenetic probe that controls Rap1 activity in *Drosophila* could help elucidate the role of this GTPase in these processes. Thus, another open area for future research is the development of additional optogenetic probes that control other proteins known to regulate morphogenesis and polarization.

If and when the development of new optogenetic probes is undertaken, a few considerations should be addressed. First, optogenetic probe design is of the utmost importance. Ideally, the recruitable protein should be inert in the dark state and divorced from all endoge-

nous regulation. One example of the importance of probe design can be seen by comparing two optogenetic probes that were used to ask whether RhoA activation is sufficient to induce a cleavage furrow to form. One study generated a photorecruitable version of Ect2, a RhoA and Cdc42 GEF that activates RhoA during cleavage furrow formation, by fusing full length Ect-2 to photosensitive CRY2. Recruiting Ect2-CRY2 to a pole of a HeLa cell, the region where the cleavage furrow would not normally form, induced a furrow to form at the equator of the cell, the region where the cleavage furrow would normally form [Kotýnková et al., 2016]. Furthermore, activation protocols that globally recruited Ect2-CRY2 to the plasma membrane of HeLa cells still induced cleavage furrow formation at the equatorial cortex, where it would normally form. These results differ from an approach that optogenetically activated RhoA by recruiting just the catalytic domain of a RhoA GEF (PDZ-LARG(DH)) [Wagner and Glotzer, 2016]. When PDZ-LARG(DH) was recruited to the poles of mammalian tissue culture cells, it *did* induce a furrow to form in the ectopic location, proving that RhoA activation is sufficient to induce cleavage furrow formation. These results suggest that photorecruitable full length Ect2 (Ect2-CRY2) still needs to be activated by endogenous factors, such as centralspindlin; regardless of where full length Ect2 was recruited to the plasma membrane, it was only activated RhoA at the equatorial cortex. Thus, Ect2-CRY2, unlike PDZ-LARG(DH), does not assay the ability of RhoA to effect cell biological processes but rather reveals when and where cells permit Ect2 to activate RhoA.

Another illustration of the importance of optogenetic probe design can be seen by comparing the two probes that have been developed to control Rho1 activation in *Drosophila* embryos. One approach engineered a recruitable version of RhoGEF2, the GEF that drives Rho1 activation during ventral furrow formation [Izquierdo et al., 2018]. This recruitable RhoGEF2 (CRY2-RhoGEF2(DHPH)) included both the Dbl homology (DH) domain and the pleckstrin homology (PH) domain of RhoGEF2. Rho1 activation via optogenetic recruitment of CRY2-RhoGEF2(DHPH) yielded pulsatile Rho1 activity over a variety of activation proto-

cols, suggesting that Rho1 exhibits a propensity towards pulsatile activity in the *Drosophila* embryonic epithelium. A second approach, reported in Chapter 2, activated Rho1 by recruiting a different engineered Rho1/RhoA GEF, SspB-LARG(DH). Importantly, this recruitable GEF includes only the catalytic DH domain of LARG. Rho1 activation via SspB-LARG(DH) never induced pulsatile Rho1 behavior (see Chapter 2). Furthermore, expressing the DHPH domains of RhoGEF2 in the context of our LOV domain-based optogenetic system impaired the viability of flies, even in the absence of membrane recruitment. The adverse effect of RhoGEF2(DHPH) expression was alleviated by mutating residues in RhoGEF2's PH domain that are thought to be involved in binding active Rho1-GTP. This suggests that the prior study, using CRY2-RhoGEF2(DHPH), observed pulsatile Rho1 activity not because Rho1 has a propensity to pulse in the *Drosophila* epithelium but rather because the optogenetic probe used has a propensity to induce pulsatile Rho1 activity (Figure 4.4). The above examples demonstrate that regulatory domains included in photorecruitable probes can synergize with photoactivation to alter the localization and/or activity profiles of the probes. Thus, the inclusion of domains in photorecruitable probes that may confound the interpretations of optogenetic experiments should be avoided.

A second consideration is that the scale of the biological question matches the precision of the optogenetic approach. For example, it would be quite exciting to expand the lab's work on modulating cleavage furrow formation from mammalian tissue culture cells to cells within *Drosophila* tissues [Wagner and Glotzer, 2016]. Is Rho1 activity still sufficient to induce a cleavage furrow to form when a cell exists within an epithelium? How does the presence of intercellular adhesions, such as adherens junctions, affect the response to Rho1 activation? However, until Rho1 can be reliably activated with subcellular precision in *Drosophila* cells, this question cannot be answered.

Finally, novel optogenetic probes and experiments should be designed to generate new knowledge, not just new technologies. The most insightful optogenetic studies in cell biology

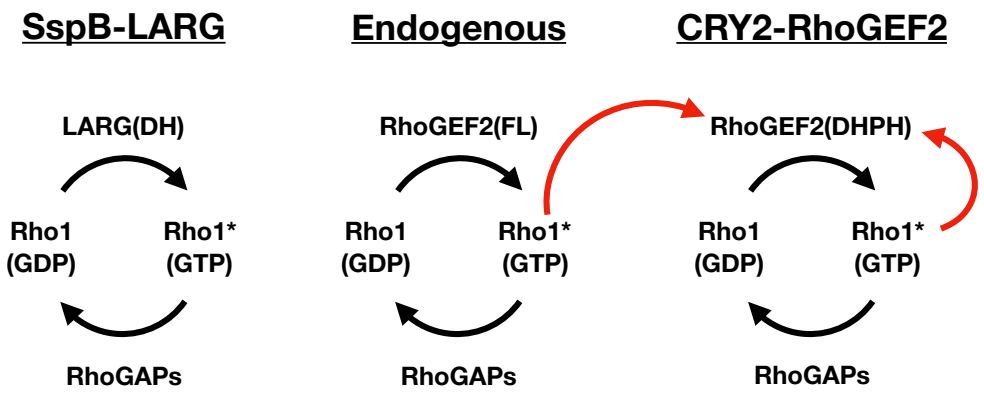

Figure 4.4: **Hypothesis for optogenetic induction of pulsatile Rho1 activity with CRY2-RhoGEF2(DHPH).** CRY2-RhoGEF2(DHPH) induces pulsatile Rho1 activity over a range of optogenetic activation protocols [Izquierdo et al., 2018]. SspB-LARG(DH) never induces pulsatile Rho1 activity (Chapter 2). CRY2-RhoGEF2(DHPH) includes a PH domain, which may enable CRY2-RhoGEF2(DHPH) bind active Rho1-GTP at the membrane (Right). This Rho1-GTP could be generated both by endogenous full-length RhoGEF2 and optogenetic CRY2-RhoGEF2(DHPH) (Red arrows). Combing this feedforward activation with negative feedback from Rho1 GAPs could yield the pulsatile Rho1 activity induced by CRY2-RhoGEF2(DHPH) (Right). SspB-LARG(DH) does not include a PH domain, and therefore, does not induce pulsatile Rho1 activity following optogenetic activation (Left).

to date are those that not only demonstrate light dependent control of protein activity but also use this inducible protein activity to deepen the understanding of a biological process. For example, optogenetic recruitment of Cdc24, a GEF, and Bem1, a scaffold, showed that each are sufficient to induce budsite selection in *S. cerevisae*. More importantly, Bem1, but not Cdc24, requires Cdk1 activity to specify a bud site [Witte et al., 2017]. Thus, exploiting the temporal precision of these probes revealed a novel cell-cycle regulation step in budding yeast symmetry breaking. In a separate study, optogenetic recruitment of RhoA to the cortex of mammalian cells showed that RhoA activation was sufficient to induce a cleavage furrow to form in anaphase-arrested cells. More importantly, though, the optogenetic probe for Rho1 activity was subsequently used to demonstrate that RhoA was able to induce a cleavage furrow to form regardless of the position of the mitotic spindle or the cell cycle stage [Wagner and Glotzer, 2016]. These and other similarly informative optogenetic experiments in single cells should inspire the use of optogenetics in developing organisms.

While a necessary proof of concept, moving proteins around cells and demonstrating that a given protein activity is sufficient to effect a biological process should not be end goals. Rather, optogenetic tools should be used to glean new information about the biological systems in which they are deployed. For example, in Chapter 2, we revealed a fundamental difference between the ventral and dorsal embryonic epithelia, which affects how these two tissues respond to Rho1 activation. The acute, spatiotemporal precision afforded by our optogenetic Rho1 probe enabled this discovery. Furthermore, the application of an optogenetic system that recruits SOS to the plasma membrane to activate ERK signaling proved that it is the cumulative load, not duration, of ERK signaling that informs cell fate decisions in the early *Drosophila* embryo [Johnson and Toettcher, 2019, Johnson et al., 2017]. These are exciting first steps towards deploying optogenetic tools to answer outstanding questions in developmental biology. Addressing the technological hurdles discussed above as well as developing additional optogenetic probes promises to make optogenetic tools standard members of the developmental biologist's experimental toolkit.

4.6 Conclusion

The generation of subcellular asymmetries remains a focus of developmental cell biology. My thesis work investigated how cells build contractile domains and use those domains to drive cell and tissue shape changes. It also explored how subcellular cortical domains are generated and how they contribute to asymmetric cell division. These processes are inherently dynamic, and the ability to image the molecular components responsible for forming these subcellular asymmetries with high spatial and temporal resolution transformed our mechanistic understanding of these processes. Optogenetic tools, such as those developed here, promise to move our understanding of these processes forward yet again, as they enable the manipulation of protein activity in real time, with high spatial and temporal precision. A key finding of the work presented here is that the dorsal and ventral embryonic epithelia

of *Drosophila* embryos exhibit dramatically different responses to identical spatial patterns of optogenetic Rho1 activation, suggesting a fundamental molecular and mechanical difference between these two epithelia. The ability to acutely activate Rho1 in a spatially defined manner made this discovery possible. As the above discussion emphasizes, many questions remain about the dynamic processes of morphogenesis and cell polarization. However, the research presented here as well as the research from several other groups [Krueger et al., 2019, 2018, Johnson and Toettcher, 2019, Izquierdo et al., 2018, Johnson et al., 2017, Sako et al., 2016] suggest that optogenetic approaches will be one key to answering these outstanding questions and formulating new questions about these developmental events.

References

Donato Aceto, Melissa Beers, and Kenneth J Kemphues. Interaction of PAR-6 with CDC-42 is required for maintenance but not establishment of PAR asymmetry in C. elegans. *Development*, 299(2):386–397, November 2006.

M Ahmad and A R Cashmore. HY4 gene of A. thaliana encodes a protein with characteristics of a blue-light photoreceptor. *Nature Publishing Group*, 366(6451):162–166, November 1993.

Benoit Aigouy, Reza Farhadifar, Douglas B Staple, Andreas Sagner, Jens-Christian Röper, Frank Jülicher, and Suzanne Eaton. Cell flow reorients the axis of planar polarity in the wing epithelium of Drosophila. *Cell*, 142(5):773–786, September 2010.

Jun Allard and Alex Mogilner. Traveling waves in actin dynamics and cell motility. *Current Opinion in Cell Biology*, 25(1):107–115, February 2013.

Dorian C Anderson, Jason S Gill, Ryan M Cinalli, and Jeremy Nance. Polarization of the C. elegans embryo by RhoGAP-mediated exclusion of PAR-6 from cell contacts. *Science*, 320(5884):1771–1774, June 2008.

Scott X Atwood and Kenneth E Prehoda. aPKC Phosphorylates Miranda to Polarize Fate Determinants during Neuroblast Asymmetric Cell Division. *Current Biology*, 19(9):723–729, May 2009.

Scott X Atwood, Chiswili Chabu, Rhiannon R Penkert, Chris Q Doe, and Kenneth E Prehoda. Cdc42 acts downstream of Bazooka to regulate neuroblast polarity through Par-6 aPKC. *Journal of Cell Science*, 120(Pt 18):3200–3206, September 2007.

Matthew J Bailey and Kenneth E Prehoda. Establishment of Par-Polarized Cortical Domains via Phosphoregulated Membrane Motifs. *Developmental Cell*, 35(2):199–210, October 2015.

K Barrett, M Leptin, and J Settleman. The Rho GTPase and a putative RhoGEF mediate a signaling pathway for the cell shape changes in Drosophila gastrulation. *Cell*, 91(7): 905–915, December 1997.

Alexander Beatty, Diane Morton, and Kenneth Kemphues. The C. elegans homolog of Drosophila Lethal giant larvae functions redundantly with PAR-2 to maintain polarity in the early embryo. *Development*, 137(23):3995–4004, December 2010.

Alexander Beatty, Diane G Morton, and Kenneth Kemphues. PAR-2, LGL-1 and the CDC-42 GAP CHIN-1 act in distinct pathways to maintain polarity in the C. elegans embryo. *Development*, 140(9):2005–2014, May 2013.

Melissa Beers and Kenneth Kemphues. Depletion of the co-chaperone CDC-37 reveals two modes of PAR-6 cortical association in C. elegans embryos. *Development*, 133(19):3745–3754, October 2006.

Bruno Bello, Heinrich Reichert, and Frank Hirth. The brain tumor gene negatively regulates neural progenitor cell proliferation in the larval central brain of Drosophila. *Development*, 133(14):2639–2648, July 2006.

William M Bement, Marcin Leda, Alison M Moe, Angela M Kita, Matthew E Larson, Adriana E Golding, Courtney Pfeuti, Kuan-Chung Su, Ann L Miller, Andrew B Goryachev, and George von Dassow. Activator-inhibitor coupling between Rho signalling and actin assembly makes the cell cortex an excitable medium. *Nature Cell Biology*, 17(11):1471–1483, November 2015.

S Ben-Yaacov, R Le Borgne, I Abramson, F Schweisguth, and E D Schejter. Wasp, the Drosophila Wiskott-Aldrich syndrome gene homologue, is required for cell fate decisions mediated by Notch signaling. *The Journal of Cell Biology*, 152(1):1–13, January 2001.

Richard Benton and Daniel St Johnston. A conserved oligomerization domain in drosophila Bazooka/PAR-3 is important for apical localization and epithelial polarity. *Current Biology*, 13(15):1330–1334, August 2003a.

Richard Benton and Daniel St Johnston. Drosophila PAR-1 and 14-3-3 inhibit Bazooka/PAR-3 to establish complementary cortical domains in polarized cells. *Cell*, 115(6):691–704, December 2003b.

Joerg Betschinger, Karl Mechtler, and Juergen A Knoblich. Asymmetric segregation of the tumor suppressor brat regulates self-renewal in Drosophila neural stem cells. *Cell*, 124(6): 1241–1253, March 2006.

Erfei Bi and Hay-Oak Park. Cell polarization and cytokinesis in budding yeast. *Genetics*, 191(2):347–387, June 2012.

J R Bischoff, L Anderson, Y Zhu, K Mossie, L Ng, B Souza, B Schryver, P Flanagan, F Clairvoyant, C Ginther, C S Chan, M Novotny, D J Slamon, and G D Plowman. A homologue of Drosophila aurora kinase is oncogenic and amplified in human colorectal cancers. *The EMBO Journal*, 17(11):3052–3065, June 1998.

Sarah K Bowman, Ralph A Neumüller, Maria Novatchkova, Quansheng Du, and Juergen A Knoblich. The Drosophila NuMA Homolog Mud regulates spindle orientation in asymmetric cell division. *DEVCEL*, 10(6):731–742, June 2006.

L Boyd, S Guo, D Levitan, D T Stinchcomb, and K J Kemphues. PAR-2 is asymmetrically distributed and promotes association of P granules and PAR-1 with the cortex in C. elegans embryos. *Development*, 122(10):3075–3084, October 1996.

Edward S Boyden, Feng Zhang, Ernst Bamberg, Georg Nagel, and Karl Deisseroth. Millisecond-timescale, genetically targeted optical control of neural activity. *Nature Neuroscience*, 8(9):1263–1268, September 2005.

R P Brendza, L R Serbus, J B Duffy, and W M Saxton. A function for kinesin I in the posterior transport of oskar mRNA and Staufen protein. *Science*, 289(5487):2120–2122, September 2000.

Clare E Buckley, Rachel E Moore, Anna Reade, Anna R Goldberg, Orion D Weiner, and Jonathan D W Clarke. Reversible Optogenetic Control of Subcellular Protein Localization in a Live Vertebrate Embryo. *Developmental Cell*, 36(1):117–126, January 2016.

L J Bugaj, D P Spelke, C K Mesuda, M Varedi, R S Kane, and D V Schaffer. Regulation of endogenous transmembrane receptors through optogenetic Cry2 clustering. *Nature Communications*, 6(1):6898, April 2015.

Lukasz J Bugaj, Atri T Choksi, Colin K Mesuda, Ravi S Kane, and David V Schaffer. Optogenetic protein clustering and signaling activation in mammalian cells. *Nature Methods*, 10(3):249–252, March 2013.

Danfeng Cai, Shann-Ching Chen, Mohit Prasad, Li He, Xiaobo Wang, Valerie Choesmel-Cadamuro, Jessica K Sawyer, Gaudenz Danuser, and Denise J Montell. Mechanical feedback through E-cadherin promotes direction sensing during collective cell migration. *Cell*, 157(5):1146–1159, May 2014.

Jose A. Campos-Ortega and Volker Hartenstein. *The Embryonic Development of Drosophila melanogaster*. Springer-Verlag, 1985.

Kate E Cavanaugh, Michael F Staddon, Edwin Munro, Shiladitya Banerjee, and Margaret L Gardel. RhoA Mediates Epithelial Cell Shape Changes via Mechanosensitive Endocytosis. *Developmental Cell*, 52(2):152–166.e5, January 2020.

Byeong-Jik Cha, Laura R Serbus, Birgit S Koppetsch, and William E Theurkauf. Kinesin I-dependent cortical exclusion restricts pole plasm to the oocyte posterior. *Nature Cell Biology*, 4(8):592–598, August 2002.

Emily Chan and Jeremy Nance. Mechanisms of CDC-42 activation during contact-induced cell polarization. *Journal of Cell Science*, 126(Pt 7):1692–1702, April 2013.

L N Chan and W Gehring. Determination of blastoderm cells in Drosophila melanogaster. *Proceedings of the National Academy of Sciences of the United States of America*, 68(9): 2217–2221, September 1971.

Zhe Chen, Frank Medina, Mu-ya Liu, Celestine Thomas, Stephen R Sprang, and Paul C Sternweis. Activated RhoA binds to the pleckstrin homology (PH) domain of PDZ-RhoGEF, a potential site for autoregulation. *The Journal of Biological Chemistry*, 285 (27):21070–21081, July 2010.

Jian-Geng Chiou, Mohan K Balasubramanian, and Daniel J Lew. Cell Polarity in Yeast. *Annual Review of Cell and Developmental Biology*, 33:77–101, October 2017.

J M Christie, P Reymond, G K Powell, P Bernasconi, A A Raibekas, E Liscum, and W R Briggs. Arabidopsis NPH1: a flavoprotein with the properties of a photoreceptor for phototropism. *Science*, 282(5394):1698–1701, November 1998.

John M Christie, Stephanie B Corchnoy, Trevor E Swartz, Mark Hokenson, In-Seob Han, Winslow R Briggs, and Roberto A Bogomolni. Steric interactions stabilize the signaling state of the LOV2 domain of phototropin 1. *Biochemistry*, 46(32):9310–9319, August 2007.

Neophytos Christodoulou and Paris A Skourides. Cell-Autonomous Ca(2+) Flashes Elicit Pulsed Contractions of an Apical Actin Network to Drive Apical Constriction during Neural Tube Closure. *CellReports*, 13(10):2189–2202, December 2015.

M Costa, E T Wilson, and E Wieschaus. A putative cell signal encoded by the folded gastrulation gene coordinates cell shape changes during Drosophila gastrulation. *Cell*, 76 (6):1075–1089, March 1994.

Carrie R Cowan and Anthony A Hyman. Centrosomes direct cell polarity independently of microtubule assembly in C. elegans embryos. *Nature*, 431(7004):92–96, September 2004.

Carrie R Cowan and Anthony A Hyman. Acto-myosin reorganization and PAR polarity in C. elegans. *Development*, 134(6):1035–1043, March 2007.

Richard Crane, Bedrick Gadea, Laurie Littlepage, Hua Wu, and Joan V Ruderman. Aurora A, meiosis and mitosis. *Biological Procedures Online*, 96(3):215–229, April 2004.

Rachel E Dawes-Hoang, Kush M Parmar, Audrey E Christiansen, Chris B Phelps, Andrea H Brand, and Eric F Wieschaus. folded gastrulation, cell shape change and the control of myosin localization. *Development*, 132(18):4165–4178, September 2005.

Victoria E Deneke, Alberto Puliafito, Daniel Krueger, Avaneesh V Narla, Alessandro De Simone, Luca Primo, Massimo Vergassola, Stefano De Renzis, and Stefano Di Talia. Self-Organized Nuclear Positioning Synchronizes the Cell Cycle in Drosophila Embryos. *Cell*, 177(4):925–941.e17, May 2019.

Daniel J Dickinson, Francoise Schwager, Lionel Pintard, Monica Gotta, and Bob Goldstein. A Single-Cell Biochemistry Approach Reveals PAR Complex Dynamics during Cell Polarization. *Developmental Cell*, 42(4):416–434.e11, August 2017.

Elliot Dine, Agnieszka A Gil, Giselle Uribe, Clifford P Brangwynne, and Jared E Toettcher. Protein Phase Separation Provides Long-Term Memory of Transient Spatial Stimuli. *Cell systems*, 6(6):655–663.e5, June 2018.

Konstantin Doubrovinski, Joel Tchoufag, and Kranthi Mandadapu. A simplified mechanism for anisotropic constriction in Drosophila mesoderm. *Development*, 145(24), December 2018.

Boris Egger, James M Chell, and Andrea H Brand. Insights into neural stem cell biology from flies. *Philosophical Transactions of the Royal Society B: Biological Sciences*, 363 (1489):39–56, January 2008.

B Etemad-Moghadam, S Guo, and K J Kemphues. Asymmetrically distributed PAR-3 protein contributes to cell polarity and spindle alignment in early C. elegans embryos. *Cell*, 83(5):743–752, December 1995.

Wei Feng, Hao Wu, Ling-Nga Chan, and Mingjie Zhang. The Par-3 NTD adopts a PB1-like structure required for Par-3 oligomerization and membrane localization. *The EMBO Journal*, 26(11):2786–2796, June 2007.

Lars-Eric Fielmich, Ruben Schmidt, Daniel J Dickinson, Bob Goldstein, Anna Akhmanova, and Sander van den Heuvel. Optogenetic dissection of mitotic spindle positioning in vivo. *eLife*, 7:219, August 2018.

V E Foe and B M Alberts. Studies of nuclear and cytoplasmic behaviour during the five mitotic cycles that precede gastrulation in Drosophila embryogenesis. *Journal of Cell Science*, 61:31–70, May 1983.

Donald T Fox and Mark Peifer. Abelson kinase (Abl) and RhoGEF2 regulate actin organization during cell constriction in Drosophila. *Development*, 134(3):567–578, February 2007.

Guo-Jie Jason Gao, Michael C Holcomb, Jeffrey H Thomas, and Jerzy Blawzdziewicz. Embryo as an active granular fluid: stress-coordinated cellular constriction chains. *Journal of physics. Condensed matter : an Institute of Physics journal*, 28(41):414021, October 2016.

Alain Garcia De Las Bayonas, Jean-Marc Philippe, Annemarie C Lellouch, and Thomas Lecuit. Distinct RhoGEFs Activate Apical and Junctional Contractility under Control of G Proteins during Epithelial Morphogenesis. *Current biology : CB*, 29(20):3370–3385.e7, October 2019.

E Gateff. Malignant neoplasms of genetic origin in Drosophila melanogaster. *Science*, 200 (4349):1448–1459, June 1978.

Michael A Gelbart, Bing He, Adam C Martin, Stephan Y Thiberge, Eric F Wieschaus, and Matthias Kaschube. Volume conservation principle involved in cell lengthening and nucleus movement during tissue morphogenesis. *Proceedings of the National Academy of Sciences*, 109(47):19298–19303, November 2012.

Daniel G Gibson, Lei Young, Ray-Yuan Chuang, J Craig Venter, Clyde A Hutchison, and Hamilton O Smith. Enzymatic assembly of DNA molecules up to several hundred kilobases. *Nature Methods*, 6(5):343–345, May 2009.

Darren Gilmour, Martina Rembold, and Maria Leptin. From morphogen to morphogenesis and back. *Nature*, 541(7637):311–320, January 2017.

D M Glover, M H Leibowitz, D A McLean, and H Parry. Mutations in aurora prevent centrosome separation leading to the formation of monopolar spindles. *Cell*, 81(1):95–105, April 1995.

Bob Goldstein and Jeremy Nance. Caenorhabditis elegans Gastrulation: A Model for Understanding How Cells Polarize, Change Shape, and Journey Toward the Center of an Embryo. *Genetics*, 214(2):265–277, February 2020.

Pierre Gönczy and Lesilee S Rose. Asymmetric cell division and axis formation in the embryo. *WormBook*, pages 1–20, October 2005.

M Gotta, M C Abraham, and J Ahringer. CDC-42 controls early cell polarity and spindle orientation in C. elegans. *Current Biology*, 11(7):482–488, April 2001.

Mélanie Gracia, Sophie Theis, Amsha Proag, Guillaume Gay, Corinne Benassayag, and Magali Suzanne. Mechanical impact of epithelial-mesenchymal transition on epithelial morphogenesis in Drosophila. *Nature Communications*, 10(1):2951, July 2019.

Viviana Gradinaru, Murtaza Mogri, Kimberly R Thompson, Jaimie M Henderson, and Karl Deisseroth. Optical deconstruction of parkinsonian neural circuitry. *Science*, 324(5925): 354–359, April 2009.

Chiharu Graybill, Brett Wee, Scott X Atwood, and Kenneth E Prehoda. Partitioning-defective protein 6 (Par-6) activates atypical protein kinase C (aPKC) by pseudosubstrate displacement. *The Journal of Biological Chemistry*, 287(25):21003–21011, June 2012.

Erik E Griffin. Cytoplasmic localization and asymmetric division in the early embryo of Caenorhabditis elegans. *Wiley Interdisciplinary Reviews: Developmental Biology*, 4(3): 267–282, May 2015.

Michael Grusch, Karin Schelch, Robert Riedler, Eva Reichhart, Christopher Differ, Walter Berger, Álvaro Inglés Prieto, and Harald Janovjak. Spatio-temporally precise activation of engineered receptor tyrosine kinases by light. *The EMBO Journal*, 33(15):1713–1726, August 2014.

Gurkan Guntas, Ryan A Hallett, Seth P Zimmerman, Tishan Williams, Hayretin Yumerefendi, James E Bear, and Brian Kuhlman. Engineering an improved light-induced dimer (iLID) for controlling the localization and activity of signaling proteins. *Proceedings of the National Academy of Sciences*, 112(1):112–117, January 2015.

H Guo, H Yang, T C Mockler, and C Lin. Regulation of flowering time by Arabidopsis photoreceptors. *Science*, 279(5355):1360–1363, February 1998.

S Guo and K J Kemphues. par-1, a gene required for establishing polarity in C. elegans embryos, encodes a putative Ser/Thr kinase that is asymmetrically distributed. *Cell*, 81 (4):611–620, May 1995.

U Häcker and N Perrimon. DRhoGEF2 encodes a member of the Dbl family of oncogenes and controls cell shape changes during gastrulation in Drosophila. *Genes & Development*, 12(2):274–284, January 1998.

Saori L Haigo, Jeffrey D Hildebrand, Richard M Harland, and John B Wallingford. Shroom Induces Apical Constriction and Is Required for Hingepoint Formation during Neural Tube Closure. *Current Biology*, 13(24):2125–2137, December 2003.

K Han. An efficient DDAB-mediated transfection of Drosophila S2 cells. *Nucleic Acids Research*, 24(21):4362–4363, November 1996.

Matthew Robert Hannaford, Anne Ramat, Nicolas Loyer, and Jens Januschke. aPKC-mediated displacement and actomyosin-mediated retention polarize Miranda in Drosophila neuroblasts. *eLife*, 7:166, January 2018.

Shannon M Harper, Lori C Neil, and Kevin H Gardner. Structural basis of a phototropin light switch. *Science*, 301(5639):1541–1544, September 2003.

Tony J C Harris. Adherens junction assembly and function in the Drosophila embryo. *International review of cell and molecular biology*, 293:45–83, 2012.

Tony J C Harris and Ulrich Tepass. Adherens junctions: from molecules to morphogenesis. *Nature Reviews Molecular Cell Biology*, 11(7):502–514, July 2010.

Volker Hartenstein and Andreas Wodarz. Initial neurogenesis in Drosophila. *Wiley Interdisciplinary Reviews: Developmental Biology*, 2(5):701–721, September 2013.

Tomohiro Haruta, Rahul Warrior, Shigenobu Yonemura, and Hiroki Oda. The proximal half of the Drosophila E-cadherin extracellular region is dispensable for many cadherin-dependent events but required for ventral furrow formation. *Genes to Cells*, 15(3):193–208, March 2010.

Michael A Herman and Mingfu Wu. Noncanonical Wnt signaling pathways in C. elegans converge on POP-1/TCF and control cell polarity. *Frontiers in bioscience : a journal and virtual library*, 9(1-3):1530–1539, May 2004.

Yoshinori Hirano, Sosuke Yoshinaga, Ryu Takeya, Nobuo N Suzuki, Masataka Horiuchi, Motoyuki Kohjima, Hideki Sumimoto, and Fuyuhiko Inagaki. Structure of a cell polarity regulator, a complex between atypical PKC and Par6 PB1 domains. *Journal of Biological Chemistry*, 280(10):9653–9661, March 2005.

Carsten Hoege, Alexandru-Tudor Constantinescu, Anne Schwager, Nathan W Goehring, Prateek Kumar, and Anthony A Hyman. LGL can partition the cortex of one-cell Caenorhabditis elegans embryos into two domains. *Current biology : CB*, 20(14):1296–1303, July 2010.

Ryan W Holly, Kimberly Jones, and Kenneth E Prehoda. A Conserved PDZ-Binding Motif in aPKC Interacts with Par-3 and Mediates Cortical Polarity. *Current Biology*, 30(5): 893–898.e5, March 2020.

Anqi Huang, Christopher Amourda, Shaobo Zhang, Nicholas S Tolwinski, and Timothy E Saunders. Decoding temporal interpretation of the morphogen Bicoid in the early Drosophila embryo. *eLife*, 6:197, July 2017.

T J Hung and K J Kemphues. PAR-6 is a conserved PDZ domain-containing protein that colocalizes with PAR-3 in Caenorhabditis elegans embryos. *Development*, 126(1):127–135, January 1999.

H Ikeshima-Kataoka, J B Skeath, Y Nabeshima, C Q Doe, and F Matsuzaki. Miranda directs Prospero to a daughter cell during Drosophila asymmetric divisions. *Nature Publishing Group*, 390(6660):625–629, December 1997.

Takanari Inoue, Won Do Heo, Joshua S Grimley, Thomas J Wandless, and Tobias Meyer. An inducible translocation strategy to rapidly activate and inhibit small GTPase signaling pathways. *Nature Methods*, 2(6):415–418, June 2005.

Y T Ip, R E Park, D Kosman, K Yazdanbakhsh, and M Levine. dorsal-twist interactions establish snail expression in the presumptive mesoderm of the Drosophila embryo. *Genes & Development*, 6(8):1518–1530, August 1992.

Keiji Itoh, Olga Ossipova, and Sergei Y Sokol. GEF-H1 functions in apical constriction and cell intercalations and is essential for vertebrate neural tube closure. *Journal of Cell Science*, 127(Pt 11):2542–2553, June 2014.

Emiliano Izquierdo, Theresa Quinkler, and Stefano De Renzis. Guided morphogenesis through optogenetic activation of Rho signalling during early Drosophila embryogenesis. *Nature Communications*, 9(1):2366, June 2018.

Yasushi Izumi, Nao Ohta, Kanako Hisata, Thomas Raabe, and Fumio Matsuzaki. Drosophila Pins-binding protein Mud regulates spindle-polarity coupling and centrosome organization. *Nature Cell Biology*, 8(6):586–593, June 2006.

Aron B Jaffe and Alan Hall. Rho GTPases: biochemistry and biology. *Annual Review of Cell and Developmental Biology*, 21:247–269, 2005.

Mamta Jaiswal, Radovan Dvorsky, and Mohammad Reza Ahmadian. Deciphering the molecular and functional basis of Dbl family proteins: a novel systematic approach toward classification of selective activation of the Rho family proteins. *Journal of Biological Chemistry*, 288(6):4486–4500, February 2013.

V Jantsch-Plunger, P Gonczy, A Romano, H Schnabel, D Hamill, R Schnabel, A A Hyman, and M Glotzer. CYK-4: A Rho family gtpase activating protein (GAP) required for central spindle formation and cytokinesis. *The Journal of Cell Biology*, 149(7):1391–1404, June 2000.

Jens Januschke and Cayetano Gonzalez. The interphase microtubule aster is a determinant of asymmetric division orientation in Drosophila neuroblasts. *The Journal of Cell Biology*, 188(5):693–706, March 2010.

J Jiang, D Kosman, Y T Ip, and M Levine. The dorsal morphogen gradient regulates the mesoderm determinant twist in early Drosophila embryos. *Genes & Development*, 5(10): 1881–1891, October 1991.

Tao Jiang, R F Andrew McKinley, Melanie A McGill, Stephane Angers, and Tony J C Harris. A Par-1-Par-3-Centrosome Cell Polarity Pathway and Its Tuning for Isotropic Cell Adhesion. *Current biology : CB*, 25(20):2701–2708, October 2015.

G Joberty, C Petersen, L Gao, and I G Macara. The cell-polarity protein Par6 links Par3 and atypical protein kinase C to Cdc42. *Nature Cell Biology*, 2(8):531–539, August 2000.

Jeanne N Jodoin, Jonathan S Coravos, Soline Chanet, Claudia G Vasquez, Michael Tworoger, Elena R Kingston, Lizabeth A Perkins, Norbert Perrimon, and Adam C Martin. Stable Force Balance between Epithelial Cells Arises from F-Actin Turnover. *Developmental Cell*, 35(6):685–697, December 2015.

Heath E Johnson and Jared E Toettcher. Signaling Dynamics Control Cell Fate in the Early Drosophila Embryo. *Developmental Cell*, 48(3):361–370.e3, February 2019.

Heath E Johnson, Yogesh Goyal, Nicole L Pannucci, Trudi Schüpbach, Stanislav Y Shvartsman, and Jared E Toettcher. The Spatiotemporal Limits of Developmental Erk Signaling. *Developmental Cell*, 40(2):185–192, January 2017.

Sukriti Kapoor and Sachin Kotak. Centrosome Aurora A regulates RhoGEF ECT-2 localisation and ensures a single PAR-2 polarity axis in C. elegans embryos. *Development*, 146 (22), November 2019.

A J Kay and C P Hunter. CDC-42 regulates PAR protein localization and function to control cellular and embryonic polarity in C. elegans. *Current Biology*, 11(7):474–481, April 2001.

K J Kemphues, J R Priess, D G Morton, and N S Cheng. Identification of genes required for cytoplasmic localization in early C. elegans embryos. *Cell*, 52(3):311–320, February 1988.

Matthew J Kennedy, Robert M Hughes, Leslie A Peteya, Joel W Schwartz, Michael D Ehlers, and Chandra L Tucker. Rapid blue-light-mediated induction of protein interactions in living cells. *Nature Methods*, 7(12):973–975, December 2010.

Stephen Kerridge, Akankshi Munjal, Jean-Marc Philippe, Ankita Jha, Alain Garcia de las Bayonas, Andrew J Saurin, and Thomas Lecuit. Modular activation of Rho1 by GPCR signalling imparts polarized myosin II activation during morphogenesis. *Nature Cell Biology*, 18(3):261–270, January 2016.

Nury Kim, Jin Man Kim, Minji Lee, Cha Yeon Kim, Ki-Young Chang, and Won Do Heo. Spatiotemporal control of fibroblast growth factor receptor signals by blue light. *Chemistry & Biology*, 21(7):903–912, July 2014.

Kerstin Klinkert, Nicolas Levernier, Peter Gross, Christian Gentili, Lukas von Tobel, Marie Pierron, Coralie Busso, Sarah Herrman, Stephan W Grill, Karsten Kruse, and Pierre Gönczy. Aurora A depletion reveals centrosome-independent polarization mechanism in Caenorhabditis elegans. *eLife*, 8:316, February 2019.

Kristin M Klueg, Diego Alvarado, Marc A T Muskavitch, and Joseph B Duffy. Creation of a GAL4/UAS-coupled inducible gene expression system for use in Drosophila cultured cell lines. *genesis*, 34(1-2):119–122, September 2002.

Clint S Ko and Adam C Martin. The cellular and molecular mechanisms that establish the mechanics of Drosophila gastrulation. *Current topics in developmental biology*, 136: 141–165, 2020.

Johannes Kohl, Julian Ng, Sebastian Cachero, Ernesto Ciabatti, Michael-John Dolan, Ben Sutcliffe, Adam Tozer, Sabine Ruehle, Daniel Krueger, Shahar Frechter, Tiago Branco, Marco Tripodi, and Gregory S X E Jefferis. Ultrafast tissue staining with chemical tags. *Proceedings of the National Academy of Sciences*, 111(36):E3805–14, September 2014.

Verena Kölsch, Thomas Seher, Gregorio J Fernandez-Ballester, Luis Serrano, and Maria Leptin. Control of Drosophila gastrulation by apical localization of adherens junctions and RhoGEF2. *Science*, 315(5810):384–386, January 2007.

Kalyn Kono, Shigeki Yoshiura, Ikumi Fujita, Yasushi Okada, Atsunori Shitamukai, Tatsuo Shibata, and Fumio Matsuzaki. Reconstruction of Par-dependent polarity in apolar cells reveals a dynamic process of cortical polarization. *eLife*, 8:386, June 2019.

Kristýna Kotýnková, Kuan-Chung Su, Stephen C West, and Mark Petronczki. Plasma Membrane Association but Not Midzone Recruitment of RhoGEF ECT2 Is Essential for Cytokinesis. *CellReports*, 17(10):2672–2686, December 2016.

Michael P Krahn, Diane Egger-Adam, and Andreas Wodarz. PP2A antagonizes phosphorylation of Bazooka by PAR-1 to control apical-basal polarity in dividing embryonic neuroblasts. *Developmental Cell*, 16(6):901–908, June 2009.

Michael P Krahn, Dieter R Klopfenstein, Nannette Fischer, and Andreas Wodarz. Membrane targeting of Bazooka/PAR-3 is mediated by direct binding to phosphoinositide lipids. *Current biology : CB*, 20(7):636–642, April 2010.

Jana Krauss, Sonia López de Quinto, Christiane NUsslein-Volhard, and Anne Ephrussi. Myosin-V regulates oskar mRNA localization in the Drosophila oocyte. *Current biology : CB*, 19(12):1058–1063, June 2009.

R Kraut, W Chia, L Y Jan, Y N Jan, and J A Knoblich. Role of inscuteable in orienting asymmetric cell divisions in Drosophila. *Nature Publishing Group*, 383(6595):50–55, September 1996.

Daniel Krueger, Pietro Tardivo, Congtin Nguyen, and Stefano De Renzis. Downregulation of basal myosin-II is required for cell shape changes and tissue invagination. *The EMBO Journal*, 37(23):775, December 2018.

Daniel Krueger, Theresa Quinkler, Simon Arnold Mortensen, Carsten Sachse, and Stefano De Renzis. Cross-linker-mediated regulation of actin network organization controls tissue morphogenesis. *The Journal of Cell Biology*, 218(8):2743–2761, August 2019.

K.V. Kumar, J.S. Bois, F. Julicher, and S.W. Grill. Pulsatory Patterns in Active Fluids. *Phys. Rev. Lett.*, 112(208101), 2014.

Kraig T Kumfer, Steven J Cook, Jayne M Squirrell, Kevin W Eliceiri, Nina Peel, Kevin F O'Connell, and John G White. CGEF-1 and CHIN-1 regulate CDC-42 activity during asymmetric division in the Caenorhabditis elegans embryo. *Molecular Biology of the Cell*, 21(2):266–277, January 2010.

Charles F Lang and Edwin Munro. The PAR proteins: from molecular circuits to dynamic self-stabilizing cell polarity. *Development (Cambridge, England)*, 144(19):3405–3416, October 2017.

P Lasko. RNA sorting in Drosophila oocytes and embryos. *The FASEB Journal*, 13(3): 421–433, March 1999.

C Lee, H M Scherr, and J B Wallingford. Shroom family proteins regulate -tubulin distribution and microtubule architecture during epithelial cell shape change. *Development*, 134(7):1431–1441, February 2007.

Cheng-Yu Lee, Ryan O Andersen, Clemens Cabernard, Laurina Manning, Khoa D Tran, Marcus J Lanskey, Arash Bashirullah, and Chris Q Doe. Drosophila Aurora-A kinase inhibits neuroblast self-renewal by regulating aPKC/Numb cortical polarity and spindle orientation. *Genes & Development*, 20(24):3464–3474, December 2006a.

Cheng-Yu Lee, Kristin J Robinson, and Chris Q Doe. Lgl, Pins and aPKC regulate neuroblast self-renewal versus differentiation. *Nature*, 439(7076):594–598, February 2006b.

Cheng-Yu Lee, Brian D Wilkinson, Sarah E Siegrist, Robin P Wharton, and Chris Q Doe. Brat is a Miranda cargo protein that promotes neuronal differentiation and inhibits neuroblast self-renewal. *DEVCEL*, 10(4):441–449, April 2006c.

Jen-Yi Lee and Bob Goldstein. Mechanisms of cell positioning during C. elegans gastrulation. *Development*, 130(2):307–320, January 2003.

Jen-Yi Lee, Daniel J Marston, Timothy Walston, Jeff Hardin, Ari Halberstadt, and Bob Goldstein. Wnt/Frizzled signaling controls C. elegans gastrulation by activating actomyosin contractility. *Current Biology*, 16(20):1986–1997, October 2006d.

Sangkyu Lee, Hyerim Park, Taeyoon Kyung, Na Yeon Kim, Sungsoo Kim, Jihoon Kim, and Won Do Heo. Reversible protein inactivation by optogenetic trapping in cells. *Nature Methods*, 11(6):633–636, June 2014.

M Leptin. Gastrulation in Drosophila: the logic and the cellular mechanisms. *The EMBO Journal*, 18(12):3187–3192, June 1999.

M Leptin and B Grunewald. Cell shape changes during gastrulation in Drosophila. *Development*, 110(1):73–84, September 1990.

M Leptin, J Casal, B Grunewald, and R Reuter. Mechanisms of early Drosophila mesoderm formation. *Development (Cambridge, England). Supplement*, pages 23–31, 1992.

Anselm Levskaya, Orion D Weiner, Wendell A Lim, and Christopher A Voigt. Spatiotemporal control of cell signalling using a light-switchable protein interaction. *Nature*, 461(7266): 997–1001, October 2009.

Miranda Lewis, Christopher J Arnot, Helen Beeston, Airlie McCoy, Alison E Ashcroft, Nicholas J Gay, and Monique Gangloff. Cytokine Spatzle binds to the Drosophila immunoreceptor Toll with a neurotrophin-like specificity and couples receptor activation. *Proceedings of the National Academy of Sciences*, 110(51):20461–20466, December 2013.

Bingsi Li, Heon Kim, Melissa Beers, and Kenneth Kemphues. Different domains of C. elegans PAR-3 are required at different times in development. *Development*, 344(2):745–757, August 2010a.

Jin Li, Heon Kim, Donato G Aceto, Jeffrey Hung, Shinya Aono, and Kenneth J Kemphues. Binding to PKC-3, but not to PAR-3 or to a conventional PDZ domain ligand, is required for PAR-6 function in C. elegans. *Development*, 340(1):88–98, April 2010b.

Susana Q Lima and Gero Miesenbock. Remote control of behavior through genetically targeted photostimulation of neurons. *Cell*, 121(1):141–152, April 2005.

D Lin, A S Edwards, J P Fawcett, G Mbamalu, J D Scott, and T Pawson. A mammalian PAR-3-PAR-6 complex implicated in Cdc42/Rac1 and aPKC signalling and cell polarity. *Nature Cell Biology*, 2(8):540–547, August 2000.

E Liscum and W R Briggs. Mutations in the NPH1 locus of Arabidopsis disrupt the perception of phototropic stimuli. *The Plant cell*, 7(4):473–485, April 1995.

Hongtao Liu, Xuhong Yu, Kunwu Li, John Klejnot, Hongyun Yang, Dominique Lisiero, and Chentao Lin. Photoexcited CRY2 interacts with CIB1 to regulate transcription and floral initiation in Arabidopsis. *Science*, 322(5907):1535–1539, December 2008.

Nicolas Loyer and Jens Januschke. The last-born daughter cell contributes to division orientation of Drosophila larval neuroblasts. *Nature Communications*, 9(1):3745, September 2018.

B Lu, M Rothenberg, L Y Jan, and Y N Jan. Partner of Numb colocalizes with Numb during mitosis and directs Numb asymmetric localization in Drosophila neural and muscle progenitors. *Cell*, 95(2):225–235, October 1998.

Wen Lu, Margot Lakonishok, Rong Liu, Neil Billington, Ashley Rich, Michael Glotzer, James R Sellers, and Vladimir I Gelfand. Competition between kinesin-1 and myosin-V defines Drosophila posterior determination. *eLife*, 9, February 2020.

Alyssa J Manning, Kimberly A Peters, Mark Peifer, and Stephen L Rogers. Regulation of epithelial morphogenesis by the G protein-coupled receptor mist and its ligand fog. *Science Signaling*, 6(301):ra98–ra98, November 2013.

Daniel J Marston, Christopher D Higgins, Kimberly A Peters, Timothy D Cupp, Daniel J Dickinson, Ariel M Pani, Regan P Moore, Amanda H Cox, Daniel P Kiehart, and Bob Goldstein. MRCK-1 Drives Apical Constriction in C. elegans by Linking Developmental Patterning to Force Generation. *Current biology : CB*, 26(16):2079–2089, August 2016.

Adam C Martin and Bob Goldstein. Apical constriction: themes and variations on a cellular mechanism driving morphogenesis. *Development*, 141(10):1987–1998, May 2014.

Adam C Martin, Matthias Kaschube, and Eric F Wieschaus. Pulsed contractions of an actin-myosin network drive apical constriction. *Nature*, 457(7228):495–499, January 2009.

Adam C Martin, Michael Gelbart, Rodrigo Fernandez-Gonzalez, Matthias Kaschube, and Eric F Wieschaus. Integration of contractile forces during tissue invagination. *The Journal of Cell Biology*, 188(5):735–749, March 2010.

Frank M Mason, Shicong Xie, Claudia G Vasquez, Michael Tworoger, and Adam C Martin. RhoA GTPase inhibition organizes contraction during epithelial morphogenesis. *The Journal of Cell Biology*, 127:jcb.201603077, August 2016.

Sam J Mathew, Martina Rembold, and Maria Leptin. Role for Traf4 in polarizing adherens junctions as a prerequisite for efficient cell shape changes. *Molecular and Cellular Biology*, 31(24):4978–4993, December 2011.

Frank Medina, Angela M Carter, Olugbenga Dada, Stephen Gutowski, Jana Hadas, Zhe Chen, and Paul C Sternweis. Activated RhoA is a positive feedback regulator of the Lbc family of Rho guanine nucleotide exchange factor proteins. *The Journal of Biological Chemistry*, 288(16):11325–11333, April 2013.

Hui Miao, Timothy E Vanderleest, Cayla E Jewett, Dinah Loerke, and J Todd Blankenship. Cell ratcheting through the Sbf RabGEF directs force balancing and stepped apical constriction. *The Journal of Cell Biology*, 218(11):3845–3860, November 2019.

Jonathan B Michaux, François B Robin, William M McFadden, and Edwin M Munro. Excitable RhoA dynamics drive pulsed contractions in the early C. elegans embryo. *The Journal of Cell Biology*, 217(12):4230–4252, December 2018.

Abhinava K Mishra, James A Mondo, Joseph P Campanale, and Denise J Montell. Coordination of protrusion dynamics within and between collectively migrating border cells by myosin II. *Molecular Biology of the Cell*, 30(19):2490–2502, September 2019.

Jun Miyoshi and Yoshimi Takai. Molecular perspective on tight-junction assembly and epithelial polarity. *Advanced drug delivery reviews*, 57(6):815–855, April 2005.

Keiko Mizuno, Atsushi Suzuki, Tomonori Hirose, Koichi Kitamura, Koichi Kutsuzawa, Masaaki Futaki, Yoshiko Amano, and Shigeo Ohno. Self-association of PAR-3-mediated by the conserved N-terminal domain contributes to the development of epithelial tight junctions. *Journal of Biological Chemistry*, 278(33):31240–31250, August 2003.

Eurico Morais-de Sa, Vincent Mirouse, and Daniel St Johnston. aPKC phosphorylation of Bazooka defines the apical/lateral border in Drosophila epithelial cells. *Cell*, 141(3): 509–523, April 2010.

D Morisato and K V Anderson. Signaling pathways that establish the dorsal-ventral pattern of the Drosophila embryo. *Annual Review of Genetics*, 29(1):371–399, 1995.

P Morize, A E Christiansen, M Costa, S Parks, and E Wieschaus. Hyperactivation of the folded gastrulation pathway induces specific cell shape changes. *Development*, 125(4): 589–597, February 1998.

Fumio Motegi and Asako Sugimoto. Sequential functioning of the ECT-2 RhoGEF, RHO-1 and CDC-42 establishes cell polarity in Caenorhabditis elegans embryos. *Nature Cell Biology*, 8(9):978–985, September 2006.

Fumio Motegi, Seth Zonies, Yingsong Hao, Adrian A Cuenca, Erik Griffin, and Geraldine Seydoux. Microtubules induce self-organization of polarized PAR domains in Caenorhabditis elegans zygotes. *Nature Cell Biology*, 13(11):1361–1367, October 2011.

Akankshi Munjal, Jean-Marc Philippe, Edwin Munro, and Thomas Lecuit. A self-organized biomechanical network drives shape changes during tissue morphogenesis. *Nature*, 524 (7565):351–355, August 2015.

Edwin Munro, Jeremy Nance, and James R Priess. Cortical flows powered by asymmetrical contraction transport PAR proteins to establish and maintain anterior-posterior polarity in the early C. elegans embryo. *DEVCEL*, 7(3):413–424, September 2004.

Georg Nagel, Tanjef Szellas, Wolfram Huhn, Suneel Kateriya, Nona Adeishvili, Peter Berthold, Doris Ollig, Peter Hegemann, and Ernst Bamberg. Channelrhodopsin-2, a directly light-gated cation-selective membrane channel. *Proceedings of the National Academy of Sciences of the United States of America*, 100(24):13940–13945, November 2003.

Jeremy Nance and James R Priess. Cell polarity and gastrulation in C. elegans. *Development*, 129(2):387–397, January 2002.

Jeremy Nance, Jen-Yi Lee, and Bob Goldstein. Gastrulation in C. elegans. *WormBook*, pages 1–13, September 2005.

Amanda L Neisch, Olga Speck, Beth Stronach, and Richard G Fehon. Rho1 regulates apoptosis via activation of the JNK signaling pathway at the plasma membrane. *The Journal of Cell Biology*, 189(2):311–323, April 2010.

M Ni, J M Tepperman, and P H Quail. Binding of phytochrome B to its nuclear signalling partner PIF3 is reversibly induced by light. *Nature Publishing Group*, 400(6746):781–784, August 1999.

Kelly K Nikolaidou and Kathy Barrett. A Rho GTPase signaling pathway is used reiteratively in epithelial folding and potentially selects the outcome of Rho activation. *Current Biology*, 14(20):1822–1826, October 2004.

Rick W Nipper, Karsten H Siller, Nicholas R Smith, Chris Q Doe, and Kenneth E Prehoda. Galphai generates multiple Pins activation states to link cortical polarity and spindle orientation in Drosophila neuroblasts. *Proceedings of the National Academy of Sciences of the United States of America*, 104(36):14306–14311, September 2007.

Patrick W Oakes, Elizabeth Wagner, Christoph A Brand, Dimitri Probst, Marco Linke, Ulrich S Schwarz, Michael Glotzer, and Margaret L Gardel. Optogenetic control of RhoA reveals zyxin-mediated elasticity of stress fibres. *Nature Communications*, 8:15817, June 2017.

Masako Okumura, Toyoaki Natsume, Masato T Kanemaki, and Tomomi Kiyomitsu. Dynein-Dynactin-NuMA clusters generate cortical spindle-pulling forces as a multi-arm ensemble. *eLife*, 7:3453, May 2018.

Chet Huan Oon and Kenneth E Prehoda. Asymmetric recruitment and actin-dependent cortical flows drive the neuroblast polarity cycle. *eLife*, 8:723, May 2019.

Mojgan Padash Barmchi, Stephen Rogers, and Udo Häcker. DRhoGEF2 regulates actin organization and contractility in the Drosophila blastoderm embryo. *The Journal of Cell Biology*, 168(4):575–585, February 2005.

Isabel M Palacios and Daniel St Johnston. Kinesin light chain-independent function of the Kinesin heavy chain in cytoplasmic streaming and posterior localisation in the Drosophila oocyte. *Development*, 129(23):5473–5485, December 2002.

Hay-Oak Park and Erfei Bi. Central roles of small GTPases in the development of cell polarity in yeast and beyond. *Microbiology and Molecular Biology Reviews*, 71(1):48–96, March 2007.

S Parks and E Wieschaus. The Drosophila gastrulation gene concertina encodes a G alpha-like protein. *Cell*, 64(2):447–458, January 1991.

Francis C Peterson, Rhiannon R Penkert, Brian F Volkman, and Kenneth E Prehoda. Cdc42 regulates the Par-6 PDZ domain through an allosteric CRIB-PDZ transition. *Molecular Cell*, 13(5):665–676, March 2004.

Mark Petronczki and Juergen A Knoblich. DmPar-6 directs epithelial polarity and asymmetric cell division of neuroblasts in Drosophila. *Nature Cell Biology*, 3:43–49, January 2001.

Alisa J Piekny and Michael Glotzer. Anillin Is a Scaffold Protein That Links RhoA, Actin, and Myosin during Cytokinesis. *Current Biology*, 18(1):30–36, January 2008.

Kenneth E Prehoda. Polarization of Drosophila neuroblasts during asymmetric division. *Cold Spring Harbor Perspectives in Biology*, 1(2):a001388–a001388, August 2009.

P H Quail. Phytochrome: a light-activated molecular switch that regulates plant gene expression. *Annual Review of Genetics*, 25(1):389–409, 1991.

Peter H Quail. Phytochrome photosensory signalling networks. *Nature Reviews Molecular Cell Biology*, 3(2):85–93, February 2002.

Matteo Rauzi, Pierre-François Lenne, and Thomas Lecuit. Planar polarized actomyosin contractile flows control epithelial junction remodelling. *Nature*, 468(7327):1110–1114, December 2010.

Matteo Rauzi, Uros Krzic, Timothy E Saunders, Matej Krajnc, Primož Ziherl, Lars Hufnagel, and Maria Leptin. Embryo-scale tissue mechanics during Drosophila gastrulation movements. *Nature Communications*, 6(1):8677, October 2015.

David J Reiner and Erik A Lundquist. Small GTPases. *WormBook*, 2018:1–65, August 2018.

Fabian A Renschler, Susanne R Bruekner, Paulin L Salomon, Amrita Mukherjee, Lars Kullmann, Mira C Schütz-Stoffregen, Christine Henzler, Tony Pawson, Michael P Krahn, and Silke Wiesner. Structural basis for the interaction between the cell polarity proteins Par3 and Par6. *Science Signaling*, 11(517):eaam9899, February 2018.

François B Robin, William M McFadden, Baixue Yao, and Edwin M Munro. Single-molecule analysis of cell surface dynamics in Caenorhabditis elegans embryos. *Nature Methods*, 11 (6):677–682, June 2014.

Josana Rodriguez, Florent Peglion, Jack Martin, Lars Hubatsch, Jacob Reich, Nisha Hirani, Alicia G Gubieda, Jon Roffey, Artur Ribeiro Fernandes, Daniel St Johnston, Julie Ahringer, and Nathan W Goehring. aPKC Cycles between Functionally Distinct PAR Protein Assemblies to Drive Cell Polarity. *Developmental Cell*, 42(4):400–415.e9, August 2017.

Minna Roh-Johnson, Gidi Shemer, Christopher D Higgins, Joseph H McClellan, Adam D Werts, U Serdar Tulu, Liang Gao, Eric Betzig, Daniel P Kiehart, and Bob Goldstein. Triggering a cell shape change by exploiting preexisting actomyosin contractions. *Science*, 335(6073):1232–1235, March 2012.

Melissa M Rolls, Roger Albertson, Hsin-Pei Shih, Cheng-Yu Lee, and Chris Q Doe. Drosophila aPKC regulates cell polarity and cell proliferation in neuroblasts and epithelia. *The Journal of Cell Biology*, 163(5):1089–1098, December 2003.

Chantal Roubinet, Anna Tsankova, Tri Thanh Pham, Arnaud Monnard, Emmanuel Caussinus, Markus Affolter, and Clemens Cabernard. Spatio-temporally separated cortical flows and spindle geometry establish physical asymmetry in fly neural stem cells. *Nature Communications*, 8(1):1383, November 2017.

Anne Royou, William Sullivan, and Roger Karess. Cortical recruitment of nonmuscle myosin II in early syncytial Drosophila embryos: its role in nuclear axial expansion and its regulation by Cdc2 activity. *The Journal of Cell Biology*, 158(1):127–137, July 2002.

Anne Royou, Christine Field, John C Sisson, William Sullivan, and Roger Karess. Reassessing the role and dynamics of nonmuscle myosin II during furrow formation in early Drosophila embryos. *Molecular Biology of the Cell*, 15(2):838–850, February 2004.

Laure Saias, Jim Swoger, Arturo D'Angelo, Peran Hayes, Julien Colombelli, James Sharpe, Guillaume Salbreux, and Jérôme Solon. Decrease in Cell Volume Generates Contractile Forces Driving Dorsal Closure. *Developmental Cell*, 33(5):611–621, June 2015.

Anne Sailer, Alexander Anneken, Younan Li, Sam Lee, and Edwin Munro. Dynamic Opposition of Clustered Proteins Stabilizes Cortical Polarity in the C. elegans Zygote. *Developmental Cell*, 35(1):131–142, October 2015.

Keisuke Sako, Saurabh J Pradhan, Vanessa Barone, Álvaro Inglés Prieto, Patrick Müller, Verena Ruprecht, Daniel Čapek, Sanjeev Galande, Harald Janovjak, and Carl Philipp Heisenberg. Optogenetic Control of Nodal Signaling Reveals a Temporal Pattern of Nodal Signaling Regulating Cell Fate Specification during Gastrulation. *CellReports*, 16(3):866–877, July 2016.

Jessica K Sawyer, Nathan J Harris, Kevin C Slep, Ulrike Gaul, and Mark Peifer. The Drosophila afadin homologue Canoe regulates linkage of the actin cytoskeleton to adherens junctions during apical constriction. *The Journal of Cell Biology*, 186(1):57–73, July 2009.

M Schaefer, A Shevchenko, and J A Knoblich. A protein complex containing Inscuteable and the Galpha-binding protein Pins orients asymmetric cell divisions in Drosophila. *Current Biology*, 10(7):353–362, April 2000.

E D Schejter and E Wieschaus. bottleneck acts as a regulator of the microfilament network governing cellularization of the Drosophila embryo. *Cell*, 75(2):373–385, October 1993.

Johannes Schindelin, Ignacio Arganda-Carreras, Erwin Frise, Verena Kaynig, Mark Longair, Tobias Pietzsch, Stephan Preibisch, Curtis Rueden, Stephan Saalfeld, Benjamin Schmid, Jean-Yves Tinevez, Daniel James White, Volker Hartenstein, Kevin Eliceiri, Pavel Tomancak, and Albert Cardona. Fiji: an open-source platform for biological-image analysis. *Nature Methods*, 9(7):676–682, June 2012.

D S Schneider, Y Jin, D Morisato, and K V Anderson. A processed form of the Spätzle protein defines dorsal-ventral polarity in the Drosophila embryo. *Development*, 120(5): 1243–1250, May 1994.

M Schober, M Schaefer, and J A Knoblich. Bazooka recruits Inscuteable to orient asymmetric cell divisions in Drosophila neuroblasts. *Nature Publishing Group*, 402(6761):548–551, December 1999.

Stephanie Schonegg and Anthony A Hyman. CDC-42 and RHO-1 coordinate acto-myosin contractility and PAR protein localization during polarity establishment in C. elegans embryos. *Development*, 133(18):3507–3516, September 2006.

C P Shen, L Y Jan, and Y N Jan. Miranda is required for the asymmetric localization of Prospero during mitosis in Drosophila. *Cell*, 90(3):449–458, August 1997.

Kristin Sherrard, François Robin, Patrick Lemaire, and Edwin Munro. Sequential activation of apical and basolateral contractility drives ascidian endoderm invagination. *Current biology : CB*, 20(17):1499–1510, September 2010.

Sarah E Siegrist and Chris Q Doe. Microtubule-induced Pins/Galphai cortical polarity in Drosophila neuroblasts. *Cell*, 123(7):1323–1335, December 2005.

Sarah E Siegrist and Chris Q Doe. Extrinsic cues orient the cell division axis in Drosophila embryonic neuroblasts. *Development*, 133(3):529–536, February 2006.

Karsten H Siller and Chris Q Doe. Spindle orientation during asymmetric cell division. *Nature Cell Biology*, 11(4):365–374, April 2009.

Karsten H Siller, Clemens Cabernard, and Chris Q Doe. The NuMA-related Mud protein binds Pins and regulates spindle orientation in Drosophila neuroblasts. *Nature Cell Biology*, 8(6):594–600, June 2006.

Christian A Smith, Kimberly M Lau, Zohra Rahmani, Sascha E Dho, Greg Brothers, Ye Min She, Donna M Berry, Eric Bonneil, Pierre Thibault, François Schweisguth, Roland Le Borgne, and C Jane McGlad. aPKC-mediated phosphorylation regulates asymmetric membrane localization of the cell fate determinant Numb. *The EMBO Journal*, 26:468–480, January 2007.

Lilianna Solnica-Krezel. Conserved patterns of cell movements during vertebrate gastrulation. *Current Biology*, 15(6):R213–28, March 2005.

Philipp Spahn, Alice Ott, and Rolf Reuter. The PDZ-GEF protein Dizzy regulates the establishment of adherens junctions required for ventral furrow formation in Drosophila. *Journal of Cell Science*, 125(Pt 16):3801–3812, August 2012.

Daniel St Johnston and Julie Ahringer. Cell polarity in eggs and epithelia: parallels and diversity. *Cell*, 141(5):757–774, May 2010.

D Stein and C Nusslein-Volhard. Multiple extracellular activities in Drosophila egg perivitelline fluid are required for establishment of embryonic dorsal-ventral polarity. *Cell*, 68 (3):429–440, February 1992.

D Stein, S Roth, E Vogelsang, and C Nusslein-Volhard. The polarity of the dorsoventral axis in the Drosophila embryo is defined by an extracellular signal. *Cell*, 65(5):725–735, May 1991.

Devin Strickland, Yuan Lin, Elizabeth Wagner, C Matthew Hope, Josiah Zayner, Chloe Antoniou, Tobin R Sosnick, Eric L Weiss, and Michael Glotzer. TULIPs: tunable, light-controlled interacting protein tags for cell biology. *Nature Methods*, 9(4):379–384, March 2012.

Atsushi Suzuki and Shigeo Ohno. The PAR-aPKC system: lessons in polarity. *Journal of Cell Science*, 119(Pt 6):979–987, March 2006.

Makoto Suzuki, Hitoshi Morita, and Naoto Ueno. Molecular mechanisms of cell shape changes that contribute to vertebrate neural tube closure. *Development, growth & differentiation*, 54(3):266–276, April 2012.

D Sweeton, S Parks, M Costa, and E Wieschaus. Gastrulation in Drosophila: the formation of the ventral furrow and posterior midgut invaginations. *Development*, 112(3):775–789, July 1991.

Y Tabuse, Y Izumi, F Piano, K J Kemphues, J Miwa, and S Ohno. Atypical protein kinase C cooperates with PAR-3 to establish embryonic polarity in Caenorhabditis elegans. *Development*, 125(18):3607–3614, September 1998.

Jeffrey H Thomas and Eric Wieschaus. src64 and tec29 are required for microfilament contraction during Drosophila cellularization. *Development*, 131(4):863–871, February 2004.

Jared E Toettcher, Orion D Weiner, and Wendell A Lim. Using optogenetics to interrogate the dynamic control of signal transmission by the Ras/Erk module. *Cell*, 155(6):1422–1434, December 2013.

Zongtian Tong, Xiang-Dong Gao, Audrey S Howell, Indrani Bose, Daniel J Lew, and Erfei Bi. Adjacent positioning of cellular structures enabled by a Cdc42 GTPase-activating protein-mediated zone of inhibition. *The Journal of Cell Biology*, 179(7):1375–1384, December 2007.

Yu Chung Tse, Michael Werner, Katrina M Longhini, Jean-Claude Labbe, Bob Goldstein, and Michael Glotzer. RhoA activation during polarization and cytokinesis of the early Caenorhabditis elegans embryo is differentially dependent on NOP-1 and CYK-4. *Molecular Biology of the Cell*, 23(20):4020–4031, October 2012.

F R Turner and A P Mahowald. Scanning electron microscopy of Drosophila melanogaster embryogenesis. II. Gastrulation and segmentation. *Development*, 57(2):403–416, June 1977.

Silvia Urbansky, Paula González Avalos, Maike Wosch, and Steffen Lemke. Folded gastrulation and T48 drive the evolution of coordinated mesoderm internalization in flies. *eLife*, 5:563, September 2016.

F van Eeden and D St Johnston. The polarisation of the anterior-posterior and dorsal-ventral axes during Drosophila oogenesis. *Current opinion in genetics & development*, 9 (4):396–404, August 1999.

G von Dassow and G Schubiger. How an actin network might cause fountain streaming and nuclear migration in the syncytial Drosophila embryo. *The Journal of Cell Biology*, 127(6 Pt 1):1637–1653, December 1994.

Elizabeth Wagner and Michael Glotzer. Local RhoA activation induces cytokinetic furrows independent of spindle position and cell cycle stage. *The Journal of Cell Biology*, 213(6): 641–649, June 2016.

Huashan Wang, Yu Cai, William Chia, and Xiaohang Yang. Drosophila homologs of mammalian TNF/TNFR-related molecules regulate segregation of Miranda/Prospero in neuroblasts. *The EMBO Journal*, 25(24):5783–5793, December 2006.

Hui Wang, Marco Vilela, Andreas Winkler, Miroslaw Tarnawski, Ilme Schlichting, Hayretin Yumerefendi, Brian Kuhlman, Rihe Liu, Gaudenz Danuser, and Klaus M Hahn. LOVTRAP: an optogenetic system for photoinduced protein dissociation. *Nature Methods*, 13 (9):755–758, September 2016.

Xiaobo Wang, Li He, Yi I Wu, Klaus M Hahn, and Denise J Montell. Light-mediated activation reveals a key role for Rac in collective guidance of cell movement in vivo. *Nature Cell Biology*, 12(6):591–597, June 2010.

Yu-Chiun Wang, Zia Khan, and Eric F Wieschaus. Distinct Rap1 activity states control the extent of epithelial invagination via α-catenin. *Developmental Cell*, 25(3):299–309, May 2013.

R M Warga and C B Kimmel. Cell movements during epiboly and gastrulation in zebrafish. *Development*, 108(4):569–580, April 1990.

J L Watts, B Etemad-Moghadam, S Guo, L Boyd, B W Draper, C C Mello, J R Priess, and K J Kemphues. par-6, a gene involved in the establishment of asymmetry in early C.

elegans embryos, mediates the asymmetric localization of PAR-3. *Development*, 122(10): 3133–3140, October 1996.

Alexander N R Weber, Monique Gangloff, Martin C Moncrieffe, Yann Hyvert, Jean-Luc Imler, and Nicholas J Gay. Role of the Spatzle Pro-domain in the generation of an active toll receptor ligand. *Journal of Biological Chemistry*, 282(18):13522–13531, May 2007.

Mo Weng and Eric Wieschaus. Myosin-dependent remodeling of adherens junctions protects junctions from Snail-dependent disassembly. *The Journal of Cell Biology*, 212(2):219–229, January 2016.

Christian Wenzl, Shuling Yan, Philip Laupsien, and Jörg Großhans. Localization of RhoGEF2 during Drosophila cellularization is developmentally controlled by Slam. *Mechanisms of Development*, 127(7-8):371–384, July 2010.

Frederik Wirtz-Peitz, Takashi Nishimura, and Juergen A Knoblich. Linking cell cycle to asymmetric division: Aurora-A phosphorylates the Par complex to regulate Numb localization. *Cell*, 135(1):161–173, October 2008.

Kristen Witte, Devin Strickland, and Michael Glotzer. Cell cycle entry triggers a switch between two modes of Cdc42 activation during yeast polarization. *eLife*, 6:231, July 2017.

A Wodarz, A Ramrath, U Kuchinke, and E Knust. Bazooka provides an apical cue for Inscuteable localization in Drosophila neuroblasts. *Nature Publishing Group*, 402(6761): 544–547, December 1999.

A Wodarz, A Ramrath, A Grimm, and E Knust. Drosophila atypical protein kinase C associates with Bazooka and controls polarity of epithelia and neuroblasts. *The Journal of Cell Biology*, 150(6):1361–1374, September 2000.

Yi I Wu, Daniel Frey, Oana I Lungu, Angelika Jaehrig, Ilme Schlichting, Brian Kuhlman, and Klaus M Hahn. A genetically encoded photoactivatable Rac controls the motility of living cells. *Nature*, 461(7260):104–108, September 2009.

Shicong Xie and Adam C Martin. Intracellular signalling and intercellular coupling coordinate heterogeneous contractile events to facilitate tissue folding. *Nature Communications*, 6(1):7161, May 2015.

Masayuki Yazawa, Amir M Sadaghiani, Brian Hsueh, and Ricardo E Dolmetsch. Induction of protein-protein interactions in live cells using light. *Nature Biotechnology*, 27(10):941–945, October 2009.

Hannah G Yevick, Pearson W Miller, Jörn Dunkel, and Adam C Martin. Structural Redundancy in Supracellular Actomyosin Networks Enables Robust Tissue Folding. *Developmental Cell*, 50(5):586–598.e3, September 2019.

Shigeki Yoshiura, Nao Ohta, and Fumio Matsuzaki. Tre1 GPCR signaling orients stem cell divisions in the Drosophila central nervous system. *Developmental Cell*, 22(1):79–91, January 2012.

F Yu, X Morin, Y Cai, X Yang, and W Chia. Analysis of partner of inscuteable, a novel player of Drosophila asymmetric divisions, reveals two distinct steps in inscuteable apical localization. *Cell*, 100(4):399–409, February 2000.

Boris V Zemelman, Nasri Nesnas, Georgia A Lee, and Gero Miesenbock. Photochemical gating of heterologous ion channels: remote control over genetically designated populations of neurons. *Proceedings of the National Academy of Sciences of the United States of America*, 100(3):1352–1357, February 2003.

Feng Zhang, Viviana Gradinaru, Antoine R Adamantidis, Remy Durand, Raag D Airan, Luis de Lecea, and Karl Deisseroth. Optogenetic interrogation of neural circuits: technology for probing mammalian brain structures. *Nature Protocols*, 5(3):439–456, March 2010.

Yongwei Zhang, Uwe Werling, and Winfried Edelmann. SLiCE: a novel bacterial cell extract-based DNA cloning method. *Nucleic Acids Research*, 40(8):e55, April 2012.

Peng Zhao, Xiang Teng, Sarala Neomi Tantirimudalige, Masatoshi Nishikawa, Thorsten Wohland, Yusuke Toyama, and Fumio Motegi. Aurora-A Breaks Symmetry in Contractile Actomyosin Networks Independently of Its Role in Centrosome Maturation. *Developmental Cell*, 48(5):631–645.e6, March 2019.

Diana Zitserman and Fabrice Roegiers. Live-cell imaging of sensory organ precursor cells in intact Drosophila pupae. *Journal of Visualized Experiments*, (51), May 2011.

Seth Zonies, Fumio Motegi, Yingsong Hao, and Geraldine Seydoux. Symmetry breaking and polarization of the C. elegans zygote by the polarity protein PAR-2. *Development*, 137 (10):1669–1677, May 2010.